THE ASTRONOMICAL JOURNAL

PUBLISHED BY THE AMERICAN INSTITUTE OF PHYSICS
FOR THE AMERICAN ASTRONOMICAL SOCIETY

VOLUME 65 | 1960 August ~ No. 1281 | NUMBER 6

Abstracts of Papers Presented at the 105th Meeting of the American Astronomical Society, April 18–21, 1960 at the University of Pittsburgh

The Frequency of Binaries among Metallic-Line ars. HELMUT A. ABT, *Kitt Peak National Observa-ry, Tucson, Arizona.*—Several astronomers have spected that the percentage of metallic-line (Am) ars which are members of spectroscopic binaries ay be unusually high. Radial-velocity catalogues t many of these stars as possibly being variable t conclusive observations and orbits are often un-ailable, even among the fourth-magnitude stars. A systematic study of 25 Am stars, picked effec-vely at random, was made. An average of 11 ectra (18–20 A/mm) of each was obtained with e McDonald 82-inch coudé and Mt. Wilson 60-ch Cassegrain spectrographs. Of the 25, 21 (84%) ve variable radial velocities and are definitely ectroscopic binaries. Orbits have been obtained r all of these, except for four double-lined binaries which the line separations were generally too all for good measures. After allowance for orbits en nearly pole-on, for long-period systems, and r cases of unsuitable distribution of observations, is clear that all Am stars are members of spectro-opic binaries.

Of the 21 stars with variable radial velocity, 11 2%) are double-lined binaries. The mass ratios d the relative luminosities in the pairs seem con-tent with the mass-luminosity relation. The riods range from one to 361 days with a median of out ten days. Some binaries, including one with a -day period, show variations in line intensities ith phase like those in the B1 dwarf Alpha Virginis.

The Use of Telescope-Image Orthicon Systems ith Hypersensitization at Readout. R. AIKENS, G. ARTON, J. A. HYNEK, *Smithsonian Astrophysical bservatory,* AND W. A. BAUM AND J. KIMMEL, *Mt. Vilson and Palomar Observatories.*—For the past o years a small "image-orthicon observatory" has en operated by the Smithsonian Astrophysical bservatory in conjunction with its Satellite Track-ing Station at Organ Pass, New Mexico, using, for the most part, modified RCA circuitry and GE image orthicons with a 10-inch Baker cine theodolite optical system.

In late 1959, the apparatus was removed to Mount Palomar and attached to the 20-inch Cassegrainian telescope for tests with this larger instrument. An appropriate refrigeration system was constructed for this purpose through the support of the Carnegie Image Tube Committee.

In these tests the phenomenon of memory on the part of the image orthicon was clearly demonstrated; illusory gains of 500 times over 103a-O emulsion were obtained, while real gains of approximately 30 times were obtained. It was shown that upon readout only a small fraction of the latent information was removed from the target, thus allowing fainter magnitude limits to be reached on successive readouts.

Upon return of the equipment to Organ Pass, it was subjected to a series of laboratory tests with a test object of graduated artifical stars.

By using a 4-second integration cycle, memory was again demonstrated with saturation occurring at approximately the 32nd readout. It was shown, however, that saturation could be effected much more rapidly by flashing the photocathode by either a uniform background light or by a sharp flash during readout. Not only were the effects of memory expedited by the hypersensitization but gains of more than a magnitude were obtained on the first readout.

Tests showed that the best results could be obtained by dispensing with hypersensitization with light and substituting hypersensitization by appropriate bias pulsing of the target and of the G-5 grid. In the most recent laboratory tests, the limiting magnitude was increased by 2.5 mag. on first readout, indicating that a large fraction of the latent information on the target can be utilized on the first sweep, with a relatively small amount remain-

ing to contribute to tube memory. Thus a tenfold gain over ordinary image orthicon usage and total gains of the order of 100 seem indicated by these tests.

Lunar Eclipse, Low Budget and Student Ingenuity. IVAN ARON, *Heidelberg College.*—Eleven students in an undergraduate optics course at Heidelberg College built equipment for observing the total lunar eclipse of March 13, 1960. A restricted budget and considerations of effective teaching led to the use of "on hand" equipment, including much obtained through state educational surplus sources. Two cameras were constructed. A view camera without lens was fitted directly to an $f/1.4$-in. Alvan Clark refractor. A surplus Turner-Reich anastigmat aerial-camera lens of 25-in. focal length was threaded to a $2\frac{1}{2}$- to 3-in. cast-iron pipe coupling, which was threaded for focusing to a length of 3-in. pipe. To the other end of the pipe were fitted standard 2-sided $2\frac{1}{4}\times3\frac{1}{4}$-in. film holders. This $f/14.5$ camera was equatorially mounted with scrap lumber and plumbers fittings, a type X-1 reflex sight providing a bearing and drive gears. A photometer was made by fitting an RCA 926 phototube to a Mark 17 eight-power elbow telescope. The eyepiece was removed, and a positive lens in a cardboard mailing-tube was used to project an image of convenient size and position. Switches at each observing position caused the note of an audio oscillator to be recorded on tape which also recorded WWV signals for precise timing. Except for the tape recorder, all electronic equipment was standard teaching-laboratory material.

Preliminary Results with a Maser Radiometer at λ3.45 cm. M. E. BAIR, A. H. BARRETT, J. J. COOK, L. G. CROSS, AND R. W. TERHUNE, *University of Michigan Observatory and Willow Run Laboratories, Ann Arbor, Michigan.*—A 4-level ruby maser radiometer operating at 8700 Mc has been built by the Willow Run Laboratories and installed on the University of Michigan 85-foot radio telescope. The bandwidth is 8 Mc, as restricted by the post-amplifiers, with a maser gain of 20 db. The rms fluctuations observed are 0.05 ± 0.01°K with an integration time of 2 sec. A liquid nitrogen temperature calibration has been incorporated. Continuous operation at liquid helium temperatures for a period of 13 hr has been obtained.

The radio source Hydra A (IAU09S1A) has been observed with an antenna temperature of 0.45 ± 0.10°K corresponding to a point source flux of 4.8×10^{-26} w m^{-2} (c/s)$^{-1}$ at 8700 Mc with a tentative error of 30%.

Microwave Absorption and Emission in th Atmosphere of Venus. ALAN H. BARRETT. *Unive sity of Michigan Observatory, Ann Arbor, Michiga* —The temperature of Venus determined by radi astronomy is about 600°K in the centimeter wave length region and approximately 400°K in the mill meter region. By infrared methods and the intensit distribution of CO_2 bands the temperature is foun to be slightly under 300°K which undoubtedly refe to the atmosphere at or above the clouds.

If the radio temperature of 600°K is the surfac temperature of Venus and the temperature abov the clouds is 285°K, information about the atmo phere below the clouds may possibly be obtaine from measurements in the millimeter range. Th radio spectrum of Venus for $\lambda\geq1$ mm has been ca culated assuming an atmosphere of 75% CO_2, 22 25% N_2, and 0–3% H_2O. The additional assump tions of adiabatic equilibrium below the cloud cov and isothermal equilibrium above the clouds wer made. These conditions imply an average tempera ture gradient of 9°K/km below the clouds, a clou height of 33 km, a scale height of 6.86 km, and pressure at the cloud level of 0.038 of the surfac pressure.

The mechanism of absorption results from th collision-induced dipole moment in CO_2 and N_2 an the rotational lines of H_2O. The optical depth any height has been computed and the radio brigh ness calculated from that. A surface pressure of (terrestrial) atmospheres for 0% H_2O or 10 atm f 3% H_2O is needed to match the radio data. Thu assuming a surface temperature of 600°K, fairl high surface pressures are indicated unless an u known atmospheric constituent is a strong absorb of microwave energy. Further millimeter measur ments are indicated, and these could be coupled wi the possible detection of other molecules by the radio spectral lines. These include O_2 at 5 and 2. mm, CO at 2.6 and 1.3 mm, NO at 1.99 and 1. mm, NO_2 at 1.13 cm, and N_2O at 1.19 cm, 5.9 2.98, and 2.39 mm.

New Measurements of the Helium-3 and H lium-4 Contents of Meteorites. CARL A. BAUE *The Pennsylvania State University, University Par Pennsylvania.*—Forty-nine measurements of th helium contents of 31 metallic meteorites were ma with the special mass spectrometer at the Universi of Minnesota. It is a double-focusing mass spe trometer (Hoffman and Nier, 1958, *Phys. Rev.* 11 2122) that was especially designed and construct for simultaneously measuring the helium-3 an helium-4 in gas samples.

One specific aim was to determine the range the helium contents better and the ratio of helium to helium-4 existing in metallic meteorites. Two

ıe meteorites selected for this study showed helium ntents far above that of any of the few previously easured for both isotopes separately or of the proximately 60 measured for total helium. Deep prings has a total helium content about 1.7 times ıd Clark County about 1.4 times greater than lorden, the metallic meteorite that previously had ıe greatest known helium content.

The ratio of helium-3 to helium-4 in Deep Springs ıd Clark County are 0.27 and 0.25, respectively. ınce these values are not particularly high these eteorites must have had moderate amounts of ielding and thus their exposure ages must be long. he preliminary estimates of their exposure ages is the order of 3.5 and 5.5 billion years, respectively, hich is considerably longer than the 2.4 billion ears found for Williamstown (Schaeffer, 1960, *hys. Today*, **13**, 18).

The helium contents of the nickel-rich ataxites e distributed much like that of the medium octaedrites. However, the hexahedrites investigated e distinct from other classes of meteorites in that ieir helium contents are unusually low and also ieir helium-3 to helium-4 ratios average much wer than other meteorites, ranging from 0.07 to 24. This is important because it indicates, for the rst time, that these meteorites, as a class, have had very different exposure history from other classes.

This work was supported by a grant from the ational Aeronautics and Space Administration.

An Approximation to Effective Temperature from ıe Curve of Growth. W. R. BEARDSLEY, *Allegheny bservatory, University of Pittsburgh.*—The value of tellar opacity as determined from curve of growth nalysis by Greenstein's method is used to calculate n absorption temperature. The same basic assumptions as made by Greenstein are involved, namely: 1) Abundance is quantitatively the same as α ersei. (2) Iron exists nearly all as *Fe* II. In addion, a standard stellar abundance scale must also e assumed. For this I chose that of Aller as given y Suess and Urey, (1956, *Revs. Modern Phys.* **28**, 6). This is used to calculate electron scattering om electron pressure and ionization temperature nd to determine a value for hydrogen abundance. he negative hydrogen absorption is calculated om electron pressure and the H^- absorption cofficient is as given by Chandrasekhar and Breen sing ionization temperature to enter the table. ubtracting the electron scattering and the H^- abprption from the stellar opacity gives the hydrogen bsorption. Correcting this value for induced emision, ionization, and abundance, one can then use it ı the fundamental relation between hydrogen abprption and temperature, solving for absorption temperature. The solution leads to a very sensitive determination of temperature. However, since H^- absorption was originally derived using ionization temperature, one must now use this temperature to get a new value of H absorption and then re-solve for a new absorption temperature. Three such iterations are usually sufficient to achieve a change in temperature of less than 5°. A final absorption temperature is then adopted to be the nearest multiple of 25°. The true probable error is difficult to estimate, however, an absorption temperature so determined should be of the same order of accuracy as the ionization temperature.

Results for supergiants in the range F0 to F8 give temperatures very close to the effective temperatures for this range as derived by Popper from the recently determined interferometric diameter of Sirius. Results for dwarfs give temperatures very much in excess, particularly those for the sun. This difficulty can be directly traced to the assumed hydrogen abundance. When improved values of the hydrogen abundance become available, this method should provide reasonable approximation to effective temperatures.

The Light Variation and Orbital Elements of AH Virginis. L. BINNENDIJK, *Flower and Cook Observatory, University of Pennsylvania.*—See this issue, p. 358, for complete article.

The Space Distribution of Meteoric Dust Particles. ROBERT E. BRIGGS (introduced by L. G. JACCHIA), *Smithsonian Astrophysical Observatory.*—An integral formula due to Haug is used to compute the space density of meteoric dust particles at many points in the solar system. The formula assumes the distribution of dust particles to have rotational symmetry about an axis through the sun which is normal to the ecliptic and also to have plane symmetry about the ecliptic. Data needed for the integration must be in the form of a joint frequency distribution for three orbital parameters of a particle's orbit, namely, inclination, eccentricity, and semi-major axis. Observed meteor orbits published by meteor analysis projects at Harvard were assumed to be typically representative of interplanetary meteoric particles. For simplicity of integration the foregoing parameters were further assumed to be independently distributed, and probability distributions for each were determined empirically. A tabulation of the resulting densities shows a strong concentration in the plane of the ecliptic with a sharp maximum at a distance of 0.06 a.u. from the sun. In planes parallel to the ecliptic the maxima become flatter and appear much farther from the sun as distance from the ecliptic increases. A sphere of

radius 0.02 a.u. around the sun appears to be a region of avoidance for meteor particles which is consistent with the implications of other physical considerations.

Theoretical Evaluation of Atmospheric Drag Effects in the Motion of an Artificial Satellite. DIRK BROUWER AND GEN-ICHIRO HORI, *Yale University Observatory*. If the atmospheric density above perigee height is represented by $\rho = A\exp(-\alpha r)$, the well-known expressions for the drag accelerations are

$$X_j = -C_D A(\dot{x}_j + \delta_j) V \exp(-\alpha r),$$

$$V^2 = \mu\left[\frac{2}{r} - \frac{1}{a}\right] - 2\omega(x_1\dot{x}_2 - x_2\dot{x}_1) + \omega^2(x_1^2 + x_2^2),$$

$x_j (j = 1, 2, 3)$ being the Cartesian coordinates; $\delta_1 = +\omega x_2$, $\delta_2 = -\omega x_1$, $\delta_3 = 0$.

In the Delaunay variables L_k, l_k (for L, G, H, l, g, h), the equations become

$$\frac{dL_k}{dt} = \frac{\partial F}{\partial l_k} + P_k, \quad \frac{dl_k}{dt} = -\frac{\partial F}{\partial L_k} - Q_k,$$

$$P_k = \sum X_j \frac{\partial x_j}{\partial l_k}, \quad Q_k = \sum X_j \frac{\partial x_j}{\partial L_k}.$$

Similarly, the equations after the elimination of the periodic terms, both short and long, become

$$\frac{dL_k''}{dt} = P_k'', \quad \frac{dl_k''}{dt} = -\frac{\partial F^{**}}{\partial L_k''} - Q_k'',$$

$$P_k'' = \sum P_j \frac{\partial l_j}{\partial l_k''} + \sum Q_j \frac{\partial L_j}{\partial l_k''},$$

$$Q_k'' = \sum P_j \frac{\partial l_j}{\partial L_k''} + \sum Q_j \frac{\partial L_j}{\partial L_k''}.$$

By ignoring the rotation of the atmosphere (i.e., putting $\omega = 0$), let p_k, q_k, p_k'', q_k'' be the functions obtained by replacing X_j by $\dot{x}_j$. Then it is easily found that

$$p_1 = L_1\left(\frac{2a}{r} - 1\right) \qquad q_1 = 2e\sin E + \frac{2}{e}\frac{L_2}{L_1}\sin f$$

$$p_2 = L_2 \qquad q_2 = -\frac{2}{e}\sin f$$

$$p_3 = L_3 \qquad q_3 = 0.$$

The solution of the problem with $\omega = 0$ is therefore reduced to that of the equations

$$\frac{dL_k''}{dt} = -C_D A V p_k'' \exp(-\alpha r),$$

$$\frac{dl_k''}{dt} = -\frac{\partial F^{**}}{\partial L_k''} + C_D A V q_k'' \exp(-\alpha r).$$

The quantities p_k'', q_k'' have been obtained from the theory (Brouwer, 1959, *Astron. J.* **64**, 378) to the first power of k_2 (or J) in the periodic terms, to the second power in the secular terms. No infinite series appear in these expressions. In the development of $V\exp(-\alpha r)$ infinite series expressions in e are unavoidable. A development to the fourth power of e has been made.

The final differential equations are solved by iteration. The investigation has not been completed but it appears that the procedure adopted is a powerful method for dealing with the simultaneous analytic solution of the effects of oblateness and drag in the motion of an artificial satellite.

Perturbations in Perigee Height of Vanguard I. R. BRYANT, A. BAILIE, AND P. MUSEN, *Theoretical Division, Goddard Space Flight Center*.—The effect of solar radiation pressure on the perigee height of Satellite 1958 β_2 (Vanguard I) has been considered.

A previous perturbation theory of this satellite contained the second, third, and fourth harmonics in the development of the earth's potential and lunar and solar gravitational effects. Comparison between the observed and calculated perigee heights left an unexplained discrepancy of 1 to 3 km.

The inclusion of solar radiation pressure leads to close agreement between the orbit data and the theoretical results except for a short period oscillation which becomes noticeable in the second year of observation.

The Barred Spiral Galaxy NGC 7479. E. M. BURBIDGE, G. R. BURBIDGE, AND K. H. PRENDERGAST, *Yerkes Observatory and Enrico Fermi Institute for Nuclear Studies, University of Chicago, and McDonald Observatory, University of Texas*.—The galaxy NGC 7479 has been classified SBb in Hubble's original scheme, and fB2 by Morgan. As compared with the essentially stellar bars of many barred spirals, the bar in NGC 7479 appears to have many HII regions along it, making it a promising object for a study of rotation by means of the $H\alpha$ emission line. Velocities along the bar and at a few points outside have been measured with the prime-focus spectrograph of the 82-inch telescope, by

eans of the $H\alpha$ and [NII] emission lines. The tation curve for the bar and points outside is own. A preliminary estimate of the mass of the r is given, and some ideas concerning the struc- re of barred spirals are discussed.

Heat Transfer Coefficient for Meteors Shielded an Air Cap. ALLAN F. COOK, *Harvard College bservatory.*—The equation of heat conduction is lved for the following model: The presentation ea of the meteoroid is a flat circular surface nor- al to the direction of flight. Only rotational and anslational degrees of freedom are activated within e air cap. Vibrational and electronic degrees of eedom are assumed to require much longer times r activation than the average duration of the ansit of an air molecule through the air cap. The undary conditions are the surface temperature at e meteoroid and at the front of the air cap, those taining immediately behind a shock wave travel- g at the velocity of the meteoroid. Isobaric con- tions are assumed within the air cap. The equation continuity is also employed. The results indicate at transfer coefficients ranging from $\frac{1}{3}$ at a ve- city of 12 km/sec^{-1} to 1/20 at a velocity of 72 m/sec^{-1} provided the meteoroid is larger than a ean free path of a high velocity air molecule in the r. These values are increased by about 40% for a rbulent boundary layer.

Narrow Band Photoelectric Photometry for G and Giants. D. L. CRAWFORD, *Kitt Peak National Ob- rvatory.*—Narrow band photoelectric photometry as been done on a number of G and K giant stars. he three filters used measured the break in the ectrum at the G band and at a *CN* band. The nge in each parameter is about 0.300 mag. and e mean error of one observation is ±0.007. A od correlation with spectral type, luminosity, age space velocity, and line strength is shown. In ldition, *UBV* colors are available for a few of these ars and these colors strengthen the correlation. eculiar *CN* stars stand out clearly.

The Structure of Sunspot Penumbras. ROBERT . DANIELSON, *Princeton University Observatory.*— Many sunspot photographs having a resolution of bout $\frac{1}{3}$ second of arc were obtained last summer uring Project Stratoscope. These photographs ow the penumbra resolved into a complex array of redominantly radial filaments. Most of these fila- ents have an apparent width of about 300 km (which is the diffraction width of the 12-inch tele- scope) and a length of 5000 to 10 000 km (the width of an average penumbra). Thus it is possible that the filaments have an actual width smaller than 300 km.

The filaments are, for the most part, brighter than the umbra, but not as bright as the granulation. Many of the filaments are recognizable after 10 minutes even though noticeable changes can occur in a few minutes. A few filaments have been traced for 40 minutes. Thus their lifetime is definitely longer than the lifetime of the granulation.

The filaments cannot be explained as hot material flowing up at the inner edge of the penumbra in tubes of 300 km diameter (or less) and flowing across the penumbra along magnetic lines of force. The reason is that the time for cooling by radiation of a 300-km filament is of the order of 1 minute while the time for material to flow across the penumbra (Evershed effect) is of the order of 100 minutes. Because of this short cooling time, the only macro- scopic flow which is capable of explaining the fila- ments is convective rolls with the axis of the roll along the magnetic field. It is thought that most of the penumbral filaments can be explained in this fashion. Some filaments, however, are seen to cross other filaments while some are observed in places where they cannot be convective rolls. These fila- ments must therefore lie above the surface of the sunspot and are therefore structures in the chromo- sphere above the sunspot.

This work was sponsored by the Office of Naval Research and the National Science Foundation.

A Report on Experiments with the Image Orthi- con As a Light Receiver. JOHN H. DEWITT, JR., *Dyer Observatory, Vanderbilt University.*—Work was begun in May, 1956 on the "Mars" project which was designed to explore the possibility of using the television image orthicon tube, then available, as a light receiver at the output of a telescope for the indirect photography of planetary images. A system was developed using an electronic image stabilizing device which overcame some of the deleterious effects of atmospheric instability.

When the General Electric Z-5294 orthicon utiliz- ing a magnesium oxide target became available in the fall of 1958 it was apparent that its superior storage characteristics would permit photography of very faint objects and possibly show a large im- provement over the sensitivity of the photographic plate. Subsequent trials at the output of the 24-inch Cassegrain telescope indicated that eleventh magni- tude could be reached in 1/30th sec and fifteenth magnitude in 8 sec or less. Equipment now being designed and constructed to explore further possi-

bilities of the image orthicon in photography of star fields, nebulae and spectra will be described.

The work is being carried out under a National Science Foundation Grant.

The Occultation of the Crab Nebula by the Solar Corona in June 1959. WILLIAM C. ERICKSON, *Convair Scientific Research Laboratory, San Diego 11, California.*—During June 1959, observations were made of the occultation of the Crab nebula by the solar corona at the Clark Lake radio astronomy station. The observing frequency was 26.3 Mc/sec (11.4 m wavelength). These observations extend the work of other observers to this lower frequency. Effects due to the scattering of radio waves in the solar corona have been found to a distance of 25 solar radii. These results are in agreement with those of other observers when scaled to their frequencies; however, they extend the observations to larger distances from the sun than those over which effects have previously been observed.

A Model for the Decimeter Radiation by Jupiter. GEORGE B. FIELD, *Princeton University Observatory.*—The model is based on emission at the cyclotron frequency by electrons trapped in Jupiter's magnetic field. The decimeter waves originate close to the magnetic poles, where the field strength must exceed 1200 gauss. The theoretical spectrum is proportional to $\lambda^{\frac{1}{2}}$ and agrees satisfactorily with the observed one. The polarization should be almost completely linear, with the magnetic vector parallel to Jupiter's magnetic axis. The required electron densities are of the order of 10^{-2} cm^{-3} if the electron energies are about 40 kev, as for the outer radiation belt of the Earth. The solar wind appears capable of supplying many times the radio-frequency energy.

The source and observable effects of such a strong magnetic field are considered. It is shown that the field can be primordial, being frozen in the metallic-hydrogen core of the planet, provided that the interior temperature does not exceed 800°K. The polarization of 20 Mc bursts can be explained provided their source is between 30° and 40° latitude. Both Zeeman effects and aurorae should be observable on Jupiter.

Meteoric Dust Particles and the Anomolous Polarization of Jupiter. GEORGE B. FIELD AND JOHN E. GAUSTAD, *Princeton University Observatory.*—It is suggested that the polarization in the polar regions of Jupiter is due to meteoric dust suspended in the atmosphere. The dust is accreted gravitationally from the interplanetary medium, and, because its electric charge acquired from the free electro in space, is funnelled by Jupiter's magnetic fie toward the poles. The rate of accretion, the requir magnetic field, and the mechanism of polarizati are discussed quantitatively.

The Protection of Frequencies for Radio A tronomy. J. W. FINDLAY, *National Radio Astronon Observatory, Green Bank, West Virginia.*—The A ministrative Radio Conference of the Internation Telecommunications Union completed its work Geneva just before Christmas 1959. The final ac of the Conference, which will be incorporated in t new radio regulations, will come into force in Ma 1961. These radio regulations will contain conside able material of importance to radio astronome The amount of frequency protection for radio a tronomers contained in the acts of the Conferen will be described.

In addition to the clearance of the hydrogen li (1400–1427 Mc), bands of frequency were des nated by the Conference and given various degre of protection at points throughout the radio spe trum from 2.5 Mc to 31.5 kMc. The value of th protection to radio astronomers will be discuss and suggestions made for further work by rad astronomers to improve the protection for the s ence in the future.

The Flux Density of Radiation from Cassiope A at 1400 Mc. J. W. FINDLAY AND H. HVATU *National Radio Astronomy Observatory, Green Ba West Virginia.*—As a part of the program of sou calibration at the National Radio Astronomy C servatory experiments have been started to meas the flux density from the Cas A source. One ma experimental difficulty in such measurements is determine exactly the effective collecting area of t antenna that is used. To minimize this difficulty horn antenna of about 10 square meters collecti area has been built. This horn is large enough give an antenna temperature from the Cas A sou of about 8°K. The gain of such a horn can be cal lated from its linear dimensions to a high accura The horn is fixed in position at an elevation an of 30° and is used as a transit instrument. It 120-ft in length and is made of sheet aluminum w all joints internally welded to ensure high electri conductivity. The design of the antenna and of t associated receiving equipment will be briefly scribed, and first measurements of the flux dens from the Cas A source at frequencies near 1400 will be reported.

Photography of the Infrared Coronal Lines 10 747 nd 10 798 A with Image Tubes. JOHN FIROR, *Department of Terrestrial Magnetism, Carnegie Institution of Washington*, AND HAROLD ZIRIN, *High Altitude Observatory, University of Colorado.*—The two nfrared lines of *Fe*XIII represent the $^3P_1 \rightarrow {}^3P_0$ nd $^3P_2 \rightarrow {}^3P_1$ transitions in the ground term of p^2. t sufficiently high coronal electron densities their atio of intensities should vary somewhat from the ormally observed ratio of about 2:1. This effect similar to that observed in planetary nebulae by eaton and Osterbrock. As the atomic parameters r *Fe*XIII are not known, it is not certain at what ensity the deviation should be observed.

Normal photographic methods with hypersensized I-Z emulsion require at least 30 minutes for roper exposure of the lines with the Climax coronograph—an impracticable exposure time if a region f the corona is to be explored for variations of line ntensity ratio. We have used electrostatically ocused, single stage tubes, loaned to us by the arnegie Image Tube Committee, to speed up exposure. The image on the output phosphor of the tube as photographed on 35-mm film using a fast lens t roughly unity magnification. With a selected tube nd a dispersion of about 15 A/mm, a 28-mm diam olar image and a 50-μ slit width, the exposure time s one minute on Plus-X film. The coronal lines of *Fe*X, XI, XIV, and XV are also obtained by normal ethods within a few hours of these exposures.

Quantitative measurements of the spectra are ow being made.

Nuclear Cosmochronology. WILLIAM A. FOWLER ND F. HOYLE, *California Institute of Technology.*—n the studies described in this paper we make uantitative use of the radioactive decays of uraium and thorium in cosmochronology in much the ame manner as these decays have been employed in eochronology. The paper is divided into two quite ifferent parts representing different views as to the mmediate source of the material that now constitutes the solar system.

Model 1. The Autonomous Galaxy. From its origin, he Galaxy has been an autonomous system—no urther important additions of material from interalactic space have taken place at subsequent times. tar formation, stellar evolution, and nucleosynthesis have declined at a steady exponential rate over he whole lifetime of the Galaxy. The duration of ucleosynthesis is found to be independent of this ate over rather wide limits.

Model 2. Steady-State Cosmology and Galactic-ntergalactic Exchange of Matter. The abundance of he elements in intergalactic matter has reached a teady state through interchange with galaxies in which stars produce elements beyond hydrogen. As a consequence of this same point of view, the Galaxy acquired significant quantities of intergalactic material at various times. This occurred particularly about one billion years before the sun and solar system were formed. Except at epochs of addition of new gas, stellar activity has declined exponentially, as in Model 1.

Consideration of the decay of the radioactive isotopes Th^{232}, U^{235}, U^{238}, according to Model 1, leads to the conclusion that the age of the Galaxy is $15_{-3}{}^{+5} \times 10^9$ years. Similar considerations according to Model 2 lead to the conclusion that the reciprocal of the Hubble constant is $11 \pm 6 \times 10^9$ years. The error can be reduced to $\pm 2 \times 10^9$ years if the present thorium-uranium ratio is chosen to give a Pb^{208}/Pb^{206} age for the solar system concordant with that given by Pb^{207}/Pb^{206}, namely 4.5×10^9 years.

Observing Close Binaries using Image Intensifiers and High-Speed Photography. LAURENCE W. FREDRICK, *Lowell Observatory, Flagstaff, Arizona.*—A two-stage cascaded image intensifying tube and motion picture cameras have been used to observe close binaries of 0".3 separation and larger. At this separation the mean errors appear to be $\pm 0''.05$ in the separation and $\pm 3°$ in position angle. These improve as the separation increases. The internal errors and distortion pattern are discussed, and means of improving these are presented. A regular observing program is being initiated. This has been supported in part by a grant made by the NSF to Carnegie Institute of Washington entitled, Development of Image Tubes for Telescopes.

On Energy Production in Colliding Galaxies. HOWARD D. GREYBER, *General Electric Research Laboratory, Schenectady, New York.* (Now at Geophysics Corporation of America, Boston, Massachusetts.)—A number of very strong radio sources in the sky have been identified visually as two galaxies in collision. One of these, Cygnus A, emits radio energy at the enormous rate of 10^{44} ergs/sec. A factor not mentioned in previous discussions on energy production in colliding galaxies is the surprising observation that very large energy production rates may be obtained from deuterium thermonuclear reactions in the extremely rare hot gas that is formed by the collision. It is shown that for one deuteron in 20 nuclei in the gas of the galaxies, the thermonuclear energy output of Cygnus A would be roughly equal to the radio noise output observed. The possibility of detecting $d+d$ reactions in a strong radio source by looking for the high-energy gamma rays from an earth satellite will be discussed.

Solar Radio Emission and Solar Cosmic Rays. F. T. HADDOCK AND M. R. KUNDU, *The Observatory, University of Michigan.*—Ionospheric absorption of cosmic noise in polar cap regions (PCA) is caused by fast protons (10–50 Mev) from the sun after a flare within 1 to 50 hr. Broad-band centimeter-wave outbursts (BCO) and meter-wave bursts of continuum radiation (type IV)—supposedly of the same nature (as indicated by dynamic spectrum observations of centimeter-wave outbursts obtained here)—have been found to be closely associated with PCA events. The PCA events have a tendency to start within 5 hr of intense BCO. For less intense BCO, the delay appears to be greater.

Ten out of 12 *intense* BCO are associated with PCA events. Type IV outbursts on meter waves is not as closely associated with polar absorption events.

The duration of the PCA events is closely related to the duration on the sun of "active regions" of noise storms (which in turn are associated with BCO or type IV flares) after the occurrence of BCO (or type IV) events, but is not related to the presence of "active regions" before the onset of the BCO. The PCA starts within several hours after a BCO event and lasts approximately as long as the "active region" is present.

Our results support the suggestion that these solar cosmic rays are accelerated by the same process as the fast electrons which are responsible for BCO or type IV radio emission near the sun and are trapped in the same region of the solar atmosphere associated with "active regions" of noise storms; they are not stored in interplanetary space. The energetic electrons lose their energy rapidly by this radiation, whereas radiation damping of the protons is negligible.

The Red Shift in Clusters of Galaxies. GERALD S. HAWKINS, *Boston University and Harvard College Observatory.*—The measurements of Humason, Mayall, and Sandage have been used to investigate the variation of the red shift within the Coma and Virgo clusters of galaxies. For each cluster the mea recession velocity was found for galaxies in t central region and galaxies at the edge, the resul being given in Table I. The "error in the mean" taken as $\sigma(n-1)^{-\frac{1}{2}}$, where σ is the standard devi tion and n is the number in the sample. The Con cluster shows an increase in the red shift betwe galaxies at the center and at the edge. An applic tion of the student's t criterion shows that th difference is significant at the 90% level. For t Virgo cluster only an upper limit can be set sin the observed value is less than the probable erro It seems difficult to reconcile this radial effect wi physical motions of the galaxies.

TABLE I.

	Coma	Virgo
Radius; inner, outer	0°.2, 0°.5	2°.8, 7°.0
Number; inner, outer	10, 11	27, 27
Velocity, inner, km sec^{-1}	+6254	+976
Velocity, outer, km sec^{-1}	+6885	+1094
Excess redshift, edge	+631 km sec^{-1}	+118 km sec^{-1}
Error in mean velocity	±320 km sec^{-1}	±130 km sec^{-1}

A Color-Absolute Magnitude Diagram for Extr galactic Radio Sources. D. S. HEESCHEN, *Nation Radio Astronomy Observatory, Green Bank, We Virginia.*—Observations have been made of th radio emission from nine galaxies, at wavelengt of 68.2 and 21.4 cm. Observed flux densities a given in terms of apparent radio magnitudes, usi the relation (Brown and Hazard 1952) $m_\lambda = -53$ $-2.5 \log S_\lambda$, where S_λ is the flux density at wav length λ. A radio-frequency "color" index C is d fined by $C = m_{21.4} - m_{68.2}$. This parameter is propo tional to the spectral index of the radio emissio over the wavelength range in question. Absolu magnitudes at 68.2 cm were obtained from th apparent magnitudes and adopted distances. Est mated uncertainties in C and $M_{68.2}$ are, for most the sources, $\pm 0^m.1$ and $\pm 1^m$, respectively. exclusiv of possible zero-point errors.

A plot of $M_{68.2}$ vs C gives a well-defined colo absolute magnitude sequence, running betwee $M = -15$, $C = 0$ and $M = -35$, $C = +1$. In terms spectral index, the sequence suggests that th spectral index of an extragalactic source is propo tional to its absolute luminosity.

The physical characteristics of the galaxies ob served differ widely, ranging from the collidin galaxies in Cygnus to the normal Sc spiral M33. I is somewhat surprising that such divergent type of objects should show as pronounced a radio colo magnitude sequence as is observed. While the co relation cannot be considered well established on th basis of the scanty data presently available, it i rather improbable that the high degree of correla tion shown between $M_{68.2}$ and C is entirely fortu tous, or due to selection effects. If the correlatio is real, it suggests that the sources have the sam emission mechanism, presumably the synchrotro mechanism, and that coupling exists between th energy distribution of relativistic electrons an either the magnetic field or the relativistic electro density, or both.

Relative Abundances in the High Velocity Star HD 25329. ARNOLD M. HEISER, *Yerkes Observatory.*—A curve-of-growth analysis is used to determine the abundances in HD 25329, a high-velocity K1V star, relative to the normal dwarf 70 Oph A (K0V). If plausible values for the necessary physical quantities are assumed, then certain elements are underabundant by factors of 200 to 1000 in HD 25329 relative to 70 Oph A. These results are compared with various relative abundance determinations in other high-velocity stars.

A Color-Magnitude Diagram for a Portion of the Large Magellanic Cloud. PAUL W. HODGE, *Harvard College Observatory and Smithsonian Astrophysical Observatory.*—Measures of 1000 stars in a section of the northern part of the Large Magellanic Cloud have provided a color-magnitude diagram for the field stars of the region. Photographic measures were calibrated by a photoelectric sequence obtained by Arp. The survey in the section studied was complete to $V=17.5$.

The resulting diagram shows a populous main sequence which accounts for about half of the stars. The remainder lie in the giant and supergiant area, forming two broad sequences, one intermediate in color and one very red, as well as a normal giant branch similar to those of nearby globular clusters. The location of stars in the evolved part of the diagram is unlike that for Milky Way stars, as determined by galactic clusters.

Forty-four of the 1000 stars are variable in brightness. Five of these are Cepheids, all but one of which have periods of four days. Five are very red irregular variables, two are irregular yellow variables, two are eclipsing binaries, and the remaining 30 form a sequence of peculiar variables with highly unusual properties. Details will be published elsewhere.

Very Restricted Four-Body Problem. SU-SHU HUANG, *Goddard Space Flight Center, National Aeronautics and Space Administration.*—Qualitative behavior of artificial satellites in the earth-moon-sun system has been discussed in terms of a very restricted four-body problem of masses m_1, m_2, m_3, and m such that $m_1 \gg m_2+m_3 \gg m$. If the separation between m_2 and m_3 is very much smaller than the distance of their center of mass from m_1, we can first idealize a state of motion (with approximation) of the three bodies m_1, m_2, and m_3 in such a way that m_2 and m_3 revolve around each other in circular orbits and furthermore the center of mass O' of m_2 and m_3 revolves around m_1 in a circular orbit too. By choosing a coordinate system with the origin at O' and revolving together with m_2 and m_3, we derive an integral which is the counterpart to Jacobi's integral in the restricted three-body problem. The position of m_1 enters into the integral through the angle subtended at O' by m_1 and m. Therefore no stationary zero-velocity surface can be defined in the present problem. However, we can introduce the conception of osculating zero-velocity surfaces which provide the instantaneous limiting surfaces that m of a given initial condition cannot pass through.

Double points of the zero-velocity surfaces have also been studied. In the restricted three-body problem these points are fixed in the rotating frame of reference and are the solution of the problem. It is not so in the very restricted four-body problem studied here. The double points rotates in the xy plane as m_1 moves with respect to the m_2-m_3 system. A study of the motion of these points leads to an interesting result that under certain conditions depending upon the mass of m_1 and its distance from O', the critical zero-velocity surfaces which pass through two double points become degenerated into one single surface. On both sides of degeneracy, the zero-velocity surfaces have fundamentally different appearances. It can be shown from these surfaces that any artificial satellite around the moon has to be close, in order to be stable.

Experiment to Determine Accurately the Polarization and Intensity of the Light from the Solar Corona. W. F. HUCH, E. P. NEY, R. W. MAAS, AND P. J. KELLOGG (introduced by MARTIN SCHWARZSCHILD), *University of Minnesota.*—Kellogg and Ney presented a theory that the solar corona may consist of charged particles trapped on a solar magnetic field. In order to test the possibility that synchrotron radiation in the visible might be detected from the solar corona, equipment has been constructed which measures the absolute intensity of polarized and unpolarized light from the corona, at wavelengths of 4500 A and 8500 A. It consists essentially of television cameras attached to telescopes, using photomultipliers as detectors. The accuracy of the equipment is such that the absolute intensities of polarized and unpolarized light from the corona may be measured to 5%, and the direction of the polarization angle may be measured to an accuracy of ± 0.8 deg. This equipment was successfully used on two sites in the Sahara Desert to measure the polarization of the corona during the eclipse of October 2, 1959. At each of these two sites, successful data were obtained for five complete scans of the corona in each color of light. Results are presented in the accompanying paper by Ney, Kellogg and Huch (p. 352). This research was supported by the ONR, the NSF, and the NASA.

Some Remarks on the Problem of Stellar Populations. WILHELMINA IWANOWSKA (introduced by PHILIP C. KENNAN), *Perkins Observatory, Delaware, Ohio (on leave from the Observatory of Copernicus University, Torun, Poland).*—An alternative approach to the problem of stellar populations is considered which seems to be more flexible for further research.

Stars are assigned to Population II or I according to their probable origin in one of the two main condensations of matter in the galaxy: the central spheroid, or the disk with spiral arms in it. The present state and position of a star is considered to be a result of its initial endowment (the population type) and its age, with the mass of the star as an important parameter for its physical-chemical evolution and its kinematical behavior. It is assumed that the galactic system is roughly halfway to or from the equipartition of energy: (1) on a large scale between the energy of random motions in the spheroid and the energy of rotation in the disk, (2) on the small local scale in random motions in each of the main population sites.

In this scheme different species of stars: red or blue giants, dwarfs, white dwarfs, planetary nebulae, novae or other kinds of variable stars are not uniquely assigned to one population type, but are regarded as variational phenomena inherent in both population types. Room is left for considerable range of ages with the possibility of present star formation in both population types. This possibility for the Population II type is left open owing to our poor knowledge of the situation in the central regions of the galactic nucleus, of globular clusters and elliptical nebulae, where more massive and younger stars may exist, in symbiosis with interstellar gas.

The fundamental problem of chemical composition differences, whether initial or present, needs further investigation both observational and theoretical.

Periodic Drag Perturbations of Artificial Satellites. IMRE G. IZSAK, *Smithsonian Astrophysical Observatory.*—The most important air drag perturbation upon the motion of an artificial satellite is the secular decrease of the elements a and e. There also exists a small secular decrease in i and small long-periodic perturbations in Ω and ω, due to the rotation of the atmosphere. Beside these effects, short-periodic perturbations are present in each element. This paper presents an investigation of the nature of these variations in the elements a, e, ω, and M. The essence of the method is a development into Fourier series of the right sides of the differential equations for the orbital elements. The mean density distribution in the atmosphere is approximated by $\rho = 10^{-1.35}(h-55)^{-5}$. The computation of the perturbations has been programed for the IBM 704.

A New Explanation of Martian Phenomena. C. C. KIESS, S. KARRER, AND HARRIET K. KIESS, *Georgetown College Observatory, Washington, D. C., and U. S. Naval Weapons Laboratory, Dahlgren, Virginia.*—The existence of water vapor and oxygen in the atmosphere of Mars in amounts too small for spectroscopic detection justifies the assumption that the observed Martian phenomena may be due to the oxides of nitrogen. Thus, absorption by the peroxide will explain the low albedos of Mars in green, blue, and violet light; and chalky-white deposits of tetroxide will explain the polar caps, their yellowish tint being due to dioxide in equilibrium with the solid N_2O_4. The dark belt bordering the melting cap is regarded as liquid N_2O_4 with NO and/or N_2O_3 in solution, or as wetting of the substrate. The spread of heavy gaseous N_2O_4 over the dark areas, toward the equator, will account for the seasonal changes of color shown by them, according to the nature of the mineral structure of the Martian soil. In the atmosphere of Mars the oxides of nitrogen may exist in both gaseous and solid phases, and, in these forms, account for the observed meteorological phenomena. In minute crystals, at the temperatures prevailing at various altitudes and latitudes, they may account for the haze and the transient blue and white clouds that are known to occur. In the gaseous phase absorption by the peroxide will account for the loss of blue and violet light, known as Wright's phenomenon. The occasional blue-clearing is, then, due to a shift in equilibrium from NO_2 to N_2O_4 owing to a cold wave. During a heat wave the shift will be in the direction of higher concentration of NO_2, thus accounting for the yellow clouds, which, at times, may be planet-wide in extent. If this view is correct Mars may be considered as a gigantic photochemical nitrogen-fixation process. Further, the well-known toxic effects of these oxides argue against existence of living organisms on the planet.

Tables for Correcting Observed Distribution Functions in Proper Motion for the Effect of Accidental Errors of Measurement. JOOST H. KIEWIET DE JONGE, *Allegheny Observatory, University of Pittsburgh.*—The Kapteyn-van Rhijn integral equation relating the observed distribution function in proper motion to the true distribution function in proper motion is inverted into a double infinite integral over the observed distribution function. It is shown that, in the case of meaningful solutions, the

der of integration in the iterated integral may be terchanged, provided the upper limit of the outer tegral is finite rather than infinite. A finite limit r what is then the inner integral assumes the role a precision parameter in the solution, and a umerical evaluation of this definite integral yields practical solution of the problem in the form of a uble entry table.

This solution, therefore, does not involve the pansions in orthogonal functions required in previously suggested solutions.

The Tables have been computed for a wide range probable error of measurement with the help of ne IBM 650 computer at the Data Processing enter at the University of Pittsburgh.

The Unseen Companion of the Fourth Nearest tar, Lalande 21185. SARAH LEE LIPPINCOTT, *proul Observatory, Swarthmore College, Swarthmore, ennsylvania.*—Lalande 21185, vis. mag. 7.46, spectrum M2V, distance 8.1 light years, has been photographed at the Sproul Observatory since 1912. Variable proper motion was established by Peter van de Kamp in 1944.

Recent studies, preliminary to a definitive least-squares solution, gave a period close to eight years or the photocentric orbit and indicated the necessity for including a secular perspective acceleration erm in addition to the proper motion because of the ong time interval and the appreciable proper motions of the reference stars.

Parallax, proper motion, secular perspective acceleration, and geometric orbital elements were determined by least squares with an IBM 650 computer. The material included 315 nights over the nterval 1912 to 1959. Two solutions, using 8.0- and .2-year periods, were made; no distinction can be nade between them on the basis of the residuals. For further use $P = 8^{y}0$, $T = 1939.9$ and $e = 0.30$ were dopted. The combined solution in right ascension nd declination yields $+0''.4039 \pm 0''.0021$ (p.e.) for ne absolute parallax, and $0''.0336 \pm 0''.0024$ for the emi-axis major of the photocentric orbit.

Reasonable extremes for the mass of the M2V tar with $M_{pv} = +10.5$ yield the following masses of ne unseen companion and the greatest separation f A and B:

$M_A + M_B$	$\Delta m = \infty$ M_B	$\Delta m = 3$ M_B	1961 d_{max}
$0.300\odot$	$0.009\odot$	$0.027\odot$	$1''.1$
0.400	0.011	0.035	$1''.2$
0.500	0.013	0.043	$1''.3$

It seems unlikely that B could be as bright as $M_{pv} = 13.5$ ($\Delta m = 3$), have a mass as small as $0.035\odot$ L726–8: $M_{pv} = 15.4$; mass $= 0.04\odot$), and have escaped visual detection at a distance of 1″. It is concluded that $\Delta m > 3$ and that the mass of the unseen companion is close to $0.01\odot$.

Assuming the companion to be extremely red some scanning photoelectric device in the infrared, taking advantage of the time of greatest elongation and the position angle might yield the positive results needed for a rigorous mass determination.

Secular and Librational Motions of the Pole. WILLIAM MARKOWITZ, *U. S. Naval Observatory.*—The polar motion is known to include 12- and 14-month periodic components. It has frequently been suggested that a secular component also exists, but its reality has hitherto been considered doubtful because of inhomogeneities in the observations.

A method of analysis is presented which enables the polar motion to be derived from the results of the northern chain of the International Latitude Service (I. L. S.) free from the effects of these inhomogeneities. The resulting polar motion is independent of errors in the positions and proper motions of the stars observed, of changes in the observing program, and of errors in the micrometer scale value.

The I. L. S. results indicate that from 1900 to 1960 polar motion had two components in addition to the 12- and 14-month terms, a progressive motion of $0''.0032$ per year along the meridian $60°W$, and a libration of period 24 years and coefficient $0''.022$ along the meridian $122°W$–$58°E$. These are mathematical representations of observed motions for which no physical causes are ascribed. The motions cannot be safely extrapolated into the past or future.

Observations of latitude and longitude made with the photographic zenith tube (PZT) at the U. S. Naval Observatory since 1915 are in agreement with the I. L. S. results.

The secular motion of the pole from 1900 to 1960 is $0''.2$. Account must be taken of the total motion of the pole in the precise determination of latitude, longitude, and time.

The north pole is moving in the general direction of eastern North America at a rate of one degree per million years. This rate is too small to account directly for the occurence of ice ages within the past 50 000 years.

Observations of Venus at 10.2-cm Wavelength. C. H. MAYER, T. P. MCCULLOUGH, AND R. M. SLOANAKER, *Radio Astronomy Branch, U. S. Naval Research Laboratory.*—The 10.2-cm emission of Venus was measured on 11 days near the inferior conjunction of September 1, 1959 using the 84-ft reflector at the Maryland Point Observatory of the U. S. Naval Research Laboratory. The apparent

blackbody disk temperature for Venus which was derived from the measurements changed from 535±65°K (p.e.) on September 17 to 675±85°K (p.e.) on October 10. The average over the whole interval was 600±65°K (p.e.). These measurements support the blackbody spectrum of the centimeter wavelength radiation from Venus which was suggested by the earlier observations at 3.15 and 9.4 cm (Mayer, McCullough, and Sloanaker, 1957, *Astrophys. J.* **127**) and at 3.37 cm (Alsop, Giordmaine, Mayer, and Townes, 1958, *Astron. J.* **63**, 301, and 1959, *URSI-IAU Paris Symposium*, p. 69).

Singlet Bands of C_2 in the Infrared Spectra of the Cool Carbon Stars. ANDREW MCKELLAR, *Dominion Astrophysical Observatory.*—It has generally been considered that the lowest triplet state of C_2 (the lower state of the Swan bands) was the normal state of the molecule. A recent investigation by Ballik and Ramsay (1959, *J. Chem. Phys.* **31**, 1128) has shown, however, that the lowest singlet state of C_2 lies about 610 cm^{-1} (0.075 ev) below the lowest triplet level, and is therefore the ground state. Hence bands arising from this lowest singlet state should be present in absorption in the spectra of the cool carbon stars.

Of the singlet systems of C_2, the one most favorably placed for astronomical observation is the Phillips System which occurs in the near infrared. A search on Victoria plates of the stars Y CVn (N3) and RY Dra (Np) has shown the Phillips bands to be present. On a grating spectrogram (7.2 A/mm) of Y CVn the 3,0 band degraded to longer wavelengths from its head at λ7714.6 is present and well resolved into its individual lines. On low dispersion three-prism plates (133 A/mm at λ10 000) the 1,0 band with head at λ10 134 is seen.

The simple and open structure of the Phillips bands makes them an advantageous agent for the investigation of the corresponding bands involving the C^{13} isotope of carbon. This subject is at present under study.

Attempted Interpretations of V/R Variation in Be Spectra. DEAN B. MCLAUGHLIN, *The Observatory, University of Michigan.*—The rotating-pulsating model for V/R variation (McLaughlin, 1931, *Publ. Am. Astron. Soc.* **7**, 31; 1933, *Proc. Natl. Acad. Sci.* **19**, 44) does not account satisfactorily for some details of the observations. In particular, it fails to yield the large shifts of emission lines in the same direction as the central absorption. Where the absorption varies in strength (as in β Mon A) it is weakest at the phase predicted for maximum strength by the rotating-pulsating model. The very large motions implied for cycles of over 1000 da are difficult to admit.

Attempts were made to account for the variatio by means of a rotating atmosphere subject to inte mittent expansion that is alternately accelerat and retarded. Qualitative agreement is obtain only with artificial assumptions that do not appe physically justifiable. Again the shifts of emissi lines are not satisfactorily represented.

All the observed phenomena do appear explicab by rotation of the line of apsides of elliptical rin of gas, as originally suggested by Struve (193 *Astrophys. J.* **73**, 94). Periastron at the recedi node gives maximum positive velocity of both emi sion and absorption, associated with $V/R>1$. Pe astron at approaching node yields $V/R<1$ a negative shifts of emission and absorption. Weake shell absorption in β Mon A corresponds to prese tation of periastron towards the observer, sin higher angular velocity then produces a minimu of density. The phase at which this occurs is co sistent with an advancing periastron. According M. Johnson (1958, *Liege Symposium* **7**, 219), o served V/R "periods" are dynamically consiste with this hypothesis.

Electron Density Distribution in the Ori Nebula. THUPPALAY K. MENON, *Flower and Co Observatory, University of Pennsylvania.*—This pap is based on observations made at a wavelength 3.75 cm using the 85-ft radio telescope at the N tional Radio Astronomy Observatory during t summer of 1959. The half-intensity beam-width the antenna was 7 minutes of arc. After correcti for the beam-width, contours of equal brightne temperature have been obtained for the Ori Nebula. Unlike the optical features, the contou show a high degree of symmetry for the regi around 10 minutes of arc of the Trapezium. Outsi of this region deviations from symmetry are fou to be correlated with optical features. In comparis with Osterbrock's model for the Orion Nebula, t present observations indicate a broader distributio Only a part of the discrepancy can be attributed the angular resolution of the antenna used for t observations. A new model of the Nebula has be derived having a radius of 12 minutes of arc and half-width of 7.5 minutes of arc for the brightne temperature distribution. From this model the ele tron density distribution has been calculated. T electron density at the center is found to be abo 1.2×10^3/cc. The predicted fluxes for various fr quencies from the present model have been co pared with observations and show reasonab agreement.

I wish to express my sincere gratitude to the st of the NRAO for their hospitality and for placi

ıe facilities of the observatory at my disposal. I ave benefited immensely from many discussions ith all of them.

Results from the Occultation of Regulus by Venus, uly 7, 1959. DONALD H. MENZEL AND G. DE AUCOULEURS, *Harvard College Observatory*.—Teams f observers from the Harvard and Smithsonian bservatories, stationed at Madrid, Le Houga, Ierate, Catania, Beirut, Shiraz, and Bloemfontein btained visual times of ingress and egress of Regu- ıs. Photoelectric light curves at ingress were re- orded at Le Houga and Bloemfontein. Analysis of ıe visual observations, supplemented by published ata from six European and two South African tations, has yielded the differential geocentric co- rdinates of the center of Venus with respect to egulus on July 7, 1959, at $14^h24^m00^s$ U.T.

$$\alpha(\text{Regulus})-\alpha(\text{Venus})=-9''.111\pm0''.013 \text{ p.e.},$$

$$\delta(\text{Regulus})-\delta(\text{Venus})=-0''.342\pm0''.012 \text{ p.e.}$$

he difference between observed (U.T.) and com- uted (E.T.) times of mid-eclipse is $-28^s.00\pm0^s.40$ p.e.). If U.T. $-$ E.T. $\approx -34^s$ for 1959.5, a provisional orrection to the ephemeris data is $O-C\approx+6^s.0$.

The radius of the atmospheric shell corresponding o half-intensity was $14''.403\pm0''.007$ p.e., or, at unit istance, $8''.500\pm0''.005$ p.e. If the optical radius is $''.41$ (ephemeris value), the corresponding altitude is 65 km above the top of the cloud layer.

Analysis of the photoelectric observations by the ıeory of differential refraction yielded the scale eight at this altitude $H(z_0)=RT/mg$, and its varia- on with z in the range $|z-z_0|<20$ km, viz.,

$$H(z_0)=6.8\pm0.2 \text{ p.e. km},$$

nd

$$(1/H)(\partial H/\partial z)=+0.010\pm0.002 \text{ p.e. km}^{-1}.$$

If the acceleration of gravity is 860 cm sec^{-2}, and ıe mean molar mass $\bar{m}=42.5$ ($CO_2=0.90$, N_2 $=0.09$, $A+\cdots=0.01$), then $T(z_0)=297\pm10$ p.e. °K nd $\partial T/\partial z=+3°$ deg km^{-1}.

The pressure at z_0 is 2.6 ± 0.13 p.e. dynes cm^{-2}, the ıass of gas above z_0 is 3.0×10^{-3} g cm^{-2}, the reduced ıickness 1.7 cm.

The observed pressure at z_0 is consistent with an tmospheric model in which the pressure is 160 mb t the top of the cloud layer.

The Automatic Machine Computation of Curves f Growth. JOSEPH PAUL MUTSCHLECNER, *The Ob- rvatory, University of Michigan*.—A program has een developed to provide for the automatic com- utation of curves of growth on an IBM 704 digital ɔmputer. The curves of growth so produced are to be used in the investigation of the solar abundance of a number of elements of special interest. The observational material for this program consists of spectral intensity tracings in the regions of the most suitable lines of each element. The tracings were obtained at the McMath-Hulbert and Mount Wilson Observatories for three or four values of $\mu(=\cos\theta)$ on the solar disk for each line.

The theoretical equivalent widths required in the curves of growth for each line are obtained by the straightforward procedure of first predicting the line profile for preset conditions and then integrating the profile over wavelength. The major features of the program are: (1) Any desired model atmosphere may be used; (2) either two or three stages of ionization may be considered; (3) the appropriate partition functions are read in explicitly for each depth; (4) the turbulent velocity is read in explicitly for each depth; (5) the line broadening may be assumed due to any desired combination of radiative damping, van der Waals interactions, and electronic or ionic quadratic Stark effect; (6) the program can yield equivalent widths for either selected values of μ or for the total flux; (7) the ionization and excitation temperatures may differ from one another at each depth if so desired.

Although all these features are not required for the particular problem at hand, they have been incorporated in order to provide a more general program applicable to other problems such as the study of line profiles and the determination of stellar abundances.

Backscatter of Cosmic Rays by the Sun's *H*II Sphere. G. A. NEWKIRK, J. W. WARWICK, AND H. ZIRIN, *High Altitude Observatory, University of Colorado*.—The phenomena of the cosmic-ray storm following the flare of February 23, 1956, have been explained by Meyer, Parker, and Simpson as due to a field-free cavity around the sun surrounded by a magnetic barrier outside the earth's orbit. This cavity was supposed to be produced by a constant "solar wind" of 500 particles/cm^3 moving at 1500 km/sec.

Several reasons are given to demonstrate the incompatibility of the constant "solar wind" with theory and observation.

The sun is surrounded by a sphere of ionized hydrogen at least several astronomical units in diameter, followed by a transition region of roughly the same thickness. The *H*II region is much hotter than the *H*I region outside. If the outer *H*I region is permeated by a galactic magnetic field, pressure balance ensures that there is virtually no field in the *H*II region and a magnetic shell at the transition region. This shell would produce the observed reflection of solar cosmic rays.

Results of the Measurement of the Polarization of Coronal Light on October 2, 1959. E. P. Ney, P. J. Kellogg, and W. F. Huch, *University of Minnesota.*—Three complete scans of the sun's corona at wavelengths of 4500 A and 8500 A have been analyzed to determine the intensities of polarized and unpolarized light during the eclipse of October 2, 1959. The measurement of polarized and unpolarized light allows one to separate the coronal light into F corona and K corona, the F corona coming from dust scattering along the line of sight, and the K corona coming from the true electron density in the corona itself. Our measurements show that the polarization of the corona was radial (in the sense of the H vector of the electromagnetic wave) within $\pm 0.8°$. They further indicate no infrared excess or deficiency larger than $\pm 10\%$. There is no time variation greater than 10% in the half-hour that elapses between our observations. Our absolute measurements indicate the same average intensity within 5% as that obtained by Von Kluber in the Khartoum eclipse in 1956.

This research was supported by the ONR, the NSF, and the NASA.

The Radial Velocity and Spectrum of HD 134646. B. E. J. Pagel (introduced by Olin J. Eggen), *Royal Greenwich Observatory.*—The star HD 134646 [Wilson 1953: No. 8768, $\alpha = 15^h06^m9$, $\delta = 63°18'$ (1950), gF2, 6.8 mag., 5B] belongs to the class of early F-type velocity variables that are of particular interest owing to the presence among them of short-period variables (Eggen 1956) and of peculiar magnetic stars. It was therefore placed on the Greenwich radial velocity program and observed intensively during the summer of 1959 with the one-prism spectrograph attached to the Yapp 36-inch reflector (dispersion 120 A/mm at $H\gamma$). The single-line orbit was obtained from 58 spectra taken between May 7 and August 18, 1959, and was found to approximate closely to a sine curve with $P = 2^d.450 \pm 0.006$ (estimated error), $K = 69.7$ km/sec ± 0.5 (p.e.), $\gamma = 1.9$ km/sec ± 1.0 (p.e.), $f(m) = 0.086$. A least-squares analysis by the method of Sterne (1941) gave the following additional elements for an elliptical orbit:

$e = 0.008 \pm 0.015$ (p.e.); ω 121°.5;
$T_0 =$ JD 2436 695^d.239 ± 0.028 (p.e., assuming ω).

The star has a 9th mag. companion at a separation of 18″ (ADS 9520). The main star appears to be F4III on the revised Yerkes system, while the companion is a G8 giant or subgiant. Both members of the pair have negligible proper motion, but at the probable distance of 144 pc, their separation is so wide that their proximity is of only marginal significance. The companion is too faint for its radial velocity to be measured with the present equipment.

The primary spectrum is moderately sharp lined and the type and orbit are reminiscent of the peculiar magnetic variable HD 98088 (Abt 1953). However, the spectrum is not peculiar and was not found to vary. A study of the magnetic field—if any—of HD 134646 would be of considerable interest.

The Distribution of Integrated Starlight in Galactic Coordinates. F. E. Roach and L. R. Megill, *Boulder Laboratories, National Bureau of Standards.*—The brightness of starlight has been calculated from the star counts listed in Groningen publication 43. Separate calculations have been made for each 10 degrees of galactic longitude and for galactic latitudes, 0, -2, ± 5, ± 10, ± 15, ± 20, ± 30, ± 40, ± 50, ± 60, ± 70, and ± 80. The results are given in number of 10th magnitude (photographic) stars per square degree for (a) each magnitude (pg) from 6 to 18, (b) the summation from $m_{pg}6$ to $m_{pg}18$, (c) the estimated contribution for $m_{pg} > 18$, and (d) the summation of (b) and (c). The extensive tabular material is on punched cards from which printouts can be made. A map has been made of the distribution of integrated starlight in galactic coordinates.

The Surface Temperature of Venus. Carl Sagan, *Yerkes Observatory.*—Recent microwave observations of Venus give brightness temperatures near 600°K. The spectrum precludes an origin as radiation from a cytherean Van Allen belt; the emission must be thermal, and must arise from just beneath the surface of Venus. The radiation temperature of an airless planet with Venus' color-corrected albedo and solar distance is ~250°K if the period of rotation is much less than the period of revolution, or if there is appreciable interhemispheric circulation; it is ~350°K if the two periods are comparable, and if there is no interhemispheric circulation. It is clear that a surface temperature of 600°K demands a very efficient greenhouse effect. From the radiation balance, the effective absorptivity of the atmosphere, integrated over wavelengths, is $\alpha = 0.995$ for rapid rotation; an equivalent atmosphere is one opaque between 1.5 and 40 μ. The only molecule which is likely to be abundant on Venus and which absorbs in the region longward of 20 μ is water.

The carbon dioxide abundance in a convective cytherean atmosphere is 18 km-atm; the total surface pressure is ~4 atm. Extrapolation to long paths of CO_2 and H_2O emissivities at elevated temperatures shows that ~10 g cm^{-2} of water vapor is required for a rapidly rotating Venus, and ~1 g cm

or a slowly rotating Venus, in order that the required greenhouse effect be achieved. As a check, the method was applied to the earth; the correct terrestrial water vapor abundance was predicted. The Venus model atmosphere has an ice-crystal cloud layer about 36 km above the surface. For rapid rotation, the predicted cloud layer is at the bolometric temperature, but has five times more water vapor above it than observed by Strong; for slow rotation, the cloud layer is 14 K° cooler than the bolometric temperature, but has 2×10^{-3} g cm^{-2} above it, as observed by Strong. If the mean cloud albedo is >0.75, the overcast is <0.90. At gaps in the clouds, there are windows near 8.7 μ, and also at many wavelengths in the near infrared and visible.

The absence of surface liquid water inhibits the establishment of the Urey equilibrium, and, incidentally, greatly reduces tidal friction. If the earth had been placed in the orbit of Venus in primitive times, the same atmospheric carbon dioxide content as on Venus would have resulted, but the surface temperature and water vapor abundance would have been much greater; thus, the earth must have been formed with $>10^4$ times more water than was Venus.

This work was supported in part by the California Institute of Technology Jet Propulsion Laboratory, National Aeronautics and Space Administration, and in part by the National Science Foundation.

On The Trumpler Shift in Early Stars. E. A. SPIEGEL, *Princeton University Observatory*.—In 1930 Trumpler measured radial velocities of late O and early B stars in order to obtain masses from the gravitational red shifts of these stars. His results indicated masses which are considerably above the masses expected for such stars, both on theoretical and observational grounds. In this note a possible explanation for Trumpler's observation is suggested.

For stars of the type studied by Trumpler (about B0) there is reason to believe that convective turbulence is moderately active (Speigel, University of Michigan Dissertation, 1958). The origin of the convection is in the *He*II ionization zone near the surfaces of such stars. By the familiar arguments in such situations, one expects that lines formed primarily in rising hot elements will be shifted to the violet and those formed in the descending cooler elements will show a corresponding red shift. It is difficult to find lines meeting the requirements for clearly showing such an effect, but where the convection is due to *He* ionization, the *He* lines should be good examples. In particular, they would be expected to show a red shift compared to the mean of the other lines. Since Trumpler's measurements were primarily of *He* lines, we might then expect that this mechanism could affect his results.

The magnitude of the red shift must surely be less than that given by the speed of sound in early-star atmospheres, about 20 km/sec. Indeed, Trumpler's shifts correspond to about 7 km/sec and this is consistent with what might be expected.

It is not difficult to check the foregoing suggestion observationally by measuring radial velocities for lines of different excitation potential. A preliminary study has been made by Struve (unpublished) on two high dispersion plates of 10 Lac (O9.5). The observations seem to corroborate the foregoing explanation to within the experimental accuracy.

Theory of the Orbit of an Artificial Satellite with Use of Spheroidal Coordinates. JOHN P. VINTI, *National Bureau of Standards, Washington, D. C.*—The author has developed the orbital theory for an artificial satellite, using a gravitational potential, (Vinti, 1959, *J. Research Nat. Bur. Standards* **63B** 105) in spheroidal coordinates, ρ, η, ϕ, which leads to quadrature solutions. This procedure accounts for all of the second harmonic (of coefficient J_2) and for most of the fourth, but omits entirely the local anomalies, drag, lunar-solar perturbations, and the odd harmonics when the origin is chosen at the earth's center of mass.

A previous report (Vinti, 1960, *Bull. Am. Phys. Soc.* **5**, 8) outlined a solution for the secular motions of ω and Ω. The complete orbital solution now requires evaluation of the integrals in the kinetic equations and their subsequent solution for ρ and η; all other quantities follow readily from these. Only the ρ integrals cause trouble; if $\rho_1\cdots\rho_4$ are the zeros of a certain quartic $F(\rho)$ that they all involve, one must first find $\rho_1+\rho_2$, $\rho_3+\rho_4$, $\rho_1\rho_2$, and $\rho_3\rho_4$, where ρ_1 and ρ_2 are those zeros of $F(\rho)$ which would reduce to the perigee and apogee radii if J_2 vanished. With this fact as a start, a method of successive approximations leads to power series in J_2 for these sums and products, the present treatment stopping with J_2^2.

Expressions of order J_2^2 follow readily for the ρ integrals and the η integrals, the former involving two angles closely related to v and E, the latter involving two other angles closely related to $\omega+v$ and $\phi-\Omega$. Here v and E are the true and eccentric anomalies, ω is the argument of perigee, and ϕ and Ω are the right ascensions of the satellite and the node. The constants that appear are all expressible in terms of initial conditions. A method of successive approximations, started by neglecting terms involving J_2, then leads to the solution for ρ and η as functions of time, through terms of order J_2^2. Calculation of the polar coordinates is then easy.

This work was supported by the U. S. Air Force, through the Office of Scientific Research of the Air Research and Development Command.

Space Velocities of Weak *CN* Giants. KENNETH M. YOSS, *Mt. Holyoke College.*—University of Michigan Curtis Schmidt objective prism plates have been searched for late-type giants with weak *CN* absorption. The spectra were obtained with the combined prisms, dispersion 110 A/mm at *H*-gamma. With this dispersion, luminosity classification, based on the strength of the *Sr*II line at 4077, can be estimated to within one luminosity class. The strength of *CN* absorption is based on the break in the continuum at the 4215 bandhead.

Approximately 10% of 900 stars brighter than photographic magnitude 9.5, which were classified within the spectral range G5 to K3 and luminosity range II–III to IV, were found to have weak *CN* absorption.

Slit spectrograms for a representative sample of 30 stars were obtained with the Mt. Wilson 60-inch reflector. Radial velocities were measured, and absolute magnitudes were obtained from microphotometer tracings. Forty standard stars, approximately half of which are high-velocity stars, were used for establishing an absolute magnitude calibration curve.

The Mt. Wilson absolute magnitudes, which have an internal mean error of ± 0.4 mag., are systematically 0.8 mag. fainter than the absolute magnitudes derived from the Schmidt luminosity classes.

Proper motions from the Yale Observatory Proper Motion Catalogues have been used with the Mt. Wilson radial velocities and absolute magnitudes to compute space velocities, corrected for solar motion. The mean space velocity for the thirty stars is 57 km/sec. If the Schmidt absolute magnitudes are used, the mean space velocity is 82 km/sec in closer agreement with the mean space velocity of Miss Roman's "weak *CN*" giants, 96 km/sec.

Relative to the Mt. Wilson absolute magnitudes, the stars either have normal or only mildly weak *CN* absorption. The fact that these stars represent the weakest *CN* giants found on the Schmidt plates suggests that the Mt. Wilson absolute magnitudes are systematically too faint.

Periodic Drag Perturbations of Artificial Satellites

IMRE G. IZSAK
Smithsonian Astrophysical Observatory, Cambridge, Massachusetts
(Received April 20, 1960)

This paper presents an investigation of the short-periodic drag perturbations of artificial satellites. The essence of the method is a development into Fourier series of the right sides of the differential equations for the elements a, e, ω, and M. The mean density distribution in the atmosphere is approximated by $\rho=10^{-1.35}(h-55)^{-5}$. Apart from secular terms in the elements a, e, and M the first-order perturbations appear in the form of Fourier series. The computation of the perturbations has been programed for the IBM 704.

THE most important air drag perturbation upon the motion of an artificial satellite is the secular decrease of the orbital elements a and e. There also exists a small secular decrease in i and small long-periodic perturbations in Ω, and ω, due to the rotation of the atmosphere. In addition to these effects, short-periodic perturbations are present in each element. This paper presents an investigation of the nature of these periodic variations in the elements a, e, ω, and M.

The differential equations of the problem are known, and we shall refer to the paper of Sterne (1959) in which the effect of a rigid rotation of the atmosphere has been taken into consideration. In order to describe this effect, he introduced the small quantity,

$$d=\omega_E n^{-1}\cos i(1-e^2)^{\frac{1}{2}},$$

where ω_E denotes the angular velocity of the earth, and n the angular velocity of the satellite, i.e., its mean motion. If we neglect quantities of the order d^2 and de^2, the time-derivatives of the orbital elements are

$$\dot{a}=-2ca^2\frac{\rho}{\rho_0}\left(\frac{1+e\cos E}{1-e\cos E}\right)^{\frac{1}{2}}[(1-2d)+(1+2d)e\cos E]\dot{E}, \quad (1)$$

$$\dot{e}=-2ca(1-e^2)\frac{\rho}{\rho_0}\left(\frac{1+e\cos E}{1-e\cos E}\right)^{\frac{1}{2}}\times\left[\cos E+d\left(\frac{e}{2}-2\cos E+\frac{7e}{2}\cos^2 E\right)\right]\dot{E}, \quad (2)$$

$$\dot{\omega}=-2c\frac{a(1-e^2)^{\frac{1}{2}}}{e}\frac{\rho}{\rho_0}\left(\frac{1+e\cos E}{1-e\cos E}\right)^{\frac{1}{2}}\times\left[1-d\left(2-\frac{7e}{2}\cos E\right)\right]\sin E\cdot\dot{E}, \quad (3)$$

$$\dot{M}=n-(1-e^2)^{\frac{1}{2}}\dot{\omega}-(2Sr/na^2). \quad (4)$$

As usual, S denotes the radial component of the disturbing force. The constant $c=(C_DA/2m)\rho_0$ is the "small parameter" of perturbations, where C_D is the aerodynamic drag coefficient, A is the cross-sectional area, m is the mass of the satellite, and ρ_0 is the atmospheric density of perigee. ρ/ρ_0 may be expressed as a function of E.

In theoretical studies on the motion of artificial satellites it is customary to consider an isothermal atmosphere which gives an exponential decrease of density with altitude:

$$\rho=\rho_0\exp[-(h-h_0)/H]. \quad (5)$$

The index 0 refers to the perigee. The constant H is the scale height, and $h-h_0=ae(1-\cos E)$. However, Fig. 1 shows that an exponential approximation to the density cannot be a very good one, if $h_0<400$ km. The small circles in this figure represent mean values formed from values obtained by Whitney (1959) and by Kallmann and Juncosa (1958). After some numerical experimentation it was found that the function

$$\rho=10^{-Q}(h-h^*)^{-N}\text{ g cm}^{-3}, \quad (6)$$

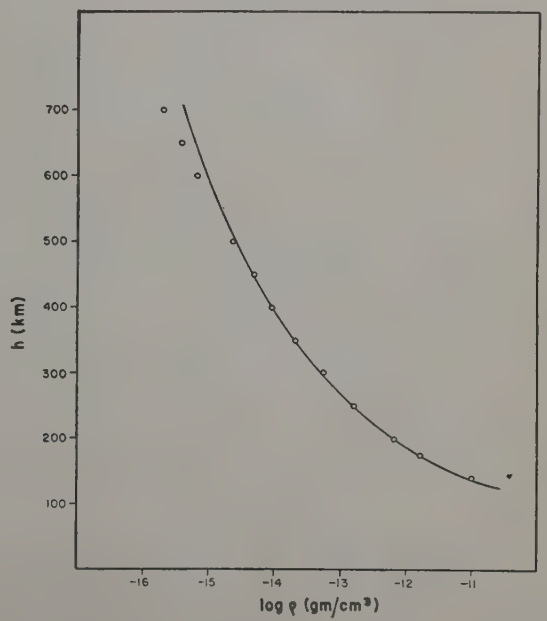

FIG. 1. Analytical representation of atmospheric density. The function $\rho=10^{-1.35}(h-55)^{-5}$ is indicated by the solid line and the circles are empirical values of density.

where $Q=1.35$, $h^*=55$, $N=5$, gives a reasonably good approximation to the actual distribution of atmospheric density as a function of height in km. The curve in Fig. 1 represents this density function. Introducing the eccentric anomaly E, we get the expression

$$\rho=\rho_0[(h-h^*)/(h_0-h^*)]^{-N} \\ =[(1-x\cos E)/(1-x)]^{-N}, \tag{7}$$

where

$$x=ae/[ae+(h_0-h^*)]<1.$$

It would be easy to integrate the expressions on the right sides of the Eqs. (1)–(4), if we could develop them into Fourier series. Such a representation can be given without difficulty for the product of the functions under the square root sign and in the brackets in the first three equations:

in Eq. (1) $f_0+2f_1\cos E+2f_2\cos 2E$

with $f_0=1-2d+\frac{3}{4}e^2$, $f_1=e$, $f_2=\frac{3}{8}e^2$;

in Eq. (2) $g_0+2g_1\cos E+2g_2\cos 2E+2g_3\cos 3E$,

with $g_0=\frac{1}{2}e+\frac{1}{4}5ed$, $g_1=\frac{1}{2}-d+\frac{3}{16}e^2$, $g_2=\frac{1}{4}e+\frac{3}{8}ed$, $g_3=\frac{1}{16}e^2$;

in Eq. (3) $2k_1\sin E+2k_2\sin 2E+2k_3\sin 3E$,

with $k_1=\frac{1}{2}-d+\frac{1}{16}e^2$, $k_2=\frac{1}{4}e+\frac{3}{8}ed$, $k_3=\frac{1}{16}e^2$.

The development of the density function is more involved, and its convergence less rapid. For the density function given by Eq. (5), it follows from the definition of the modified Bessel functions that

$$\frac{\rho}{\rho_0}=\exp(-y)\exp(y\cos E) \\ =\exp(-y)[I_0(y)+2\sum_{j=1}^{\infty}I_j(y)\cos jE],$$

where $y=ae/H$. For the case of the density function given by Eq. (7), which we shall employ in this paper, we can apply a standard method used in the theory of Keplerian motion (Smart 1953). Thus it can be shown that if we introduce the quantity

$$\xi=x[1+(1-x^2)^{\frac{1}{2}}]^{-1},$$

then our series will be

$$\left(\frac{1-x\cos E}{1-x}\right)^{-N}=\frac{1-\xi}{(1+\xi)^{2N-1}} \\ \times\{A_0{}^N(\xi^2)+2\sum_{j=1}^{\infty}A_j{}^N(\xi^2)\xi^j\cos jE\},$$

where

$$A_j{}^N(\xi^2)=\sum_{k=0}^{N-1}\binom{N-1+j}{N-1-k}\binom{N-1-j}{k}\xi^{2k}.$$

Note that

$$\sum_{k=0}^{N-1}\binom{N-1+j}{N-1-k}\binom{N-1-j}{k}=\binom{2N-2}{N-1}.$$

The number N is assumed to be a positive integer; in particular, for the present case, $N=5$. If it is not an integer, $A_j{}^N$ becomes, apart from a constant multiplier, a hypergeometric series in ξ^2.

Now let us return to the differential equations (1)–(3). The multiplication of the Fourier series in question yields equations of the form

$$\dot{a}=-2\,ca^2[F_0+2\sum_{j=1}^{\infty}F_j\cos jE]\dot{E},$$

$$\dot{e}=-2\,ca(1-e^2)[G_0+2\sum_{j=1}^{\infty}G_j\cos jE]\dot{E},$$

$$\dot{\omega}=-2ca(1-e^2)^{\frac{1}{2}}e^{-1}[2\sum_{j=1}^{\infty}K_j\sin jE]\dot{E},$$

where the coefficients F_j, G_j, K_j are linear expressions in the quantity

$$B_j{}^N=(1-\xi)\xi^jA_j{}^N/(1+\xi)^{2N-1}.$$

For instance, dropping the superscript N for convenience, we obtain

$$F_0=f_0B_0+2f_1B_1+2f_2B_2,$$
$$F_1'=f_1B_0+(f_0+f_2)B_1+f_1B_2+f_2B_3,$$
$$F_2=f_2B_0+f_1B_1+f_0B_2+f_1B_3+f_2B_4,$$
$$F_3=f_2B_1+f_1B_2+f_0B_3+f_1B_4+f_2B_5,$$
$$\cdots$$

These equations can be integrated immediately. Let the perturbations be all zero at the time $t=0$ of perigee passage, and transform the independent variable in the secular terms from E to t with Kepler's equation $E=nt+e\sin E$. Then we have the orbital elements

$$a=a(0)-2ca^2F_0\cdot nt-4ca^2\sum_{j=1}^{\infty}\frac{F_j}{j}\sin jE, \tag{8}$$

$$e=e(0)-2ca(1-e^2)G_0\cdot nt-4ca(1-e^2)\sum_{j=1}^{\infty}\frac{G_j}{j}\sin jE, \tag{9}$$

$$\omega=\omega(0)-4ca(1-e^2)^{\frac{1}{2}}e^{-1}\sum_{j=1}^{\infty}\frac{K_j}{j}(1-\cos jE). \tag{10}$$

The coefficient F_1 now means the above F_1' plus $\frac{1}{2}eF_0$, and G_1 has been transformed similarly.

Concerning perturbations of the mean anomaly we remark that the third term in Eq. (4) can be neglected, because S actually contains e as a factor; therefore it is about e^2 times smaller than the second term. On the

ther hand, since $\dot{n}=-3n\dot{a}/2a$, we have at once

$$n=n(0)+3cn^2aF_0\cdot t+6cna\sum_{j=1}^{\infty}\frac{F_j}{j}\sin jE.$$

Hence if we introduce the notation

$$K_1=\frac{1-e^2}{3e}2K_1+F_1-\frac{e}{4}F_2,$$

$$K_j=\frac{1-e^2}{3e}2K_j+\frac{F_j}{j}-\frac{e}{2}\left(\frac{F_{j-1}}{j-1}+\frac{F_{j+1}}{j+1}\right),\quad (j=2, 3, \cdots),$$

he mean anomaly will be

$$M=n(0)t+\tfrac{3}{2}cn^2aF_0\cdot t^2+6ca\sum_{j=1}^{\infty}\frac{L_j}{j}(1-\cos jE). \quad (11)$$

A numerical example of drag perturbations was omputed by Charles H. Moore on the IBM 704 by valuating the coefficient F_j, G_j, K_j, L_j and the Fourier eries (8)–(11), from the following elements:

Satellite 1958 γ (Explorer III), May 23, 1958

$a=7269$ km

$n=14.00$ rev. day^{-1}, $h_0=174$ km

$e=0.0986$, $\rho_0=1.91\times10^{-12}$ g cm^{-3}

$i=33°.3$. $c=2.56\times10^{-8}$ km^{-1}.

Figure 2 shows the drag perturbations of the elements a, ω, M. (The variation of the eccentricity is similar to hat of the semi-major axis.) In the case of the mean nomaly only the periodic part in (11) was plotted. As a visual aid, the figure also shows the secular part in he perturbation of a.

The rapidity of convergence of the above Fourier eries may be quite different for different satellites.

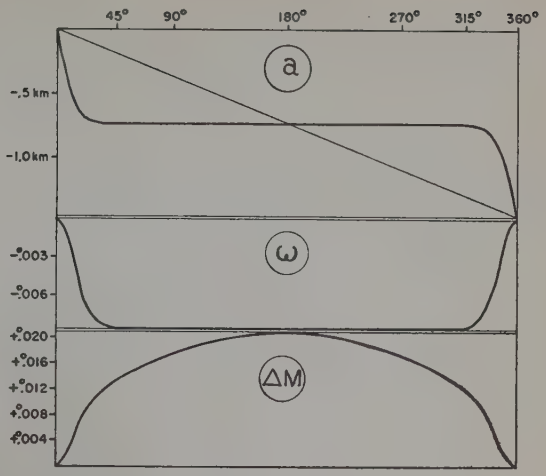

FIG. 2. The drag perturbations of the elements a, ω, and M. The abscissa is eccentric anomaly.

The convergence is more rapid the smaller the value of the parameter ξ. In the rather extreme example used in the illustration we had $\xi=0.566$, and for 2% accuracy we needed 10 terms in the Fourier-series (8), (9), (11), and an even larger number in (10).

ACKNOWLEDGMENT

I am very grateful to C. H. Moore for carrying out the programing of the relevant equations.

REFERENCES

Kallman, H. K. and Juncosa, M. L. 1958, *Project Rand Research Memorandum*, No. 2286.
Smart, W. M., 1953, *Celestial Mechanics* (Longmans, Green and Company, Ltd., London) pp. 31–36.
Sterne, T. E. 1959, *J. Am. Rocket Soc.* **29**, 777–782.
Whitney, C. A. 1959, *Spec. Report* No. 25, Smithsonian Astrophys. Obs.

The Light Variation and Orbital Elements of AH Virginis*

L. BINNENDIJK
Flower and Cook Observatory, University of Pennsylvania, Philadelphia, Pennsylvania
(Received April 9, 1960)

Photoelectric observations are presented of 1110 yellow and 1082 blue magnitudes of AH Virginis which were obtained during 22 nights of observing, mostly during the spring months of 1955 and 1957. The period is variable and the shape of the light curve changes in a short time as is shown by the observations of five consecutive nights.

One light curve observed in 1955 has an unusual appearance in that the heights of the maxima are unequal and the secondary minimum is asymmetrical and delayed. This curve was compared with a more nearly normal light curve, observed in 1957, which shows maxima of the same height and a symmetrical and undisplaced secondary minimum.

Orbital elements were computed keeping the geometrical elements such as the inclination, the sizes and shapes of the components the same, while the photometric elements such as intensity and surface brightness were considered to vary during the two-year period of observation.

A total eclipse occurs at primary minimum. Only the greater star is visible then and it is somewhat fainter in the 1955 light curve. The greatest difference between the 1955 and 1957 light curves occurs at secondary maximum (phase 0.75). It is shown that the unusual appearance of the 1955 light curve was caused by a subluminous region on the greater star. This region was located near one of the endpoints of the equatorial b axis, which exceeds the Jacobian limiting surface.

1. INTRODUCTION

THE variable AH Virginis is the bright component of the optical double star ADS 8472. The faint ($13^m.2$) companion is only $1''.30$ from the variable at position angle 17°. The variability of AH Virginis was discovered by Guthnick and Prager (1929) and a photographic light curve was published by Prager (1929). The period used by him was incorrect as was found by Lause (1934, 1935, 1937) from visual observations. Prager's observations were reduced by Chang (1948) using the correct period. This author also determined the radial velocity curves and derived the orbital elements from the combined data.

Huruhata and Nakamura (1951) gave photoelectric observations of one secondary minimum. Kitamura, Tanabe, and Nakamura (1957) observed the system photoelectrically during two nights in March and two nights in May, 1952. The mean curve obtained from these observations shows a rounded rather than a flat bottom at primary eclipse, which is not in agreement with the results of the present study. This curved appearance may be attributed to the fact that observations which were separated by a time interval of two months were combined, along with the fact that the observations were either started or terminated about the time of primary minimum. Kopal and Shapley (1956), assuming partial eclipses, used these observations to determine the orbital elements and found the system to have an inclination of 61°.

TABLE I. Variable and Comparison Stars.

Star	BD No.	R.A. (1900)	D. (1900)	Sp.
AH Virginis	+12°2437	$12^h\ 9^m15^s$	+12°22'.7	K0
Comparison	12 2443	12 12 34	+11 45.7	K0
Check star	12 2434	12 8 2	+12 29.2	K0

* Part of this work was supported by a contract with the Office of Naval Research.

Kwee (1958) published photoelectric observations of four runs through the primary minimum, each of which showed a constancy of light of about 40 minutes duration. This flatness of the primary minimum was also found from the observations of the present study. It is concluded, therefore, that AH Virginis is one of the few W Ursae Majoris systems which undergoes complete eclipses, and that the inclination is closer to 90° than to the above-mentioned value.

Another orbital computation using the Japanese observations and assuming $i=90°$ was recently made by Kitamura and Takahashi (1959), who also derived provisional elements from our earlier material (Binnendijk 1957). Their theoretical light curves show constant light for both the primary and secondary eclipses, which indicates that uniform light ($x=0$) was assumed in the solutions. However, all observations of secondary eclipse agree in showing a curved appearance, which indicates a considerable amount of limb darkening for the greater star.

2. OBSERVATIONS

In the present study the variable was observed photoelectrically in two wavelength regions with the 28-inch reflecting telescope of the Flower and Cook Observatory. A yellow filter, Corning 3384 of thickness 3.0 mm was used, with an effective wavelength of 5300 A. The combination of two filters, Corning 5543 of thickness 2.5 mm and Corning 3060 of thickness 2.0 mm was used for the blue filter, with an effective wavelength of 4420 A. The observations were made in four seasons, but the most extensive series were made during the spring months of 1955 and 1957. The output of a 1P21 photomultiplier was fed into a direct current amplifier of the Kron type and the amplified current registered by a Brown recorder. The duration of each deflection was one minute.

Table I lists the BD numbers, the position of the

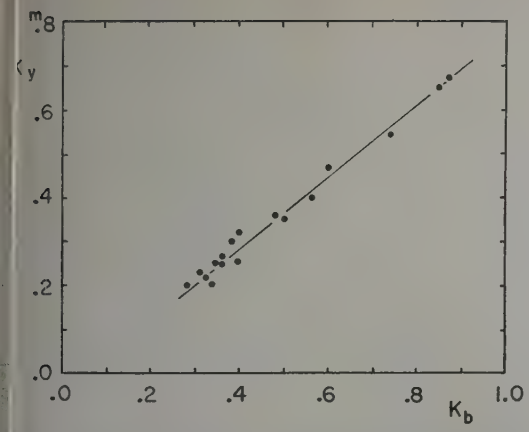

FIG. 1. Each dot represents a night on which the extinction coefficients, determined from observations of the comparison star, remained constant. The observed relation between blue and yellow extinction coefficients is a straight line which if extended does not go through the origin.

ars, and the spectral types according to the HD talogue. The magnitude difference between the comrison star and the check star was constant both in 55 and 1957, but there was a slight systematic difrence between the two values. This slight change was cribed to the application of a new aluminum coating the mirrors of the telescope.

3. EXTINCTION

The blue and yellow extinction coefficients for each ght were determined from observations of the comarison star. The correction for relative extinction was ien applied to the differences in magnitude between ie variable star and the comparison star.

For each of those nights during which the extinction oefficients remained constant, the blue extinction oefficient was plotted against the yellow one. Figure 1 ows that for practical purposes these points are tuated on a straight line. This line, if extended, does ot go through the origin. In a recent study by Hardie 1959) the same phenomenon appears in his figures and ormulae.

The following is a qualitative explanation. The exnction coefficient is the amount of the extinction in ie zenith expressed in magnitudes. Outside the earth's tmosphere the atmospheric extinction in any waveength is naturally zero. As light enters a vertical column f the atmosphere it encounters molecules of nitrogen nd oxygen which produce the well-known Rayleigh cattering. The resulting extinction is inversely proporonal to the fourth power of the wavelength. During a ight of good transparency, the humidity is usually oderate and the influence of the water vapor particles rather small. The ratio of the blue to the yellow exnction coefficients is found to be 1.5 on such a transarent night. During a night which is less transparent, the humidity is usually much higher and the water vapor particles are larger and more numerous. They cause an additional extinction which is less dependent on wavelength. The ratio of the coefficients is found to be 1.3 in this case. Finally during a night of poor transparency, fog particles appear. These have an average diameter of 0.01 mm, or 20 times the wavelength of light, and they are responsible for an additional extinction which is independent of wavelength. On such a night photoelectric observations are seldom made. According to this explanation the observed straight line is the central part of a curved line. The unobserved part of the curve goes through the origin and for extremely large extinctions it would show a slope of 45°.

4. TIMES OF MINIMA

A total of 1110 yellow and 1082 blue observations were made during 22 nights. From these, 16 times of minima were determined, using the method of Hertzsprung (1928). These are shown in Table II along with older data. Nason and Moore (1951) derived their time of minimum from one branch only. Their original tracing was made available to the author and was

TABLE II. Times of Minima and Residuals of AH Virginis.

J. D. ⊙	Min.	*O—C*	Meth.	Obs.[a]	Ref.
2425003.497	I	+0^{d}002	pg	Pr	1
5413.456	I	−0.003	pg	Pr	1
5730.295	II	−0.009	v	Ku	2
7610.392	I	+0.002	v	La	3
7925.4083	I	+0.0061	v	La	3
8284.4300	I	+0.0041	v	La	3
8634.4827	I	−0.0015	v	La	3
2431265.413	I	−0.010	v	Ze	4
3354.1581	II	−0.0004	v	H,N	5
3389.8160	I	−0.0004	pe	N,M	6
3744.364	I	+0.007	v	Sz	7
3759.434	I	−0.002	v	D,P	8
4094.41509	I	−0.0006	pe	Kw	9
4105.2169	II	+0.0019	pe	K,T,N	10
4486.44716	I	−0.0013	pe	Kw	9
4508.45296	I	−0.0014	pe	Kw	9
4841.39628	I	−0.0006	pe	Kw	9
4913.7336	II	+0.0021	pg	Ko	11
5197.77620	II	+0.0044	pe	Bi	..
5207.75545	I	−0.0005	pe	Bi	..
5243.61733	I	−0.0003	pe	Bi	..
5244.63855	II	+0.0021	pe	Bi	..
5245.65520	I	0.0000	pe	Bi	..
5573.70997	I	+0.0025	pe	Bi	..
5901.76578	I	+0.0060	pe	Bi	..
5907.67557	II	+0.0067	pe	Bi	..
5910.73091	I	+0.0057	pe	Bi	..
5921.73391	I	+0.0057	pe	Bi	..
5938.64646	II	+0.0062	pe	Bi	..
5958.61491	II	+0.0063	pe	Bi	..
5959.63316	I	+0.0057	pe	Bi	..
5961.67108	I	+0.0060	pe	Bi	..
5962.69001	II	+0.0062	pe	Bi	..
6697.65698	I	+0.0137	pe	Bi	..

[a] Pr = Prager 1 (1929); Ku = Kukarkin 2 (1929); La = Lause 3 (1934, 1935, 1937); Ze = Zessewitsch 4 (1944); H,N, = Huruhata and Nakamura 5 (1951); N,M = Nason and Moore 6 (1951); Sz = Szczepanowska 7 (1951, 1953); D,P = Domke and Pohl 8 (1953); Kw = Kwee 9 (1958); K,T,N = Kitamura, Tanabe and Nakamura 10 (1957); Ko = Koch 11 (1956); Bi = Binnendijk.

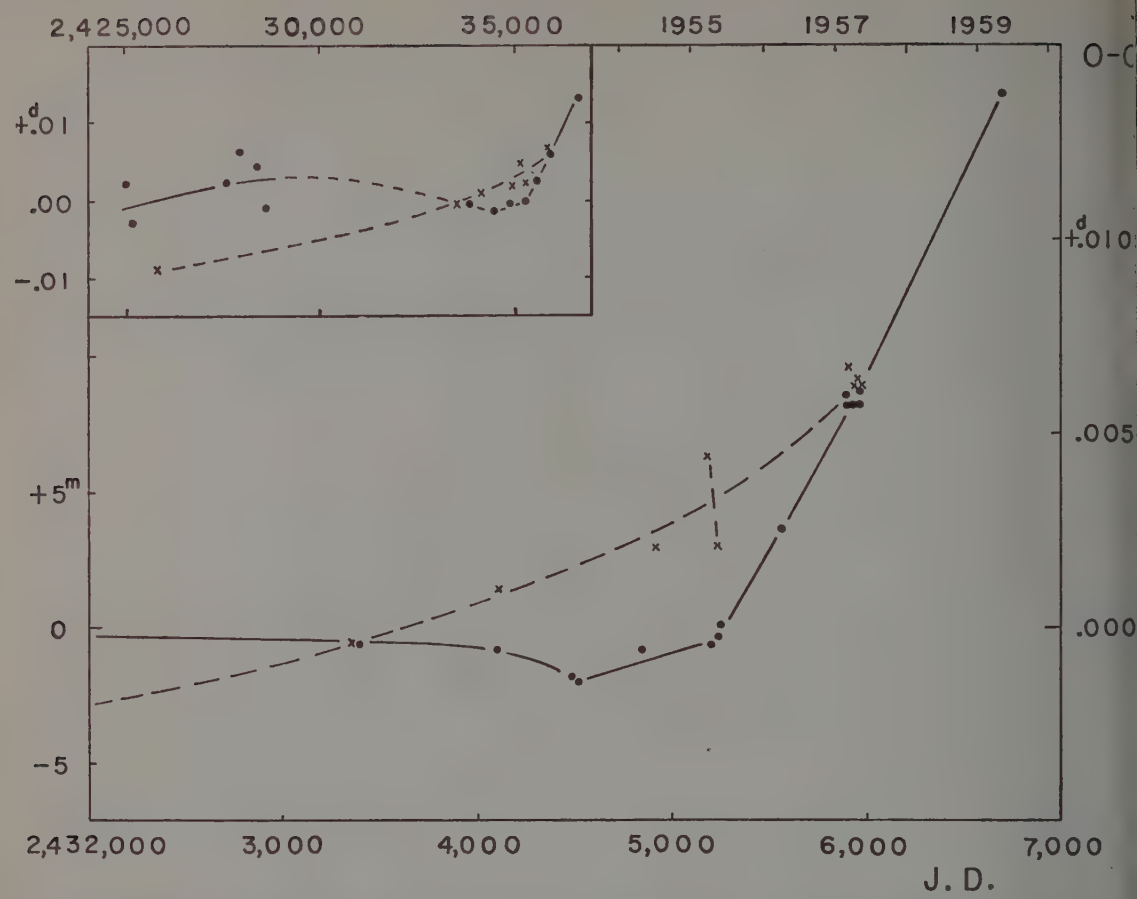

FIG. 2. Period variation of AH Virginis. The dots refer to primary minima, the crosses to secondary minima. In the upper left-hand corner the general variation is given; in the larger figure the more accurate data of recent years are plotted in more detail.

compared with the present observations. The newly determined time of minimum is given in the table and differs by 0.005 day from the value published originally. The linear ephemeris used to compute the *O–C*'s was

JD Hel. Min. I = 2435245.6552 + 0^d.4075184 *E*.

Figure 2 illustrates the changes in the period which have occurred. The dots refer to primary minima, the crosses to secondary minima. It can be seen that there is a greater scatter in the crosses than in the dots and that from 1951 to 1957 the secondary minima came later than expected but by varying amounts.

In 1953 there was a slight decrease in the period. In 1955 the period became 0^d.22 longer than during the two previous years but it has stayed constant since then. The period used in the final reduction of the present observations was

JD Hel. Min. I = 2435245.6552 + 0^d.4075218 *E*.

Tables IIIa and IIIb give the heliocentric Julian Days, the phases counted from primary minimum, and the magnitude differences between the variable star and the comparison star.

5. LIGHT CURVES AND COLOR CURVE

The observations made in the 1955 season showed very clearly that the light curve itself varies with time so that only observations made in a rather small time interval can be combined. Therefore it was necessary to divide the observing nights into two groups and normal points were computed, each of which consisted of about three observations. For convenience one zero point correction was applied to the yellow magnitudes and another to the blue magnitudes in order to make the magnitude differences at maximum approximately equal to zero. Figure 3 shows the variation of the light curves in both wavelengths. In addition to the light curves the color curves are also given. The difference between the blue and yellow magnitudes were computed at exactly the same time or phase, since such a procedure is imperative for such a short period system where the light is continuously changing.

TABLE IIIa. Yellow Observations of AH Virginis.

) Hel. 0000+	Phase	Δm	JD Hel. 2430000+	Phase	Δm	JD Hel. 2430000+	Phase	Δm	JD Hel. 2430000+	Phase	Δm
7.6171	0.1214	+0.076	5207.7831	0.0672	+0.271	5244.6549	0.5454	+0.366	5573.6260	0.7931	−0.072
.6236	0.1373	0.019	5208.5689	0.9954	+0.481	.6606	0.5594	0.298	.6275	0.7969	0.066
.6310	0.1555	0.007	.5740	0.0080	0.512	.6619	0.5625	0.299	.6334	0.8113	0.045
.6391	0.1753	−0.030	.5792	0.0207	0.481	.6666	0.5741	0.275	.6602	0.8771	+0.061
.6463	0.1929	0.085	.5847	0.0343	0.471	.6681	0.5778	0.255	.6616	0.8806	0.066
.6670	0.2438	0.117	.5972	0.0650	0.322	5245.5978	0.8591	+0.018	.6674	0.8948	0.119
.6733	0.2594	0.114	.6014	0.0753	0.271	.6040	0.8744	0.045	.6689	0.8985	0.139
.6789	0.2730	0.114	.6056	0.0855	0.190	.6055	0.8781	0.044	.6748	0.9130	0.186
.6851	0.2884	0.116	.6104	0.0974	0.131	.6139	0.8986	0.110	.6764	0.9170	0.200
.6892	0.2983	0.121	.6153	0.1094	0.097	.6153	0.9020	0.122	.6827	0.9323	0.311
.6963	0.3156	0.089	.6208	0.1230	0.077	.6207	0.9153	0.191	.6843	0.9363	0.338
.7004	0.3258	0.083	.6250	0.1332	0.022	.6222	0.9190	0.212	.6901	0.9505	0.419
.7045	0.3358	0.063	.6299	0.1451	0.018	.6262	0.9290	0.245	.6916	0.9542	0.440
.7088	0.3463	0.046	.6354	0.1588	−0.026	.6278	0.9327	0.271	.6972	0.9681	0.502
.7142	0.3597	0.019	.6396	0.1690	0.052	.6331	0.9457	0.372	.6988	0.9718	0.509
.7191	0.3716	0.007	.6452	0.1826	0.069	.6346	0.9494	0.399	.7044	0.9857	0.511
.7232	0.3818	+0.037	.6493	0.1928	0.073	.6422	0.9681	0.487	.7062	0.9900	0.509
.7289	0.3957	0.061	.6542	0.2048	0.087	.6436	0.9716	0.489	.7123	0.0050	0.497
.7336	0.4074	0.089	.6626	0.2255	0.110	.6481	0.9826	0.474	.7138	0.0087	0.485
.7441	0.4329	0.188	.6667	0.2355	0.122	.6495	0.9860	0.483	.7197	0.0232	0.499
.7507	0.4491	0.256	.6735	0.2522	0.119	.6575	0.0056	0.494	.7212	0.0269	0.511
.7581	0.4673	0.350	.6788	0.2653	0.110	.6590	0.0093	0.484	.7271	0.0414	0.467
.7636	0.4809	0.404	.6833	0.2764	0.111	.6651	0.0244	0.479	.7286	0.0451	0.442
.7678	0.4911	0.416	.6875	0.2866	0.124	.6665	0.0278	0.493	.7340	0.0584	0.345
.7733	0.5048	0.444	.6944	0.3036	0.103	.6707	0.0380	0.445	.7357	0.0624	0.322
.7775	0.5150	0.436	.6987	0.3141	0.089	.6721	0.0414	0.438	.7415	0.0766	0.252
.7831	0.5286	0.443	.7042	0.3275	0.085	.6798	0.0605	0.339	.7429	0.0800	0.215
.7882	0.5411	0.396	.7087	0.3386	0.049	.6812	0.0639	0.311	.7493	0.0959	0.152
.7956	0.5593	0.327	.7133	0.3499	0.039	.6853	0.0738	0.261	.7509	0.0999	0.137
.8017	0.5744	0.269	.7222	0.3718	+0.029	.6868	0.0775	0.226	.7570	0.1146	0.081
.8067	0.5866	0.202	.7264	0.3820	0.022	5246.5693	0.2432	−0.083	.7586	0.1186	0.067
.8136	0.6036	0.156	.7313	0.3939	0.092	.5707	0.2466	0.097	.7669	0.1391	0.024
.8192	0.6172	0.111	.7367	0.4073	0.112	.5762	0.2599	0.088	.7684	0.1427	0.024
.8232	0.6272	0.097	.7410	0.4178	0.173	.5776	0.2634	0.089	.7748	0.1584	−0.019
7.5629	0.5270	+0.444	5243.5903	0.9330	+0.288	.5852	0.2821	0.092	.7763	0.1621	0.015
.5678	0.5389	0.440	.5945	0.9433	0.367	.5867	0.2858	0.084	.7827	0.1777	0.035
.5730	0.5517	0.353	.6000	0.9569	0.444	.5928	0.3008	0.076	.7843	0.1817	0.040
.5799	0.5687	0.291	.6042	0.9671	0.500	.5942	0.3043	0.082	5901.6578	0.7363	−0.098
.5841	0.5789	0.232	.6084	0.9773	0.476	.5985	0.3147	0.078	.6593	0.7400	0.110
.5903	0.5943	0.173	.6146	0.9927	0.478	.5999	0.3182	0.076	.6662	0.7568	0.131
.5945	0.6045	0.167	.6202	0.0063	0.487	.6088	0.3400	0.036	.6676	0.7602	0.105
.6001	0.6182	0.126	.6257	0.0199	0.467	.6103	0.3437	0.032	.6787	0.7874	0.084
.6042	0.6284	0.112	.6296	0.0296	0.486	.6158	0.3571	+0.001	.6801	0.7909	0.095
.6119	0.6471	0.073	.6404	0.0560	0.362	.6173	0.3608	−0.001	.6898	0.8147	0.060
.6163	0.6579	0.045	.6445	0.0660	0.318	.6262	0.3826	+0.045	.6912	0.8181	0.078
.6237	0.6761	−0.001	.6461	0.0699	0.277	.6277	0.3863	0.045	.6981	0.8351	0.061
.6335	0.7002	0.010	.6514	0.0830	0.208	.6318	0.3966	0.087	.6995	0.8386	0.065
.6401	0.7164	0.017	.6529	0.0867	0.193	.6387	0.4133	0.151	.7217	0.8931	+0.050
.6445	0.7272	0.047	.6570	0.0966	0.150	.6402	0.4170	0.153	.7231	0.8965	0.072
.6528	0.7476	0.033	.6584	0.1000	0.127	.6456	0.4304	0.187	.7294	0.9118	0.139
.6577	0.7596	0.048	.6639	0.1137	0.079	.6471	0.4340	0.210	.7307	0.9152	0.172
.6636	0.7740	0.057	.6681	0.1239	0.054	.6526	0.4474	0.285	.7323	0.9189	0.187
.6680	0.7848	0.037	.6695	0.1273	0.049	.6540	0.4508	0.313	.7335	0.9220	0.199
.6737	0.7988	0.017	.6771	0.1460	0.022	.6603	0.4664	0.412	.7432	0.9459	0.329
.6778	0.8090	0.030	.6813	0.1563	−0.006	.6616	0.4695	0.418	.7446	0.9493	0.340
.6820	0.8192	0.019	5244.5902	0.3867	+0.071	.6673	0.4835	0.435	.7460	0.9527	0.356
.6886	0.8354	0.011	.5944	0.3969	0.100	.6688	0.4872	0.412	.7474	0.9561	0.377
.6931	0.8465	+0.034	.5958	0.4003	0.105	.6735	0.4988	0.440	.7537	0.9714	0.450
.6994	0.8618	0.047	.6020	0.4157	0.131	.6749	0.5022	0.435	.7547	0.9740	0.439
.7053	0.8763	0.081	.6034	0.4191	0.157	.6803	0.5156	0.429	.7564	0.9782	0.454
.7115	0.8916	0.093	.6110	0.4378	0.256	.6818	0.5193	0.432	.7620	0.9919	0.464
.7157	0.9019	0.175	.6124	0.4412	0.267	5573.5760	0.6704	−0.029	.7634	0.9953	0.450
.7230	0.9198	0.211	.6180	0.4549	0.344	.5776	0.6744	0.041	.7641	0.9972	0.456
.7278	0.9317	0.276	.6194	0.4583	0.355	.5856	0.6940	0.071	.7655	0.0004	0.439
.7334	0.9453	0.361	.6236	0.4685	0.403	.5870	0.6974	0.068	.7710	0.0141	0.444
.7393	0.9598	0.469	.6249	0.4719	0.398	.5931	0.7125	0.077	.7724	0.0175	0.441
.7438	0.9709	0.481	.6305	0.4855	0.436	.5946	0.7162	0.080	.7739	0.0212	0.445
.7483	0.9820	0.525	.6320	0.4892	0.429	.6005	0.7307	0.083	.7752	0.0243	0.436
.7532	0.9939	0.494	.6374	0.5026	0.462	.6020	0.7344	0.089	.7807	0.0379	0.434
.7622	0.0160	0.496	.6389	0.5063	0.434	.6084	0.7500	0.085	.7821	0.0414	0.410
.7671	0.0280	0.494	.6465	0.5247	0.440	.6099	0.7537	0.081	.7835	0.0448	0.414
.7733	0.0433	0.430	.6480	0.5284	0.436	.6158	0.7681	0.095	.7849	0.0482	0.371
.7779	0.0546	0.367	.6535	0.5420	0.387	.6174	0.7721	0.095	.7914	0.0641	0.290

TABLE IIIa. (Continued)

HD Hel. 2430000+	Phase	Δm	JD Hel. 2430000+	Phase	Δm	JD Hel. 2430000+	Phase	Δm	JD Hel. 2430000+	Phase	Δ
5901.7929	0.0678	+0.264	5907.7691	0.7324	−0.132	5921.7427	0.0218	+0.454	5938.6709	0.5610	+0
.7943	0.0712	0.237	.7746	0.7460	0.130	.7441	0.0257	0.455	.6764	0.5746	0
.7960	0.0754	0.214	.7760	0.7495	0.137	.7455	0.0286	0.448	.6778	0.5780	0
.8023	0.0907	0.136	.7775	0.7531	0.125	.7505	0.0409	0.423	.6793	0.5817	0
.8037	0.0942	0.120	.7788	0.7563	0.129	.7518	0.0440	0.393	.6806	0.5848	0
.8052	0.0979	0.103	.7844	0.7699	0.125	.7532	0.0474	0.358	.6865	0.5993	0
.8067	0.1015	0.092	.7857	0.7739	0.128	.7594	0.0627	0.281	.6878	0.6024	0
.8115	0.1135	0.068	.7871	0.7767	0.107	.7615	0.0678	0.266	.6893	0.6061	0
.8134	0.1180	0.049	.7885	0.7801	0.108	.7643	0.0747	0.222	.6905	0.6092	0
.8150	0.1220	0.028	.7941	0.7938	0.099	.7657	0.0780	0.200	.6967	0.6243	0
.8162	0.1249	0.018	.7955	0.7972	0.097	.7670	0.0814	0.184	.6981	0.6277	0
.8217	0.1385	−0.026	.7970	0.8009	0.087	.7726	0.0951	0.127	.6995	0.6311	0
.8231	0.1419	0.029	.7985	0.8046	0.077	.7740	0.0985	0.094	.7007	0.6342	−0
.8245	0.1453	0.026	.8047	0.8199	0.070	.7754	0.1019	0.089	.7133	0.6652	0
.8321	0.1640	0.047	.8061	0.8233	0.062	.7768	0.1054	0.078	.7147	0.6687	0
.8335	0.1674	0.049	.8078	0.8276	0.050	.7823	0.1189	0.050	.7161	0.6720	0
.8349	0.1708	0.062	.8093	0.8312	0.049	.7837	0.1223	0.050	.7174	0.6751	0
.8363	0.1742	0.066	.8220	0.8622	0.007	.7851	0.1258	0.036	.7236	0.6905	0
5907.6184	0.3626	−0.049	.8232	0.8653	0.019	.7865	0.1292	0.036	.7250	0.6939	0
.6198	0.3660	−0.053	.8246	0.8687	0.005	.7997	0.1615	−0.039	.7264	0.6973	0
.6309	0.3933	+0.014	.8260	0.8721	0.007	.8011	0.1649	0.047	.7278	0.7007	0
.6323	0.3967	0.024	5921.5865	0.6384	−0.002	.8025	0.1684	0.040	.7337	0.7152	0
.6337	0.4001	0.033	.5879	0.6418	−0.002	.8039	0.1718	0.057	.7353	0.7192	0
.6350	0.4035	0.045	.5893	0.6452	+0.002	.8094	0.1854	0.074	.7368	0.7228	0
.6413	0.4189	0.109	.5907	0.6487	+0.005	.8108	0.1888	0.082	.7382	0.7262	0
.6427	0.4223	0.107	.5962	0.6623	−0.044	.8122	0.1922	0.087	.7439	0.7402	0
.6441	0.4257	0.139	.5976	0.6657	0.059	.8136	0.1956	0.095	.7452	0.7433	0
.6455	0.4291	0.141	.5990	0.6691	0.051	.8191	0.2093	0.112	.7465	0.7467	0
.6510	0.4427	0.222	.6067	0.6878	0.097	.8205	0.2127	0.114	.7481	0.7504	0
.6524	0.4461	0.246	.6080	0.6913	0.109	.8219	0.2161	0.113	.7535	0.7637	0
.6538	0.4495	0.262	.6094	0.6946	0.091	.8233	0.2195	0.115	.7552	0.7680	0
.6552	0.4529	0.280	.6108	0.6980	0.088	5938.5578	0.2835	−0.101	.7584	0.7757	0
.6607	0.4665	0.340	.6164	0.7117	0.094	.5591	0.2866	0.095	.7653	0.7927	0
.6621	0.4700	0.331	.6177	0.7151	0.107	.5607	0.2906	0.103	.7667	0.7961	0
.6636	0.4737	0.356	.6191	0.7185	0.108	.5618	0.2934	0.095	.7681	0.7995	0
.6649	0.4768	0.343	.6205	0.7219	0.116	.5744	0.3244	0.062	.7696	0.8032	0
.6704	0.4904	0.380	.6261	0.7355	0.117	.5757	0.3275	0.064	.7820	0.8336	0
.6718	0.4938	0.379	.6275	0.7389	0.121	.5771	0.3309	0.051	.7834	0.8370	0
.6733	0.4975	0.385	.6289	0.7423	0.108	.5785	0.3343	0.058	.7850	0.8410	0
.6747	0.5009	0.382	.6303	0.7458	0.124	.5840	0.3479	0.025	.7861	0.8438	0
.6809	0.5160	0.375	.6358	0.7594	0.110	.5854	0.3513	0.032	.7912	0.8563	+0
.6823	0.5194	0.364	.6372	0.7628	0.113	.5868	0.3548	0.027	.7925	0.8594	0
.6838	0.5231	0.372	.6553	0.8071	0.100	.5882	0.3582	0.023	.7938	0.8626	0
.6850	0.5262	0.366	.6566	0.8105	0.098	.5938	0.3718	0.004	.7952	0.8660	0
.6906	0.5398	0.326	.6580	0.8139	0.096	.5952	0.3752	+0.005	5944.5658	0.0262	+0
.6920	0.5433	0.301	.6594	0.8173	0.084	.5965	0.3786	0.012	.5672	0.0296	0
.6935	0.5469	0.295	.6650	0.8309	0.059	.5979	0.3820	0.025	.5687	0.0333	0
.6948	0.5501	0.268	.6664	0.8344	0.062	.6038	0.3965	0.055	.5699	0.0364	0
.7003	0.5637	0.207	.6677	0.8378	0.051	.6060	0.4019	0.074	.5762	0.0518	0
.7017	0.5671	0.187	.6691	0.8412	0.049	.6077	0.4059	0.087	.5776	0.0552	0
.7032	0.5708	0.175	.6747	0.8548	0.023	.6091	0.4093	0.098	.5791	0.0588	0
.7045	0.5739	0.163	.6761	0.8582	0.016	.6147	0.4232	0.167	.5803	0.0620	0
.7100	0.5876	0.122	.6775	0.8616	0.008	.6160	0.4263	0.167	.5859	0.0756	0
.7114	0.5910	0.098	.6789	0.8650	0.005	.6175	0.4300	0.187	.5873	0.0790	0
.7128	0.5944	0.102	.6914	0.8957	+0.078	.6243	0.4468	0.270	.5888	0.0827	0
.7142	0.5978	0.087	.6927	0.8991	0.089	.6257	0.4502	0.287	.5901	0.0858	0
.7198	0.6114	0.059	.6942	0.9028	0.109	.6272	0.4539	0.303	.6012	0.1130	0
.7212	0.6148	0.036	.6955	0.9060	0.120	.6285	0.4570	0.317	.6026	0.1165	0
.7225	0.6182	0.051	.7011	0.9196	0.208	.6342	0.4709	0.377	.6041	0.1202	0
.7239	0.6216	0.033	.7039	0.9264	0.226	.6361	0.4758	0.385	.6053	0.1233	0
.7295	0.6353	−0.001	.7052	0.9298	0.240	.6375	0.4792	0.395	.6145	0.1458	0
.7309	0.6387	0.011	.7115	0.9451	0.330	.6389	0.4826	0.402	.6158	0.1489	0
.7323	0.6421	0.018	.7129	0.9485	0.344	.6452	0.4979	0.411	.6173	0.1526	−0
.7336	0.6455	0.031	.7143	0.9519	0.374	.6472	0.5030	0.416	.6185	0.1557	0
.7468	0.6779	0.081	.7157	0.9553	0.379	.6486	0.5064	0.414	.6241	0.1693	0
.7482	0.6813	0.091	.7212	0.9690	0.440	.6542	0.5200	0.391	.6270	0.1764	0
.7510	0.6881	0.100	.7226	0.9744	0.437	.6557	0.5238	0.386	.6283	0.1795	0
.7566	0.7017	0.118	.7240	0.9758	0.439	.6570	0.5269	0.390	.6345	0.1949	0
.7581	0.7054	0.110	.7254	0.9792	0.436	.6639	0.5439	0.331	.6359	0.1983	0
.7593	0.7085	0.122	.7309	0.9929	0.442	.6653	0.5473	0.325	.6374	0.2020	0
.7649	0.7222	0.128	.7323	0.9963	0.468	.6668	0.5510	0.296	.6388	0.2054	0
.7663	0.7256	0.128	.7341	0.0005	0.463	.6681	0.5542	0.276	.6442	0.2188	0
.7677	0.7290	0.131	.7414	0.0184	0.460	.6696	0.5578	0.243	.6456	0.2222	0

TABLE IIIa. (Continued)

JD Hel. 2430000+	Phase	Δm	JD Hel. 2430000+	Phase	Δm	JD Hel. 2430000+	Phase	Δm	JD Hel. 2430000+	Phase	Δm
944.6472	0.2261	−0.082	5958.7026	0.7160	−0.133	5959.7122	0.1933	−0.089	5961.6183	0.8707	+0.002
.6484	0.2290	0.092	.7039	0.7192	0.140	.7145	0.1990	0.090	.6198	0.8744	0.000
.6541	0.2429	0.093	.7053	0.7226	0.127	.7159	0.2024	0.090	.6211	0.8775	0.005
.6554	0.2460	0.089	.7111	0.7368	0.120	.7219	0.2172	0.072	.6287	0.8962	0.061
.6568	0.2497	0.075	.7125	0.7402	0.128	.7233	0.2206	0.065	.6301	0.8996	0.073
.6581	0.2528	0.085	.7140	0.7439	0.118	.7249	0.2246	0.080	.6316	0.9033	0.093
.6652	0.2701	0.088	.7152	0.7470	0.124	.7263	0.2280	0.090	.6331	0.9070	0.117
.6665	0.2733	0.075	.7206	0.7601	0.112	.7316	0.2410	0.082	.6384	0.9201	0.177
.6680	0.2770	0.082	.7229	0.7657	0.123	.7346	0.2484	0.090	.6398	0.9235	0.180
.6692	0.2801	0.080	.7244	0.7694	0.125	.7359	0.2515	0.087	.6412	0.9269	0.207
.6817	0.3108	0.066	.7257	0.7726	0.122	.7373	0.2550	0.093	.6426	0.9303	0.230
.6832	0.3145	0.046	.7272	0.7763	0.115	.7438	0.2709	0.102	.6484	0.9445	0.333
.6846	0.3179	0.062	.7284	0.7794	0.107	.7450	0.2740	0.114	.6498	0.9479	0.352
.6860	0.3213	0.056	.7358	0.7976	0.072	.7474	0.2797	0.108	.6512	0.9513	0.390
.6923	0.3366	0.042	.7372	0.8010	0.072	.7487	0.2831	0.110	.6527	0.9550	0.405
.6935	0.3397	0.048	.7389	0.8049	0.063	.7596	0.3098	0.096	.6579	0.9678	0.431
.6949	0.3431	0.040	.7402	0.8083	0.059	.7610	0.3132	0.090	.6593	0.9712	0.430
.6963	0.3466	0.034	.7458	0.8220	0.063	.7624	0.3166	0.094	.6608	0.9749	0.435
.7020	0.3605	0.003	.7472	0.8254	0.054	.7638	0.3200	0.080	.6662	0.9882	0.423
.7034	0.3639	+0.001	.7486	0.8288	0.060	5960.6447	0.4817	+0.372	.6676	0.9916	0.431
.7048	0.3673	0.003	.7500	0.8322	0.055	.6461	0.4851	0.370	.6691	0.9953	0.426
.7060	0.3704	0.002	.7559	0.8467	0.035	.6475	0.4885	0.375	.6704	0.9985	0.418
.7117	0.3843	0.035	.7574	0.8504	0.018	.6488	0.4917	0.390	.6718	0.0019	0.423
.7130	0.3874	0.060	.7589	0.8541	0.020	.6598	0.5186	0.384	.6732	0.0053	0.426
.7156	0.3940	0.087	.7603	0.8575	+0.004	.6612	0.5220	0.370	.6747	0.0090	0.433
.7173	0.3980	0.081	5959.5761	0.8593	−0.008	.6626	0.5254	0.370	.6759	0.0121	0.430
.7284	0.4252	0.141	.5775	0.8627	0.012	.6641	0.5291	0.361	.6815	0.0257	0.443
.7297	0.4284	0.157	.5788	0.8661	0.006	.6697	0.5431	0.333	.6829	0.0292	0.437
.7312	0.4321	0.182	.5802	0.8695	+0.005	.6711	0.5464	0.315	.6843	0.0325	0.452
.7324	0.4352	0.209	.5913	0.8968	0.086	.6726	0.5502	0.314	.6856	0.0359	0.437
.7383	0.4497	0.298	.5927	0.9002	0.097	.6740	0.5536	0.285	.6870	0.0394	0.400
.7395	0.4525	0.315	.5942	0.9039	0.104	.6810	0.5706	0.183	.6884	0.0428	0.399
.7417	0.4579	0.341	.5955	0.9070	0.124	.6822	0.5737	0.160	.6940	0.0564	0.313
.7433	0.4619	0.378	.6011	0.9207	0.192	.6836	0.5771	0.137	.6954	0.0598	0.293
.7445	0.4647	0.381	.6025	0.9241	0.215	.6892	0.5908	0.120	.6969	0.0635	0.273
958.5727	0.3971	+0.054	.6041	0.9280	0.284	.6906	0.5942	0.100	.6982	0.0666	0.245
.5749	0.4025	0.061	.6055	0.9315	0.281	.6920	0.5976	0.083	.7052	0.0839	0.166
.5914	0.4431	0.241	.6108	0.9445	0.344	.6934	0.6010	0.083	.7065	0.0871	0.155
.5928	0.4465	0.264	.6137	0.9516	0.406	.7003	0.6180	0.000	.7080	0.0907	0.160
.5944	0.4505	0.271	.6152	0.9553	0.428	.7017	0.6214	−0.007	.7093	0.0939	0.137
.6011	0.4670	0.370	.6212	0.9701	0.424	.7045	0.6283	0.002	.7190	0.1178	0.060
.6025	0.4704	0.376	.6226	0.9735	0.432	.7093	0.6402	0.040	.7204	0.1212	0.056
.6039	0.4738	0.377	.6240	0.9769	0.452	.7107	0.6435	0.049	.7218	0.1246	0.035
.6053	0.4772	0.376	.6254	0.9803	0.467	.7122	0.6458	0.040	.7232	0.1280	0.035
.6113	0.4919	0.400	.6318	0.9962	0.460	.7136	0.6507	0.054	.7287	0.1416	−0.007
.6128	0.4956	0.399	.6332	0.9996	0.462	.7190	0.6640	0.074	.7302	0.1453	0.009
.6143	0.4993	0.406	.6347	0.0033	0.461	.7204	0.6674	0.078	.7315	0.1484	0.012
.6201	0.5135	0.398	.6367	0.0081	0.442	.7218	0.6708	0.097	.7329	0.1518	0.022
.6215	0.5169	0.386	.6420	0.0212	0.449	.7233	0.6745	0.090	.7384	0.1655	0.045
.6231	0.5209	0.391	.6434	0.0246	0.462	.7288	0.6879	0.119	.7412	0.1723	0.062
.6282	0.5334	0.363	.6450	0.0286	0.447	.7302	0.6913	0.119	.7426	0.1757	0.066
.6296	0.5368	0.353	.6465	0.0323	0.441	.7317	0.6950	0.116	.7481	0.1893	0.073
.6318	0.5422	0.305	.6519	0.0454	0.374	.7329	0.6981	0.115	.7503	0.1947	0.068
.6332	0.5456	0.290	.6531	0.0485	0.338	.7385	0.7118	0.127	.7516	0.1978	0.073
.6345	0.5488	0.275	.6548	0.0525	0.322	.7399	0.7152	0.127	.7531	0.2015	0.071
.6458	0.5766	0.163	.6562	0.0559	0.297	.7427	0.7220	0.117	5962.5675	0.1999	−0.085
.6472	0.5800	0.155	.6617	0.0695	0.229	.7489	0.7373	0.130	.5689	0.2034	0.095
.6487	0.5837	0.141	.6633	0.0735	0.221	.7503	0.7407	0.130	.5704	0.2071	0.098
.6500	0.5868	0.115	.6651	0.0777	0.211	.7519	0.7447	0.120	.5718	0.2104	0.083
.6557	0.6010	0.062	.6666	0.0814	0.184	.7531	0.7475	0.129	.5828	0.2374	0.118
.6571	0.6044	0.045	.6719	0.0945	0.136	5961.5794	0.7752	−0.104	.5842	0.2408	0.113
.6586	0.6081	0.039	.6733	0.0979	0.110	.5808	0.7786	0.122	.5858	0.2448	0.116
.6599	0.6112	0.014	.6749	0.1019	0.118	.5824	0.7826	0.113	.5873	0.2485	0.136
.6651	0.6240	−0.006	.6764	0.1056	0.089	.5838	0.7860	0.113	.5925	0.2613	0.136
.6665	0.6274	0.015	.6824	0.1203	0.026	.5968	0.8178	0.102	.5939	0.2647	0.132
.6679	0.6308	0.013	.6837	0.1235	0.030	.5982	0.8212	0.100	.5953	0.2681	0.130
.6693	0.6342	0.023	.6853	0.1274	0.026	.5995	0.8246	0.095	.5969	0.2721	0.130
.6747	0.6476	0.023	.6915	0.1425	−0.003	.6008	0.8278	0.089	.6023	0.2852	0.118
.6760	0.6507	0.035	.6927	0.1456	0.010	.6065	0.8417	0.052	.6035	0.2883	0.112
.6774	0.6541	0.041	.6946	0.1502	0.007	.6079	0.8451	0.047	.6053	0.2925	0.103
.6788	0.6575	0.042	.6960	0.1536	0.002	.6094	0.8488	0.042	.6068	0.2962	0.101
.6999	0.7092	0.125	.6975	0.1573	0.014	.6108	0.8522	0.032	.6137	0.3133	0.088
.7012	0.7126	0.138	.7109	0.1902	0.076	.6169	0.8672	+0.002	.6156	0.3178	0.067

TABLE IIIa. (Continued)

JD Hel. 2430000+	Phase	Δm	JD Hel. 2430000+	Phase	Δm	JD Hel. 2430000+	Phase	Δm	JD Hel. 2430000+	Phase	Δm
5962.6171	0.3215	−0.057	5966.5936	0.0795	+0.188	6673.6883	0.1882	−0.050	6693.6565	0.1873	−0.0
.6185	0.3249	0.077	.5992	0.0931	0.122	.6937	0.2015	0.056	.6579	0.1907	0.0
.6240	0.3386	0.048	.6006	0.0965	0.116	.6951	0.2049	0.071	.6641	0.2061	0.0
.6254	0.3419	0.051	.6021	0.1002	0.103	.6965	0.2084	0.072	.6655	0.2095	0.0
.6270	0.3459	0.056	.6034	0.1033	0.099	.6979	0.2118	0.078	.6669	0.2129	0.0
.6284	0.3493	0.060	.6082	0.1152	0.049	.7041	0.2271	0.090	.6683	0.2163	0.1
.6400	0.3777	0.017	.6096	0.1186	0.020	.7055	0.2305	0.082	.6739	0.2299	0.1
.6413	0.3809	0.009	.6110	0.1221	0.010	.7069	0.2339	0.098	.6755	0.2339	0.1
.6431	0.3854	+0.020	.6180	0.1391	−0.032	.7083	0.2373	0.090	.6771	0.2379	0.1
.6446	0.3891	0.053	.6193	0.1425	0.041	.7145	0.2526	0.120	.6829	0.2521	0.1
.6502	0.4027	0.088	.6208	0.1462	0.052	.7159	0.2561	0.119	.6843	0.2555	0.0
.6517	0.4064	0.084	.6221	0.1493	0.056	.7173	0.2595	0.123	.6857	0.2589	0.1
.6529	0.4095	0.099	.6279	0.1635	0.076	.7187	0.2629	0.117	.6871	0.2623	0.0
.6546	0.4135	0.103	.6307	0.1703	0.069	.7245	0.2771	0.116	.6989	0.2913	0.1
.6636	0.4357	0.188	.6322	0.1740	0.072	.7259	0.2805	0.120	.7002	0.2947	0.1
.6649	0.4388	0.204	.6375	0.1871	0.085	.7274	0.2842	0.111	.7016	0.2981	0.1
.6665	0.4428	0.229	.6388	0.1902	0.078	.7290	0.2882	0.109	.7030	0.3015	0.0
.6680	0.4465	0.252	.6402	0.1936	0.086	.7347	0.3021	0.102	.7086	0.3151	0.0
.6738	0.4607	0.346	.6416	0.1970	0.087	.7361	0.3055	0.100	.7100	0.3185	0.0
.6753	0.4644	0.335	.6471	0.2107	0.108	.7375	0.3089	0.098	.7114	0.3219	0.0
.6768	0.4680	0.355	.6485	0.2141	0.114	.7389	0.3123	0.087	.7128	0.3254	0.0
.6783	0.4718	0.342	.6499	0.2175	0.119	.7507	0.3412	0.075	.7183	0.3390	0.0
.6799	0.4757	0.354	.6513	0.2209	0.124	.7521	0.3447	0.061	.7197	0.3424	0.0
.6858	0.4902	0.399	.6568	0.2345	0.125	.7536	0.3484	0.063	.7211	0.3458	0.0
.6872	0.4936	0.400	.6582	0.2379	0.136	.7548	0.3515	0.053	.7225	0.3492	0.0
.6886	0.4970	0.424	.6597	0.2416	0.130	6693.5669	0.9675	+0.488	6697.5986	0.8606	+0.0
.6901	0.5007	0.396	.6610	0.2447	0.123	.5683	0.9709	0.477	.6000	0.8641	0.0
.6916	0.5044	0.401	6673.6014	0.9749	+0.480	.5697	0.9744	0.494	.6062	0.8794	0.0
.6975	0.5189	0.385	.6027	0.9783	0.475	.5711	0.9777	0.485	.6078	0.8834	0.0
.6989	0.5223	0.375	.6041	0.9817	0.478	.5766	0.9914	0.525	.6103	0.8893	0.0
.7002	0.5254	0.362	.6055	0.9851	0.479	.5780	0.9948	0.511	.6118	0.8930	0.0
.7018	0.5294	0.353	.6118	0.0005	0.478	.5794	0.9982	0.509	.6173	0.9067	0.1
.7079	0.5445	0.295	.6132	0.0038	0.482	.5808	0.0016	0.514	.6194	0.9117	0.1
.7092	0.5476	0.284	.6145	0.0073	0.484	.5864	0.0152	0.530	.6208	0.9152	0.1
.7107	0.5513	0.278	.6159	0.0107	0.484	.5877	0.0186	0.516	.6229	0.9203	0.1
.7121	0.5547	0.251	.6215	0.0243	0.493	.5891	0.0220	0.510	.6291	0.9356	0.2
.7175	0.5680	0.184	.6229	0.0277	0.486	.5905	0.0254	0.509	.6305	0.9390	0.3
.7190	0.5717	0.156	.6243	0.0311	0.482	.5961	0.0391	0.513	.6319	0.9425	0.3
.7210	0.5766	0.149	.6257	0.0345	0.491	.5975	0.0425	0.497	.6333	0.9458	0.3
.7226	0.5805	0.127	.6319	0.0499	0.440	.5988	0.0459	0.470	.6404	0.9632	0.4
.7286	0.5953	0.076	.6333	0.0533	0.423	.6002	0.0493	0.451	.6419	0.9669	0.4
.7300	0.5987	0.068	.6347	0.0567	0.411	.6072	0.0664	0.348	.6433	0.9703	0.5
.7316	0.6027	0.065	.6368	0.0618	0.356	.6086	0.0698	0.320	.6442	0.9725	0.5
.7329	0.6058	0.048	.6382	0.0652	0.334	.6099	0.0729	0.305	.6460	0.9771	0.5
.7385	0.6194	−0.002	.6438	0.0791	0.265	.6114	0.0766	0.275	.6541	0.9970	0.5
.7398	0.6226	−0.002	.6455	0.0831	0.211	.6169	0.0902	0.203	.6558	0.0010	0.5
.7411	0.6260	+0.001	.6475	0.0882	0.187	.6183	0.0936	0.194	.6666	0.0277	0.5
.7425	0.6294	+0.008	.6493	0.0925	0.187	.6197	0.0970	0.178	.6683	0.0316	0.5
.7481	0.6430	−0.028	.6569	0.1112	0.118	.6210	0.1001	0.184	.6696	0.0350	0.4
.7496	0.6467	0.033	.6590	0.1163	0.082	.6287	0.1192	0.095	.6717	0.0401	0.4
.7510	0.6501	0.035	.6604	0.1197	0.087	.6301	0.1226	0.073	.6733	0.0441	0.4
.7522	0.6532	0.035	.6618	0.1232	0.077	.6315	0.1260	0.080	.6752	0.0487	0.4
5966.5798	0.0454	+0.389	.6680	0.1385	0.032	.6371	0.1396	0.052	.6773	0.0538	0.3
.5811	0.0488	0.386	.6694	0.1419	0.032	.6387	0.1436	0.039	.6787	0.0572	0.3
.5826	0.0525	0.344	.6708	0.1453	0.018	.6401	0.1470	0.035	.6854	0.0737	0.2
.5839	0.0556	0.309	.6722	0.1487	0.025	.6414	0.1504	0.018	.6868	0.0771	0.2
.5895	0.0692	0.250	.6840	0.1777	−0.035	.6537	0.1805	−0.011	.6882	0.0805	0.2
.5909	0.0726	0.215	.6854	0.1811	0.036	.6551	0.1839	0.043	.6895	0.0839	0.2
.5924	0.0763	0.204	.6868	0.1845	0.047						

TABLE IIIb. Blue Observations of AH Virginis.

JD Hel. 2430000+	Phase	Δm	JD Hel. 2430000+	Phase	Δm	JD Hel. 2430000+	Phase	Δm	JD Hel. 2430000+	Phase	Δm
5197.6184	0.1245	−0.236	5197.6753	0.2642	−0.429	5197.6968	0.3171	−0.391	5197.7157	0.3633	−0.330
.6247	0.1401	0.271	.6796	0.2747	0.431	.7011	0.3276	0.388	.7199	0.3736	0.327
.6324	0.1589	0.284	.6858	0.2901	0.434	.7053	0.3378	0.359	.7242	0.3841	0.282
.6677	0.2455	0.440	.6900	0.3003	0.424	.7093	0.3477	0.348	.7295	0.3972	0.228

TABLE IIIb. (Continued)

JD Hel. 2430000+	Phase	Δm	JD Hel. 2430000+	Phase	Δm	JD Hel. 2430000+	Phase	Δm	JD Hel. 2430000+	Phase	Δm
197.7345	0.4094	−0.186	5208.6632	0.2269	−0.407	5245.6488	0.9843	+0.242	5573.7204	0.0249	+0.247
.7449	0.4349	0.087	.6674	0.2372	0.438	.6502	0.9877	0.215	.7218	0.0283	0.242
.7533	0.4556	+0.004	.6743	0.2542	0.417	.6583	0.0076	0.240	.7278	0.0431	0.202
.7588	0.4690	0.091	.6795	0.2670	0.417	.6596	0.0108	0.226	.7292	0 0465	0.205
.7642	0.4824	0.145	.6840	0.2781	0.435	.6660	0.0264	0.241	.7347	0.0601	0.111
.7685	0.4929	0.166	.6882	0.2883	0.442	.6672	0.0295	0.248	.7364	0.0641	0.071
.7740	0.5065	0.175	.6953	0.3056	0.434	.6715	0.0400	0.198	.7421	0.0783	−0.048
.7781	0.5164	0.165	.6993	0.3156	0.418	.6728	0.0431	0.177	.7436	0.0820	0.076
.7838	0.5304	0.173	.7049	0.3292	0.390	.6805	0.0623	0.051	.7500	0.0976	0.133
.7892	0.5437	0.131	.7094	0.3403	0.357	.6818	0.0653	0.030	.7516	0.1016	0.133
.7965	0.5616	0.033	.7142	0.3522	0.367	.6861	0.0758	−0.035	.7577	0.1163	0.230
.8027	0.5769	−0.021	.7229	0.3735	0.278	.6874	0.0789	−0.039	.7593	0.1203	0.232
.8075	0.5886	0.098	.7271	0.3837	0.274	5246.5700	0.2449	−0.364	.7676	0.1408	0.273
.8143	0.6053	0.156	.7320	0.3956	0.180	.5714	0.2483	0.374	.7690	0.1442	0.273
.8199	0.6190	0.168	.7375	0.4093	0.139	.5770	0.2619	0.391	.7755	0.1601	0.321
.8240	0.6292	0.181	.7420	0.4203	0.103	.5784	0.2653	0.378	.7769	0.1635	0.315
207.5636	0.5287	+0.183	5243.5910	0.9347	+0.052	.5859	0.2838	0.387	.7833	0.1794	0.333
.5687	0.5412	0.162	.5952	0.9450	0.095	.5874	0.2875	0.389	.7850	0.1834	0.348
.5741	0.5545	0.100	.6007	0.9586	0.183	.5935	0.3026	0.376	5901.6585	0.7380	−0.403
.5807	0.5707	0.037	.6050	0.9691	0.224	.5950	0.3062	0.366	.6599	0.7414	0.380
.5849	0.5809	0.010	.6090	0.9790	0.228	.5992	0.3165	0.357	.6669	0.7585	0.427
.5910	0.5960	−0.109	.6163	0.9969	0.209	.6006	0.3199	0.377	.6683	0.7619	0.407
.5952	0.6062	0.122	.6208	0.0080	0.226	.6096	0.3420	0.321	.6794	0.7891	0.411
.6007	0.6198	0.159	.6264	0.0216	0.220	.6110	0.3454	0.317	.6807	0.7926	0.413
.6049	0.6301	0.187	.6306	0.0319	0.208	.6166	0.3591	0.280	.6906	0.8167	0.370
.6124	0.6485	0.244	.6353	0.0435	0.177	.6180	0.3625	0.298	.6919	0.8198	0.369
.6173	0.6605	0.255	.6411	0.0577	0.084	.6270	0.3846	0.251	.6988	0.8369	0.335
.6245	0.6780	0.281	.6469	0.0719	−0.009	.6284	0.3878	0.245	.7002	0.8403	0.341
.6344	0.7025	0.294	.6520	0.0844	0.084	.6324	0.3980	0.182	.7224	0.8948	0.229
.6407	0.7178	0.321	.6536	0.0884	0.089	.6338	0.4014	0.170	.7301	0.9136	0.122
.6452	0.7289	0.322	.6575	0.0980	0.150	.6394	0.4150	0.132	.7315	0.9170	0.079
.6535	0.7494	0.330	.6591	0.1017	0.159	.6408	0.4184	0.129	.7328	0.9203	0.090
.6584	0.7613	0.324	.6646	0.1154	0.203	.6464	0.4323	0.076	.7342	0.9237	0.066
.6643	0.7758	0.336	.6688	0.1256	0.237	.6477	0.4355	0.049	.7439	0.9476	+0.059
.6688	0.7868	0.341	.6702	0.1290	0.259	.6534	0.4494	+0.039	.7454	0.9513	0.068
.6744	0.8005	0.328	.6778	0.1477	0.283	.6546	0.4525	0.052	.7468	0.9547	0.086
.6786	0.8110	0.340	.6820	0.1581	0.302	.6610	0.4681	0.155	.7481	0.9578	0.104
.6828	0.8212	0.327	5244.5909	0.3884	−0.223	.6628	0.4726	0.156	.7544	0.9732	0.177
.6893	0.8371	0.285	.5951	0.3986	0.202	.6680	0.4852	0.166	·7557	0·9766	0·182
.6938	0.8482	0.275	.5965	0.4020	0.187	.6693	0.4886	0.176	.7571	0.9800	0.190
.7004	0.8644	0.264	.6027	0.4174	0.132	.6741	0.5002	0.187	.7628	0.9939	0.206
.7122	0.8934	0.184	.6041	0.4208	0.122	.6756	0.5039	0.189	.7648	0.9987	0.215
.7171	0.9053	0.128	.6117	0.4395	0.024	5573.5768	0.6724	−0.333	.7662	0.0021	0.206
.7240	0.9223	0.077	.6131	0.4429	0.010	.5784	0.6764	0.335	.7717	0.0158	0.190
.7296	0.9359	+0.015	.6187	0.4565	+0.071	.5862	0.6957	0.359	.7732	0.0195	0.190
.7341	0.9470	0.104	.6201	0.4600	0.071	.5875	0.6989	0.358	.7746	0.0229	0.201
.7401	0.9618	0.212	.6242	0.4702	0.116	.5938	0.7142	0.379	.7759	0.0260	0.181
.7446	0.9729	0.235	.6256	0.4736	0.149	.5952	0.7176	0.381	.7816	0.0399	0.160
.7490	0.9837	0.262	.6312	0.4872	0.179	.6012	0.7324	0.376	.7828	0.0431	0.132
.7542	0.9964	0.239	.6327	0.4910	0.173	.6028	0.7363	0.377	.7842	0.0465	0.136
.7631	0.0183	0.242	.6382	0.5045	0.182	.6090	0.7517	0.380	.7856	0.0499	0.092
.7681	0.0305	0.239	.6394	0.5074	0.183	.6104	0.7551	0.368	.7922	0.0661	0.004
.7741	0.0453	0.176	.6473	0.5267	0.186	.6165	0.7698	0.394	.7936	0.0695	−0.020
.7789	0.0569	0.099	.6487	0.5301	0.192	.6181	0.7738	0.395	.7953	0.0737	0.058
.7837	0.0688	0.000	.6542	0.5438	0.130	.6267	0.7948	0.366	.7967	0.0771	0.073
5208.5696	0.9971	+0.230	.6555	0.5469	0.104	.6280	0.7983	0.356	.8030	0.0925	0.158
.5749	0.0102	0.235	.6612	0.5608	0.039	.6341	0.8131	0.327	.8044	0.0958	0.175
.5800	0.0227	0.226	.6624	0.5639	0.010	.6607	0.8783	0.232	.8057	0.0993	0.192
.5854	0.0361	0.211	.6674	0.5761	−0.023	.6623	0.8823	0.225	.8125	0.1158	0.257
.5916	0.0511	0.108	.6688	0.5795	0.024	.6681	0.8965	0.149	.8141	0.1197	0.257
.5979	0.0668	0.033	5245.5986	0.8611	−0.269	.6695	0.8992	0.149	.8156	0.1234	0.261
.6021	0.0770	−0.024	.6048	0.8764	0.242	.6755	0.9147	0.093	.8169	0.1266	0.270
.6063	0.0872	0.085	.6062	0.8798	0.222	.6770	0.9184	0.043	.8224	0.1402	0.316
.6115	0.1000	0.134	.6146	0.9003	0.169	.6833	0.9340	+0.051	.8238	0.1436	0.313
.6160	0.1111	0.214	.6160	0.9037	0.145	.6850	0.9380	0.079	.8252	0.1470	0.322
.6214	0.1244	0.246	.6215	0.9173	0.091	.6908	0.9522	0.172	.8328	0.1657	0.359
.6257	0.1349	0.280	.6229	0.9207	0.094	.6921	0.9556	0.191	.8342	0.1691	0.371
.6306	0.1469	0.296	.6269	0.9307	0.035	.6979	0.9698	0.240	.8356	0.1725	0.375
.6361	0.1605	0.324	.6283	0.9341	+0.002	.6993	0.9732	0.247	.8370	0.1759	0.390
.6404	0.1710	0.339	.6339	0.9477	0.123	.7051	0.9874	0.250	5907.6191	0.3643	−0.354
.6458	0.1843	0.370	.6353	0.9511	0.163	.7070	0.9919	0.273	.6205	0.3677	0.339
.6500	0.1946	0.399	.6429	0.9699	0.246	.7130	0.0067	0.250	.6316	0.3950	0.256
.6549	0.2065	0.395	.6444	0.9736	0.220	.7144	0.0101	0.244	.6330	0.3984	0.256

TABLE IIIb. (Continued)

JD Hel. 2430000+	Phase	Δm	JD Hel. 2430000+	Phase	Δm	JD Hel. 2430000+	Phase	Δm	JD Hel. 2430000+	Phase	Δm
5907.6343	0.4018	−0.242	5921.5886	0.6435	−0.297	5921.8045	0.1735	−0.370	5938.7459	0.7450	−0.407
.6357	0.4052	0.243	.5900	0.6469	0.293	.8101	0.1871	0.395	.7474	0.7487	0.407
.6420	0.4206	0.197	.5915	0.6506	0.292	.8115	0.1905	0.395	.7486	0.7518	0.411
.6434	0.4240	0.175	.5969	0.6640	0.342	.8129	0.1939	0.396	.7543	0.7657	0.417
.6448	0.4274	0.160	.5983	0.6674	0.355	.8143	0.1973	0.400	.7577	0.7739	0.425
.6461	0.4308	0.145	.5997	0.6708	0.372	.8198	0.2110	0.421	.7590	0.7774	0.419
.6517	0.4444	0.043	.6073	0.6895	0.385	.8212	0.2144	0.425	.7660	0.7944	0.385
.6531	0.4478	0.028	.6087	0.6930	0.390	.8226	0.2178	0.424	.7674	0.7978	0.382
.6545	0.4512	0.004	.6101	0.6964	0.365	.8240	0.2212	0.425	.7688	0.8012	0.380
.6559	0.4546	0.008	.6115	0.6997	0.381	5938.5584	0.2849	−0.393	.7704	0.8052	0.369
.6614	0.4683	+0.060	.6170	0.7134	0.380	.5597	0.2883	0.401	.7827	0.8353	0.385
.6628	0.4717	0.059	.6184	0.7168	0.393	.5613	0.2921	0.384	.7841	0.8387	0.366
.6642	0.4751	0.071	.6198	0.7202	0.400	.5625	0.2951	0.395	.7854	0.8421	0.353
.6656	0.4785	0.074	.6212	0.7236	0.413	.5750	0.3258	0.360	.7919	0.8580	0.295
.6711	0.4921	0.120	.6268	0.7372	0.397	.5764	0.3292	0.355	.7931	0.8609	0.276
.6725	0.4955	0.120	.6282	0.7406	0.403	.5778	0.3326	0.345	.7945	0.8643	0.275
.6739	0.4989	0.123	.6295	0.7441	0.399	.5792	0.3360	0.349	.7959	0.8677	0.278
.6753	0.5023	0.114	.6309	0.7474	0.407	.5847	0.3497	0.330	5944.5665	0.0279	+0.203
.6816	0.5177	0.096	.6365	0.7611	0.396	.5861	0.3530	0.325	.5678	0.0313	0.192
.6830	0.5211	0.084	.6379	0.7645	0.387	.5875	0.3564	0.313	.5692	0.0347	0.186
.6843	0.5245	0.100	.6504	0.7952	0.395	.5889	0.3599	0.304	.5706	0.0381	0.157
.6857	0.5279	0.096	.6559	0.8088	0.396	.5945	0.3735	0.278	.5769	0.0535	0.117
.6913	0.5416	0.031	.6573	0.8122	0.403	.5957	0.3766	0.277	.5783	0.0569	0.094
.6927	0.5450	0.008	.6587	0.8156	0.387	.5972	0.3803	0.268	.5796	0.0603	0.070
.6941	0.5484	0.003	.6601	0.8190	0.383	.5986	0.3837	0.260	.5810	0.0637	0.027
.6955	0.5518	−0.001	.6657	0.8326	0.365	.6054	0.4002	0.208	.5867	0.0776	−0.062
.7010	0.5654	0.088	.6670	0.8361	0.352	.6067	0.4036	0.195	.5880	0.0807	0.072
.7024	0.5688	0.105	.6684	0.8395	0.351	.6085	0.4079	0.186	.5894	0.0841	0.111
.7038	0.5722	0.114	.6698	0.8429	0.338	.6097	0.4110	0.169	.5908	0.0875	0.119
.7052	0.5756	0.147	.6754	0.8565	0.307	.6153	0.4246	0.121	.6019	0.1148	0.192
.7107	0.5893	0.179	.6768	0.8599	0.307	.6167	0.4280	0.111	.6033	0.1182	0.218
.7122	0.5930	0.173	.6782	0.8634	0.290	.6181	0.4314	0.079	.6048	0.1219	0.252
.7135	0.5961	0.192	.6795	0.8667	0.297	.6250	0.4485	0.006	.6060	0.1250	0.265
.7149	0.5995	0.223	.6920	0.8974	0.216	.6263	0.4516	+0.009	.6151	0.1472	0.297
.7205	0.6131	0.244	.6934	0.9008	0.200	.6278	0.4553	0.025	.6165	0.1506	0.307
.7218	0.6165	0.253	.6948	0.9043	0.181	.6292	0.4587	0.051	.6178	0.1540	0.313
.7232	0.6199	0.253	.6962	0.9077	0.160	.6347	0.4723	0.129	.6192	0.1574	0.308
.7246	0.6234	0.269	.7018	0.9213	0.106	.6368	0.4775	0.141	.6248	0.1710	0.329
.7302	0.6370	0.305	.7032	0.9247	0.076	.6383	0.4812	0.147	.6263	0.1747	0.329
.7316	0.6404	0.332	.7045	0.9281	0.053	.6459	0.4996	0.141	.6277	0.1781	0.350
.7330	0.6438	0.325	.7059	0.9315	0.049	.6479	0.5047	0.148	.6290	0.1813	0.343
.7475	0.6796	0.369	.7122	0.9468	+0.064	.6563	0.5252	0.127	.6352	0.1966	0.362
.7489	0.6830	0.388	.7136	0.9502	0.077	.6584	0.5303	0.121	.6366	0.2000	0.353
.7503	0.6864	0.379	.7150	0.9536	0.117	.6646	0.5456	0.041	.6380	0.2034	0.362
.7517	0.6898	0.391	.7164	0.9570	0.122	.6660	0.5490	0.008	.6394	0.2068	0.354
.7573	0.7034	0.413	.7219	0.9707	0.167	.6675	0.5528	−0.002	.6449	0.2205	0.372
.7588	0.7071	0.404	.7233	0.9741	0.177	.6688	0.5558	0.018	.6463	0.2239	0.373
.7600	0.7102	0.419	.7247	0.9775	0.182	.6702	0.5693	0.044	.6478	0.2275	0.380
.7656	0.7239	0.421	.7261	0.9809	0.186	.6771	0.5763	0.118	.6491	0.2307	0.386
.7670	0.7273	0.425	.7316	0.9946	0.167	.6785	0.5797	0.137	.6546	0.2443	0.382
.7684	0.7307	0.437	.7330	0.9980	0.195	.6799	0.5831	0.165	.6560	0.2477	0.392
.7698	0.7341	0.437	.7420	0.0201	0.189	.6813	0.5865	0.165	.6574	0.2511	0.376
.7753	0.7477	0.437	.7434	0.0235	0.185	.6871	0.6007	0.202	.6588	0.2545	0.397
.7767	0.7512	0.437	.7448	0.0269	0.185	.6884	0.6041	0.224	.6658	0.2716	0.401
.7781	0.7546	0.422	.7511	0.0423	0.139	.6900	0.6078	0.254	.6671	0.2750	0.392
.7795	0.7580	0.441	.7525	0.0457	0.134	.6912	0.6109	0.261	.6686	0.2786	0.392
.7850	0.7716	0.426	.7539	0.0491	0.067	.6972	0.6257	0.281	.6699	0.2818	0.391
.7864	0.7750	0.413	.7601	0.0644	−0.007	.6986	0.6291	0.284	.6825	0.3128	0.351
.7878	0.7784	0.400	.7622	0.0695	0.031	.7000	0.6325	0.284	.6838	0.3159	0.342
.7892	0.7818	0.408	.7650	0.0763	0.069	.7014	0.6359	0.308	.6853	0.3196	0.361
.7948	0.7955	0.399	.7664	0.0798	0.096	.7140	0.6669	0.344	.6866	0.3227	0.359
.7962	0.7989	0.396	.7677	0.0832	0.114	.7153	0.6700	0.340	.6928	0.3380	0.336
.7979	0.8031	0.376	.7733	0.0968	0.180	.7167	0.6734	0.359	.6942	0.3415	0.351
.7992	0.8063	0.366	.7747	0.1002	0.231	.7181	0.6768	0.348	.6956	0.3449	0.350
.8054	0.8216	0.369	.7761	0.1036	0.242	.7243	0.6922	0.399	.6970	0.3482	0.339
.8068	0.8250	0.352	.7775	0.1071	0.230	.7257	0.6956	0.393	.7027	0.3622	0.297
.8087	0.8296	0.331	.7830	0.1207	0.256	.7271	0.6990	0.409	.7040	0.3653	0.294
.8100	0.8330	0.334	.7844	0.1241	0.265	.7285	0.7024	0.415	.7055	0.3690	0.283
.8225	0.8636	0.303	.7858	0.1275	0.275	.7345	0.7172	0.404	.7068	0.3724	0.279
.8239	0.8670	0.294	.7872	0.1309	0.283	.7359	0.7206	0.413	.7122	0.3855	0.264
.8253	0.8704	0.288	.8004	0.1633	0.349	.7375	0.7246	0.396	.7137	0.3892	0.228
.8267	0.8738	0.281	.8018	0.1667	0.350	.7389	0.7280	0.405	.7165	0.3960	0.200
5921.5872	0.6401	−0.294	.8032	0.1701	0.356	.7445	0.7416	0.401	.7180	0.3997	0.197

TABLE IIIb. (Continued)

JD Hel. 2430000+	Phase	Δm	JD Hel. 2430000+	Phase	Δm	JD Hel. 2430000+	Phase	Δm	JD Hel. 2430000+	Phase	Δm
5944.7291	0.4269	−0.110	5959.5920	0.8985	−0.186	5960.6802	0.5686	−0.097	5961.6877	0.0411	+0.137
.7303	0.4301	0.100	.5934	0.9019	0.172	.6817	0.5723	0.134	.6891	0.0445	0.116
.7317	0.4335	0.076	.5948	0.9053	0.166	.6829	0.5754	0.156	.6947	0.0581	0.005
.7331	0.4369	0.076	.5962	0.9087	0.141	.6899	0.5925	0.188	.6961	0.0615	−0.009
.7389	0.4511	+0.005	.6017	0.9224	0.079	.6913	0.5959	0.208	.6974	0.0649	0.040
.7410	0.4562	0.054	.6031	0.9258	0.028	.6927	0.5993	0.205	.6988	0.0683	0.053
.7424	0.4596	0.104	.6115	0.9462	+0.080	.6942	0.6030	0.216	.7058	0.0854	0.132
.7452	0.4664	0.110	.6129	0.9496	0.095	.7010	0.6197	0.287	.7072	0.0888	0.140
5958.5733	0.3988	−0.226	.6159	0.9570	0.183	.7024	0.6232	0.291	.7086	0.0922	0.161
.5754	0.4039	0.220	.6233	0.9752	0.170	.7038	0.6265	0.279	.7100	0.0956	0.173
.5921	0.4448	0.042	.6247	0.9786	0.181	.7100	0.6419	0.320	.7197	0.1195	0.250
.5935	0.4482	0.022	.6261	0.9820	0.219	.7114	0.6453	0.329	.7211	0.1229	0.251
.5949	0.4516	0.001	.6325	0.9979	0.185	.7129	0.6490	0.318	.7225	0.1263	0.255
.6018	0.4687	+0.097	.6339	0.0013	0.193	.7143	0.6524	0.335	.7238	0.1297	0.278
.6032	0.4721	0.106	.6354	0.0050	0.189	.7199	0.6660	0.359	.7294	0.1433	0.305
.6046	0.4755	0.101	.6374	0.0098	0.191	.7212	0.6694	0.378	.7308	0.1467	0.324
.6060	0.4789	0.110	.6427	0.0229	0.204	.7226	0.6728	0.386	.7322	0.1501	0.307
.6120	0.4936	0.138	.6441	0.0263	0.202	.7240	0.6763	0.401	.7336	0.1535	0.316
.6136	0.4976	0.143	.6457	0.0303	0.199	.7296	0.6899	0.410	.7391	0.1672	0.322
.6150	0.5010	0.143	.6476	0.0348	0.185	.7309	0.6930	0.410	.7406	0.1709	0.339
.6208	0.5152	0.129	.6526	0.0471	0.091	.7322	0.6964	0.408	.7419	0.1740	0.366
.6222	0.5186	0.116	.6538	0.0502	0.067	.7336	0.6998	0.392	.7433	0.1774	0.353
.6289	0.5351	0.080	.6555	0.0542	0.053	.7393	0.7138	0.419	.7488	0.1910	0.372
.6310	0.5402	0.071	.6568	0.0576	0.020	.7406	0.7169	0.413	.7509	0.1961	0.368
.6325	0.5439	0.019	.6625	0.0715	−0.017	.7420	0.7203	0.404	.7523	0.1995	0.372
.6338	0.5470	0.010	.6643	0.0758	0.059	.7434	0.7237	0.406	.7537	0.2030	0.362
.6352	0.5504	−0.006	.6659	0.0797	0.075	.7496	0.7390	0.433	5962.5682	0.2016	−0.391
.6465	0.5783	0.121	.6673	0.0831	0.106	.7511	0.7427	0.430	.5696	0.2051	0.389
.6479	0.5817	0.113	.6726	0.0962	0.156	.7525	0.7461	0.430	.5711	0.2087	0.404
.6493	0.5851	0.160	.6741	0.0999	0.174	.7538	0.7493	0.438	.5723	0.2116	0.399
.6507	0.5885	0.171	.6756	0.1036	0.174	5961.5801	0.7769	−0.419	.5835	0.2391	0.427
.6564	0.6027	0.231	.6770	0.1070	0.196	.5815	0.7804	0.415	.5849	0.2425	0.423
.6578	0.6061	0.244	.6830	0.1218	0.248	.5831	0.7843	0.413	.5865	0.2465	0.410
.6592	0.6095	0.251	.6844	0.1252	0.251	.5852	0.7894	0.409	.5879	0.2499	0.427
.6606	0.6129	0.267	.6860	0.1291	0.270	.5976	0.8198	0.405	.5932	0.2630	0.432
.6657	0.6254	0.296	.6921	0.1442	0.299	.5988	0.8229	0.403	.5946	0.2664	0.432
.6672	0.6291	0.313	.6938	0.1482	0.282	.6003	0.8266	0.395	.5962	0.2704	0.430
.6686	0.6325	0.304	.6953	0.1519	0.290	.6016	0.8298	0.377	.5976	0.2738	0.432
.6699	0.6356	0.311	.6967	0.1553	0.284	.6072	0.8434	0.347	.6030	0.2869	0.424
.6752	0.6487	0.319	.6990	0.1609	0.293	.6086	0.8468	0.328	.6046	0.2908	0.415
.6767	0.6524	0.335	.7115	0.1916	0.377	.6100	0.8502	0.326	.6076	0.2982	0.407
.6781	0.6558	0.338	.7129	0.1950	0.386	.6113	0.8536	0.323	.6143	0.3147	0.392
.6795	0.6592	0.351	.7152	0.2007	0.384	.6176	0.8690	0.313	.6161	0.3193	0.361
.7005	0.7109	0.423	.7166	0.2041	0.400	.6190	0.8723	0.300	.6178	0.3232	0.373
.7018	0.7140	0.426	.7226	0.2189	0.378	.6204	0.8758	0.286	.6193	0.3269	0.368
.7032	0.7175	0.436	.7240	0.2223	0.379	.6218	0.8792	0.267	.6247	0.3403	0.357
.7046	0.7209	0.431	.7256	0.2263	0.388	.6294	0.8979	0.239	.6261	0.3437	0.365
.7060	0.7243	0.422	.7270	0.2297	0.384	.6308	0.9013	0.215	.6277	0.3476	0.376
.7118	0.7385	0.426	.7323	0.2427	0.376	.6324	0.9053	0.185	.6291	0.3510	0.371
.7132	0.7419	0.425	.7340	0.2470	0.394	.6338	0.9087	0.171	.6407	0.3794	0.304
.7145	0.7453	0.420	.7352	0.2499	0.389	.6391	0.9218	0.114	.6424	0.3837	0.294
.7159	0.7487	0.428	.7365	0.2530	0.401	.6405	0.9252	0.103	.6437	0.3868	0.277
.7236	0.7674	0.434	.7380	0.2567	0.396	.6419	0.9286	0.054	.6453	0.3908	0.263
.7250	0.7708	0.424	.7445	0.2726	0.404	.6433	0.9320	0.046	.6509	0.4044	0.239
.7264	0.7743	0.418	.7459	0.2760	0.397	.6491	0.9462	+0.075	.6523	0.4078	0.228
.7277	0.7777	0.409	.7480	0.2814	0.403	.6505	0.9496	0.099	.6536	0.4113	0.226
.7291	0.7811	0.399	.7494	0.2848	0.407	.6518	0.9530	0.123	.6553	0.4152	0.205
.7365	0.7992	0.387	.7604	0.3118	0.378	.6534	0.9567	0.128	.6643	0.4374	0.089
.7379	0.8027	0.372	.7617	0.3149	0.395	.6586	0.9695	0.169	.6657	0.4408	0.062
.7395	0.8066	0.370	.7631	0.3183	0.369	.6600	0.9729	0.165	.6673	0.4448	0.059
.7408	0.8097	0.370	.7645	0.3217	0.368	.6613	0.9763	0.180	.6687	0.4482	0.024
.7465	0.8237	0.366	5960.6454	0.4834	+0.104	.6669	0.9899	0.170	.6760	0.4660	+0.056
.7478	0.8268	0.362	.6468	0.4868	0.122	.6683	0.9933	0.170	.6775	0.4698	0.091
.7493	0.8305	0.347	.6482	0.4902	0.122	.6697	0.9968	0.185	.6791	0.4737	0.076
.7507	0.8339	0.364	.6496	0.4936	0.136	.6711	0.0002	0.174	.6807	0.4777	0.107
.7566	0.8484	0.319	.6605	0.5203	0.105	.6725	0.0036	0.180	.6865	0.4919	0.132
.7581	0.8521	0.298	.6619	0.5237	0.105	.6738	0.0070	0.180	.6879	0.4953	0.141
.7595	0.8555	0.287	.6633	0.5272	0.123	.6752	0.0104	0.192	.6893	0.4987	0.149
.7611	0.8595	0.276	.6648	0.5308	0.091	.6766	0.0138	0.195	.6909	0.5027	0.128
5959.5768	0.8610	−0.302	.6704	0.5448	0.047	.6822	0.0274	0.197	.6923	0.5061	0.128
.5781	0.8644	0.295	.6718	0.5482	0.030	.6836	0.0308	0.192	.6981	0.5203	0.097
.5795	0.8679	0.285	.6732	0.5516	0.016	.6850	0.0343	0.175	.6995	0.5237	0.101
.5809	0.8712	0.289	.6746	0.5550	−0.020	.6864	0.0377	0.159	.7009	0.5271	0.110

TABLE IIIb. (Continued)

JD Hel. 2430000+	Phase	Δm	JD Hel. 2430000+	Phase	Δm	JD Hel. 2430000+	Phase	Δm	JD Hel. 2430000+	Phase	Δm
5962.7025	0.5311	−0.074	5966.6506	0.2192	−0.420	6673.7166	0.2577	−0.396	6693.6863	0.2606	−0.408
.7086	0.5462	0.001	.6520	0.2226	0.425	.7180	0.2612	0.409	.6877	0.2640	0.397
.7099	0.5493	0.005	.6575	0.2362	0.442	.7194	0.2646	0.403	.6996	0.2930	0.415
.7114	0.5530	0.016	.6589	0.2396	0.431	.7252	0.2788	0.400	.7009	0.2964	0.402
.7128	0.5564	0.031	.6604	0.2433	0.433	.7266	0.2822	0.412	.7023	0.2998	0.404
.7182	0.5697	0.120	.6617	0.2465	0.443	.7282	0.2862	0.397	.7037	0.3032	0.390
.7204	0.5751	0.131	6673.6021	0.9766	+0.227	.7298	0.2901	0.402	.7093	0.3168	0.377
.7217	0.5783	0.152	.6035	0.9800	0.222	.7354	0.3038	0.396	.7107	0.3203	0.384
.7233	0.5822	0.166	.6048	0.9834	0.222	.7368	0.3072	0.397	.7120	0.3236	0.375
.7293	0.5970	0.219	.6062	0.9868	0.217	.7382	0.3106	0.391	.7134	0.3270	0.378
.7307	0.6005	0.214	.6125	0.0022	0.235	.7396	0.3140	0.390	.7190	0.3407	0.365
.7322	0.6041	0.238	.6139	0.0056	0.244	.7514	0.3430	0.362	.7204	0.3441	0.347
.7335	0.6072	0.245	.6152	0.0090	0.236	.7527	0.3464	0.344	.7218	0.3475	0.352
.7391	0.6209	0.305	.6166	0.0124	0.245	.7541	0.3498	0.346	.7232	0.3509	0.351
.7404	0.6243	0.307	.6222	0.0260	0.255	.7555	0.3532	0.334	6697.5978	0.8586	−0.271
.7418	0.6277	0.318	.6236	0.0294	0.231	6693.5968	0.0408	+0.217	.5993	0.8623	0.286
.7432	0.6311	0.310	.6250	0.0328	0.255	.5982	0.0442	0.217	.6007	0.8657	0.271
.7488	0.6447	0.330	.6263	0.0362	0.251	.5996	0.0476	0.193	.6069	0.8811	0.216
.7502	0.6481	0.334	.6326	0.0516	0.194	.6009	0.0510	0.177	.6095	0.8873	0.213
.7517	0.6518	0.329	.6340	0.0550	0.153	.6079	0.0680	0.062	.6111	0.8913	0.203
.7529	0.6549	0.325	.6357	0.0592	0.145	.6093	0.0715	0.058	.6125	0.8947	0.187
5966.5805	0.0471	+0.100	.6375	0.0635	0.086	.6107	0.0749	0.027	.6180	0.9083	0.122
.5818	0.0505	0.089	.6391	0.0675	0.052	.6121	0.0783	0.006	.6201	0.9135	0.108
.5832	0.0539	0.064	.6448	0.0814	−0.040	.6176	0.0919	−0.070	.6221	0.9183	0.093
.5846	0.0573	0.035	.6463	0.0851	0.070	.6190	0.0953	0.098	.6236	0.9220	0.062
.5902	0.0709	−0.050	.6483	0.0902	0.099	.6204	0.0987	0.082	.6298	0.9373	+0.053
.5916	0.0744	0.081	.6504	0.0953	0.101	.6218	0.1021	0.096	.6312	0.9407	0.094
.5930	0.0778	0.099	.6576	0.1129	0.162	.6294	0.1209	0.214	.6326	0.9441	0.094
.5943	0.0811	0.121	.6597	0.1181	0.196	.6308	0.1243	0.232	.6347	0.9492	0.107
.5999	0.0948	0.183	.6610	0.1212	0.190	.6322	0.1277	0.239	.6411	0.9649	0.234
.6013	0.0982	0.186	.6625	0.1249	0.203	.6377	0.1413	0.263	.6426	0.9686	0.253
.6027	0.1016	0.194	.6687	0.1402	0.251	.6394	0.1453	0.249	.6470	0.9793	0.249
.6089	0.1170	0.256	.6701	0.1436	0.273	.6408	0.1487	0.273	.6527	0.9936	0.256
.6117	0.1237	0.282	.6715	0.1470	0.280	.6422	0.1521	0.273	.6547	0.9984	0.256
.6132	0.1275	0.267	.6729	0.1504	0.283	.6544	0.1822	0.343	.6569	0.0038	0.257
.6189	0.1414	0.314	.6847	0.1794	0.330	.6558	0.1856	0.333	.6676	0.0299	0.264
.6200	0.1442	0.321	.6861	0.1828	0.339	.6572	0.1890	0.350	.6689	0.0333	0.243
.6215	0.1479	0.329	.6875	0.1862	0.351	.6586	0.1924	0.359	.6706	0.0373	0.233
.6228	0.1510	0.332	.6889	0.1896	0.350	.6648	0.2078	0.371	.6724	0.0419	0.228
.6286	0.1652	0.361	.6944	0.2033	0.350	.6662	0.2112	0.369	.6745	0.0470	0.195
.6300	0.1687	0.356	.6958	0.2066	0.370	.6676	0.2146	0.371	.6761	0.0509	0.161
.6314	0.1721	0.343	.6972	0.2100	0.363	.6690	0.2180	0.375	.6780	0.0555	0.147
.6328	0.1755	0.365	.6986	0.2135	0.371	.6745	0.2316	0.407	.6798	0.0600	0.115
.6381	0.1885	0.401	.7048	0.2288	0.385	.6762	0.2356	0.393	.6861	0.0754	0.016
.6409	0.1953	0.401	.7062	0.2322	0.378	.6778	0.2396	0.406	.6875	0.0788	−0.016
.6422	0.1987	0.383	.7076	0.2356	0.392	.6836	0.2538	0.405	.6889	0.0822	0.024
.6478	0.2124	0.417	.7090	0.2390	0.397	.6850	0.2572	0.408	.6902	0.0856	0.052
.6492	0.2158	0.429	.7152	0.2543	0.419						

The color curve shows a reddening of about 0.05 mag. at both primary and secondary minima. This is expected since then the cooler and redder ends of the ellipsoidal stars caused by the combination of gravitation and reflection effects are in view. The light curves have maxima of unequal height and the secondary eclipse curve is asymmetrical and the minimum is delayed in time. It can also be noticed that the brighter maximum in the light curves corresponds to a slightly bluer color in the color curve. This indicates a change in the temperature and a change in the surface brightness. However, if the whole disk of one or both components were affected in this manner, the observed maxima of the light curve would be of the same height and the secondary minimum would be symmetrical. Apparently a disturbed local region is involved. It could be a superluminous region visible at phase 0.25 or a subluminous region visible at phase 0.75, depending upon the definition of a normal system.

During the 1957 season differences in the heights of the maxima were still found. The observing nights were now divided into four groups and the same procedure was followed as given above. Each normal point consisted of about five observations (see Fig. 4). Five consecutive nights of observations showed that the shape of the maxima of the light curve definitely changed during just a few observing nights (see Fig. 5). The depths of both minima are somewhat shallower than those observed two years before.

6. LIGHT IN THE MAXIMA

The observations of March 30, and April 9 and 10, 1955 were chosen as defining a well-observed light curve

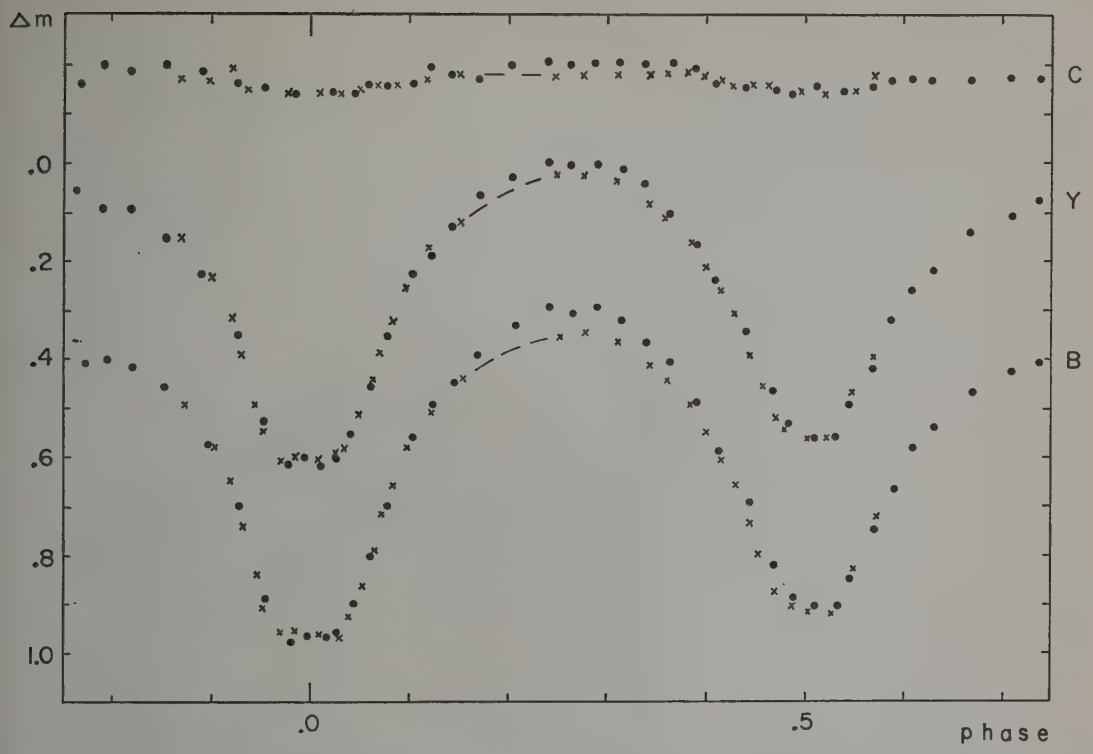

FIG. 3. The light curves and the color curve of AH Virginis in 1955. The dots refer to normal points of observations made on March 30, April 9 and 10; the crosses represent the normal points of observations made on May 15, 16, 17, and 18. The symbols are B=blue, Y=yellow, C=color.

with maxima of unequal height and an asymmetrical and delayed secondary minimum. The magnitudes and phases of the normal points were converted into intensities and phase angles. The intensities were corrected to remove the effect of the light of the $13^{m}.2$ companion. Least-squares solutions were made for the yellow and blue light in the maxima according to the formula

$$l = A_0 + A_1 \cos\theta + A_2 \cos 2\theta + B_1 \sin\theta + B_2 \sin 2\theta.$$

The coefficients and their probable errors are given in the upper part of Table IV.

The observations of May 1, 2, and 3, 1957 were chosen as defining a well-observed light curve with maxima of the same height and a symmetrical secondary minimum. While the maxima show some irregularities, this light curve is as normal as can be expected for a W Ursae Majoris system. The procedure outlined above was repeated and the coefficients and their probable errors are listed in the lower part of this table.

In this two-year time interval the reflection effect changed considerably but the coefficient of the $\cos\theta$ term has the sign predicted by theory. The coefficients of the $\cos 2\theta$ term remained constant within the probable errors.

7. ORBITAL ELEMENTS

The 1955 and 1957 light curves belong to the same system but they are very different in appearance. Therefore in determining the orbital elements the condition was imposed that the geometrical elements such as the inclination, sizes and shapes of the components should remain the same. The photometric elements such as the intensity and the surface brightness of the components were considered to vary during the time interval.

The yellow and blue intensities of the 1955 light curves were first rectified for the so-called perturbations, by the subtraction of the $\sin\theta$ and $\sin 2\theta$ terms. After this rectification the secondary minimum becomes symmetrical and occurs midway between the primary

TABLE IV. Coefficients for the Light in the Maxima.

Year	λ	A_0	A_1	A_2	B_1	B_2
1955	Y	+0.8483	−0.0035	−0.1202	+0.0334	−0.0140
		± 28	± 28	± 38	± 12	± 16
	B	+0.8369	−0.0017	−0.1183	+0.0410	−0.0227
		± 37	± 36	± 50	± 16	± 22
1957	Y	+0.8820	−0.0122	−0.1172	−0.0076	−0.0035
		± 28	± 29	± 40	± 14	± 17
	B	+0.8795	−0.0159	−0.1184	−0.0045	−0.0094
		± 30	± 31	± 43	± 15	± 19

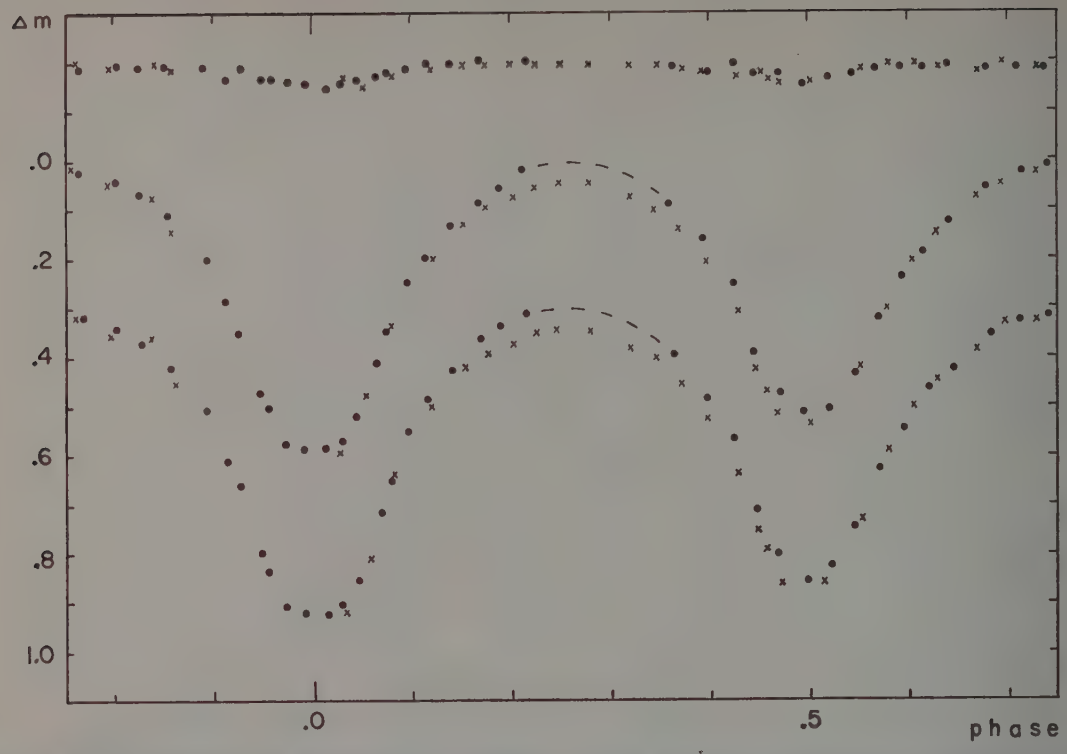

FIG. 4. The light curves and the color curve of AH Virginis in 1957. The dots refer to normal points of observations made on March 3, 9, and 23; the crosses represent the normal points of observations made on April 9 and 15. The symbols are B=blue, Y=yellow, C=color.

minima. Moreover, the duration of secondary eclipse becomes equal to that of the primary one and a circular orbit can be assumed. The difference between the reflection coefficients was found from the observed quantity A_1, and the ratio of the coefficients was found from the ratio of the depths after a provisional rectification had been made. Then the normal rectifications for reflection and oblateness were carried out separately, and the phase angles were rectified.

The computation for rectification was repeated for the 1957 light curves but it was necessary to make one change. The ratio of the depths was so close to unity that the reflection coefficients found were very unreliable. Therefore, the provisional elements of the 1955 solution were substituted into an expression for the sum of the reflection coefficients, as given in Formula 108 of a publication by Russell and Merrill (1952).

The constancy of the light during primary minimum shows that this eclipse is total. The radial velocity curves also indicate that primary minimum is an occultation, according to reasoning presented in an earlier publication (Binnendijk 1957). Also, the χ value for primary minimum is greater than for secondary minimum, which again proves that primary minimum is an occultation.

The depth relation is therefore uniquely determined. A coefficient of limb darkening $x=0.8$ was assumed for this system with late spectral type (K0). The values found from the 1955 solution were $k=0.46$ (yellow) and 0.50 (blue), while the 1957 solution gave $k=0.48$ (yellow) and 0.52 (blue). Similar values of k were found by using values in the nomographs of Merrill (1950, 1953), where the lower part of the eclipse curves are used. The shoulders of the eclipse curves suggest a somewhat higher value of k.

Next, the shape relations of the primary and secondary eclipse curves were studied in more detail with the help of the ψ functions. It was possible to get a reasonable representation of both eclipse curves in yellow and blue light for the 1955 and 1957 light curves with one set of geometrical elements but with different photometric elements. In the following list of elements $\epsilon=(a-b)/a$ is the oblateness, i is the inclination corrected for polar flattening, and I is the mean surface brightness of the components.

1955 and 1957 Light Curves

$k=0.50$	$\alpha_0{}^{oc}=1.00$	$\alpha_0{}^{tr}=1.093$
$\epsilon=0.085$	$\alpha_g=0.50$	$a_s=0.25$
$i=80°.8$	$b_g=0.46$	$b_s=0.23$

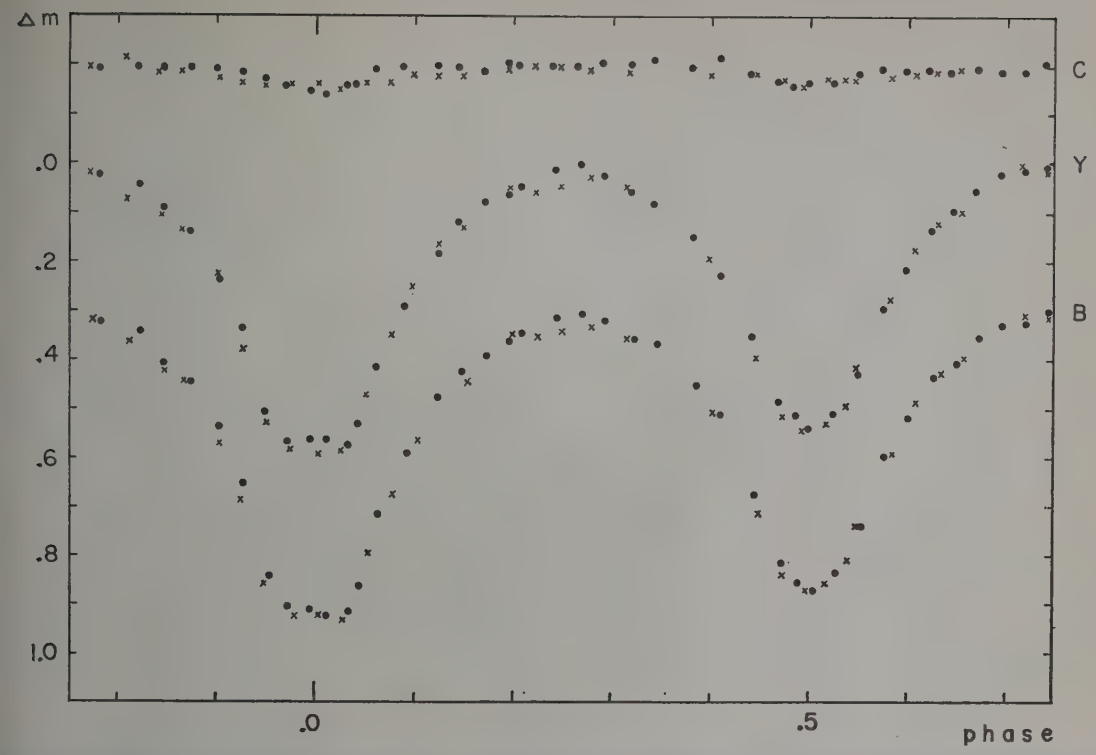

FIG. 5. The light curves and the color curve during five consecutive nights in 1957. The crosses represent the normal points of servations made on April 29 and 30; the dots refer to normal points of observations made on May 1, 2, and 3. The symbols are =blue, Y=yellow, C=color.

1955 Light Curve

Yellow	Blue
$L_g=0.785$	$L_g=0.744$
$L_s=0.215$	$L_s=0.256$
$I_g=0.916\ I_s$	$I_g=0.726\ I_s$

1957 Light Curve

Yellow	Blue
$L_g=0.796$	$L_g=0.771$
$L_s=0.204$	$L_s=0.229$
$I_g=0.973\ I_s$	$I_g=0.844\ I_s$

Fig. 6, the 1955 and 1957 light curves in yellow and ue are given for comparison along with the theoretical ht curves computed from the above elements. The obable error of the $O-C$ is $\pm 0^m0075$. The agreement therefore, very satisfactory.

In a close binary system such as is studied here tra light can be expected from a surrounding gas eam. The values θ and α in the shape relation remain e same, as do the ψ function and the k value which e found from this relation. But the extra light affects e depth of the minima and consequently the depth ation. It is found that k will increase by 0.03 if there 10% additional light involved. This is just about the amount of the estimated probable error in the determined k. Unfortunately the k's found from the depth and the shape relations are not precise enough to make such a discrimation. An upper limit is set by the value $k=0.64$, which was found from the durations of the minima for concentric eclipses ($i=90°$).

It is now possible to determine more accurately the position of the disturbed local region which was observed in the 1955 light curve. At primary minimum only the greater star is visible. Figure 6 shows that in the 1955 light curves this star was 0.05 magnitudes fainter in both wavelengths than in the 1957 light curves. The greater star was also fainter in the rectified light curves of 1955 as is evident from the orbital elements. The subluminous region is therefore situated on the greater star and it must be partially visible at primary minimum. The difference between the 1955 and 1957 light curves, in both wavelengths, is as much as 0.10 magnitudes at phase 0.75 and this subluminous region must be in full view then. The region can be located in the central part of the elliptical disk visible at this phase. At phase 0.45 the facing part of this subluminous region is almost completely hidden by the smaller star in front. This is indicated by the fact that the 1955 and 1957 light curves then coincide.

The spectroscopic data of Chang (1948), uncorrected

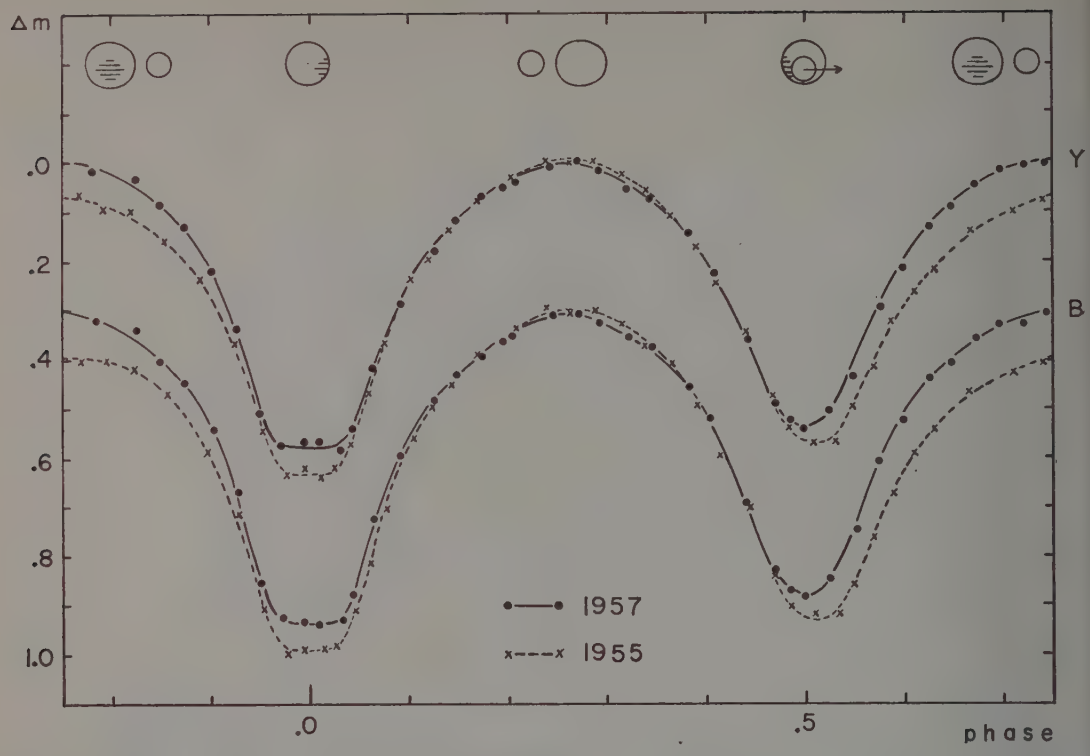

FIG. 6. A comparison of the 1955 and 1957 observations discussed in the text. The lines represent the theoretical light curve computed from the orbital elements. The deviation of the 1955 light curve can be explained by the presence of a subluminous regio situated on the larger star. It can be located in the central part of the elliptical disk visible at phase 0.75, where this greater star [ex ceeds the Jacobian limiting surface.

for reflection, were now combined with the orbital elements found from the light curves. The results were

$a_1=600000$ km	$a_2=1420000$ km
$a_g=1.47\ \odot$	$a_s=0.73\ \odot$
$b_g=1.34\ \odot$	$b_s=0.66\ \odot$
$\mathfrak{M}_g=1.38\ \odot$	$\mathfrak{M}_s=0.58\ \odot$
$\rho_g=0.52\ \odot$	$\rho_s=1.82\ \odot$
$P\sqrt{\rho_g}=0.30$	$P\sqrt{\rho_s}=0.55$

8. COMPARISON WITH THEORY

A comparison has been made between some of the observed values and those determined theoretically. First the oblateness was considered. The Roche model yields a value of 0.067 for the greater star and 0.045 for the smaller star from which the weighted mean of 0.063 was obtained. The homogeneous model gives a value of 0.157 for the weighted mean. The four values found from the four light curves agree very well and the mean value $\epsilon=0.085$ is closer to the Roche model than to the homogeneous model, which was expected.

Next the reflection effect was considered. The theoretical value does not agree with the observed one. This disagreement is usually found in studying W Ursae Majoris systems. The theory of reflection applies mos directly to stars with radii smaller then 0.20, while her both components are larger than this value. A nev theoretical treatment of the reflection effect for thes close systems is urgently needed. However, it is inter esting to note that the orbital determination show such good agreement in spite of the incomplete recti fication procedure for the reflection.

Finally, a comparison was made between the ob served sizes of the stars and the dimensions of th Jacobian limiting surface. The three axes of the com ponents were found by various methods to be $a_g=0.5$ $b_g=0.47$, $c_g=0.45$ for the greater star and $a_s=0.2$ $b_s=0.24$, $c_s=0.23$ for the smaller star. A mass ratio o 2.38, found from the radial velocity curves, wa assumed here. Both the simple theory in which bot stars are considered as mass points and the mor sophisticated theory in which each component in tur is considered to be a polytrope of index $n=3$ were use in determining the limiting surface. For the latte model, the unpublished tables of J. E. Merrill and E. G Reuning were consulted. In each case the results wer the same, namely, that the greater star exceeds th limiting surface in the direction of the equatorial b axis The solutions of the light curves frequently show tha components of eclipsing systems approach stabilit

nits first in this direction. In AH Virginis this equa-
rial b axis is pointed in our direction at phase 0.75,
hich is the phase at which evidence was found that
the 1955 curve the subluminous region was in full
ew.

Apparently the subluminous region can be identified
ith the area on the greater star from which gaseous
aterial was escaping into circumstellar space. The
riod of the system increased in 1955 and from this
crease the mass loss is estimated to be $2.4\times10^{-5}\ \odot$.
n explosion-like prominence on the advancing side of
e greater star would just decrease the period according
Wood (1950). Such a phenomenon may have
ppened in 1953 when a slight decrease in the period
as observed, but not enough information about the
ght curve was available for that year. If the period
crease in 1955 was caused by an outflow of material
om the advancing side of the larger star this outflow
as slow rather than explosive. Unfortunately no spec-
oscopic observations are available for these years.

ACKNOWLEDGMENTS

It is a great pleasure to thank Dr. J. E. Merrill for
me stimulating discussions concerning the orbital
lution.

REFERENCES

Binnendijk, L. 1957, *J. Astron. Soc. Canada* **51**, 83; *Contr. from Dominion Astrophys. Obs. Victoria* No. 53, 77; *Flower and Cook Obs. Reprint* No. 108.
Chang, Y. C. 1948, *Astrophys. J.* **107**, 96.
Domke, K. and Pohl, E. 1953, *Astron. Nachr.* **281**, 113.
Guthnick, P. and Prager, R. 1929, *Beob. Zirk.* No. 13, 32.
Hardie, R. 1959, *Astrophys. J.* **130**, 663.
Hertzsprung, E. 1928, *Bull. Astron. Inst. Neth.* **4**, 179.
Huruhata, M. and Nakamura, T. 1951, *Bull. Tokyo Obs.* No. 33, 233.
Kitamura, M., Tanaba, H., and Nakamura, T. 1957, *Publ. Astron. Soc. Japan* **9**, 119. Tokyo Reprint No. 158.
Kitamura, M. and Takahashi, C. 1959, *Tokyo Astr. Bull., second series*, No. 123.
Koch, R. H. 1956, *Astron. J.* **61**, 47.
Kopal, Z. and Shapley, M. B. 1956, *Jodrell Bank Ann.* **1**, 141.
Kukarkin, B. V. 1929, *Nishni-Novgorod Veränderliche Sterne* **1**, No. 11, 2.
Kwee, K. K. 1958, *Bull. Astron. Inst. Neth.* **14**, 131.
Lause, F. 1934, *Astron. Nachr.* **254**, 373.
——. 1935, *ibid.* **257**, 211.
——. 1937, *ibid.* **264**, 106.
Merrill, J. E. 1950, *Contr. Princeton Univ. Obs.* No. 23.
——. 1953, *ibid.* No. 24.
Nason, M. E. and Moore, R. C. 1951, *Astron. J.* **56**, 182.
Prager, R. 1929, *Kl. Veröff. Berlin-Babelsberg* **2**, No. 6, 36.
Russell, H. N. and Merrill, J. E. 1952, *Contr. Princeton Univ. Obs.* No. 26, 49.
Szczepanowska, A. 1951, *Rocznik Astronomiczny Krakow* **22**, 89.
——. 1953, *ibid.* **24**, 89.
Wood, F. B. 1950, *Astrophys. J.* **112**, 196.
Zessewitsch, V. P. 1944, *Kazan Astron. Circ.* No. 35, 9.

Photoelectric Light Curves of XY Leonis

ROBERT H. KOCH*
Flower and Cook Observatory, Philadelphia, Pennsylvania

Yellow and blue light curves of XY Leonis have been obtained. There are small differences between the best orbital elements derived at each wave length. Neither solution agrees with the one expected from spectroscopic observations. A possible cause of the discrepancy is discussed and a limiting photometric solution computed.

1. INTRODUCTION

THE light variation of XY Leonis (BD+18°2307, 356.1934, P3373, 1950: $\alpha = 9^h\,58^m.9$, $\delta = +17°39'.2$) was discovered by Hoffmeister (1934). A light curve from visual estimates and a large number of times of minimum light have been published by Zessewitsch (1954). A few other minima are listed by Ashbrook (1952, 1953) and Koch (1956). Vyssotsky and Balz (1958) give the spectral classification as G5 from the McCormick prism plates. Keenan (personal letter to Dr. J. E. Merrill) estimated the spectral type of the hot star to be about K0V. Struve and Zebergs (1959) have observed the radial velocity curves of both components. These observations show the system to be an ordinary W UMa-type binary. At the elongations *Ca* H and K emission is visible. The emission features appear to be quite complicated.

2. THE OBSERVATIONS

A total of 293 yellow and 299 blue observations were obtained from January through April, 1956 with the 36-inch telescope at the Steward Observatory. The comparison star is BD+18°2306; on each of nineteen nights it was checked at least once against BD+18°2308. Within this interval the comparison star was satisfactorily constant in light. The observations of XY Leo are listed in Table I; the yellow light curve and color curve are shown in Fig. 1. All times are heliocentric and

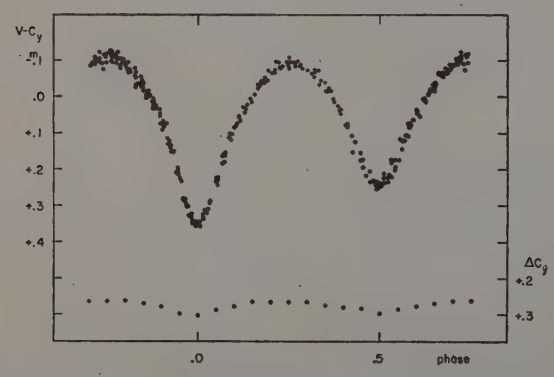

FIG. 1. The top curve shows yellow observations of XY Leo taken at the Steward Observatory. At the bottom is the mean differential color curve obtained by subtracting the averaged yellow observations from the averaged blue ones.

counted from Greenwich Mean Noon. Corrections for differential extinction are less than $0^m.001$ at each wavelength and have been neglected. A few yellow observations taken with the 28-inch reflector at the Flower and Cook Observatory are also listed in Table I.

On May 2, 1957 the comparison and check stars were tied to the (*B*, *V*) system using ρ Leo and AD Leo as standards. AD Leo is known to be a variable of the UV Cet-type, but it was constant in brightness during this night. Four observations were made of each star and the magnitudes and colors were determined by least-squares solutions. The results appear in Table II the probable error for each determination is also given. Average values of Δm were read from the light curves at four phases and the variation of XY Leo scaled on the (*B*, *V*) system. Table II gives the results. The variation of (*B*–*V*) throughout the light curve can be attributed to the gravity effect introduced by the distortion of figure and to differential reflection within the system. The small change in (*B*–*V*) indicates that the two components are not appreciably different in surface temperature.

On the night of February 19, 1956 the comparison star was observed three times in both violet and blue light and the variable was observed twice through the same filters. These observations give (*U*−*B*) for the comparison star as $+0^m.28$. For XY Leo (*U*−*B*) is $+0^m.70$ and $+0^m.73$ at phases $0^p.5917$ and $0^p.6297$ respectively.

The galactic coordinates of XY Leo are: $l = 186°$, $b = +51°$. Hubble (1934) has investigated several neighboring fields and found the distribution of galaxies to be normal. XY Leo is taken to be effectively unreddened. This conclusion points out a possible discrepancy in the color indices of the variable even when these are corrected for reflection and ellipticity effects. In the catalogue of Johnson (1955) two nearby K0V stars show (*B*−*V*) colors of $+0^m.79$, and $+0^m.86$ and (*U*−*B*) colors of $+0^m.39$ and $+0^m.56$. If these are normal K0V stars, XY Leo should have a very red component contributing an appreciable amount of light. The only alternative seems to be that the light curve in at least one wavelength is complicated in such a way that the true colors of the components are masked. If this is the case, then either the solutions at each wavelength differ significantly one from another or the observations in at least one wavelength do not lead to a satisfactory solution.

*Now at Amherst College Observatory, Amherst, Massachusetts.

TABLE Ia. Yellow Observations of XY Leo.

V—C	JD ⊙ 2435000+	Phase	V—C	JD ⊙ 2435000+	Phase	V—C	JD ⊙ 2435000+	Phase
+0m201	473.9603	0.5438	−0m121	508.9726	0.7793	+0m248	518.8394	0.5083
+0.108	.9708	0.5808	−0.074	.9813	0.8099	+0.235	.8449	0.5276
+0.049	.9781	0.6065	−0.068	.9861	0.8268	+0.192	.8501	0.5459
+0.011	.9847	0.6297	−0.021	.9913	0.8451	+0.120	.8571	0.5706
−0.028	.9916	0.6540	0.000	.9962	0.8623	+0.078	.8623	0.5889
−0.075	474.0024	0.6920	+0.032	509.0011	0.8796	+0.041	.8671	0.6058
−0.092	.0097	0.7177	+0.006	513.8244	0.8564	+0.007	.8730	0.6265
−0.093	.0180	0.7469	+0.092	.8372	0.9014	−0.014	.8772	0.6413
−0.091	.0263	0.7761	+0.142	.8432	0.9225	−0.032	.8824	0.6596
−0.071	482.9521	0.1929	+0.207	.8487	0.9419	−0.057	.8880	0.6793
−0.093	.9611	0.2246	+0.282	.8539	0.9602	−0.080	.8897	0.6853
−0.069	.9889	0.3224	+0.298	.8556	0.9662	−0.108	.8973	0.7121
−0.040	.9969	0.3506	+0.351	.8612	0.9859	−0.043	.9345	0.8430
−0.018	483.0025	0.3703	+0.359	.8668	0.0056	−0.016	.9400	0.8623
+0.024	.0077	0.3886	+0.294	.8744	0.0324	+0.025	.9456	0.8821
+0.074	.0146	0.4129	+0.181	.8855	0.0715	+0.067	.9515	0.9028
+0.108	.0188	0.4277	+0.120	.8911	0.0912	+0.154	.9595	0.9310
+0.156	.0250	0.4495	+0.060	.8970	0.1119	+0.234	.9654	0.9517
+0.219	.0302	0.4678	+0.042	.9022	0.1302	+0.302	.9710	0.9715
+0.237	.0354	0.4861	+0.007	.9070	0.1471	+0.076	522.8393	0.5867
+0.240	.0410	0.5058	−0.033	.9122	0.1654	+0.007	.8501	0.6248
+0.215	.0476	0.5290	−0.052	.9178	0.1851	−0.033	.8581	0.6529
−0.083	.9487	0.7008	−0.064	.9230	0.2034	−0.059	.8636	0.6723
−0.098	.9563	0.7275	−0.080	.9300	0.2281	−0.068	.8688	0.6906
−0.093	.9619	0.7472	−0.095	.9404	0.2647	−0.091	.8741	0.7092
−0.094	.9674	0.7666	−0.089	.9459	0.2840	−0.105	.8793	0.7275
−0.085	.9727	0.7853	−0.071	.9511	0.3023	−0.119	.8845	0.7458
−0.066	.9789	0.8071	−0.063	.9563	0.3207	−0.111	.8897	0.7641
−0.037	.9865	0.8338	−0.047	.9622	0.3414	−0.103	.8952	0.7835
−0.003	.9931	0.8571	−0.014	.9675	0.3601	−0.075	.9008	0.8032
+0.027	.9984	0.8757	+0.004	.9723	0.3770	−0.031	.9081	0.8289
+0.049	484.0036	0.8940	+0.048	.9779	0.3967	−0.034	.9136	0.8483
+0.117	.0098	0.9158	+0.083	.9827	0.4136	0.000	.9188	0.8669
+0.198	.0174	0.9426	+0.124	.9879	0.4319	+0.033	.9244	0.8863
+0.286	.0227	0.9612	+0.195	.9952	0.4576	+0.085	.9300	0.9060
+0.331	.0279	0.9796	+0.255	514.0053	0.4931	+0.154	.9362	0.9278
+0.352	.0338	0.0003	+0.123	517.8199	0.9197	−0.101	534.8086	0.7163
+0.321	.0400	0.0222	+0.208	.8268	0.9440	−0.110	.8162	0.7430
+0.231	.0484	0.0517	+0.287	.8324	0.9637	−0.112	.8211	0.7603
+0.160	.0542	0.0722	+0.347	.8383	0.9845	−0.104	.8263	0.7786
−0.032	489.9018	0.6543	+0.340	.8473	0.0162	−0.101	.8308	0.7944
−0.074	.9136	0.6959	+0.290	.8529	0.0359	−0.068	.8357	0.8117
−0.090	.9188	0.7142	+0.224	.8584	0.0553	−0.050	.8402	0.8275
−0.091	.9244	0.7339	+0.157	.8644	0.0764	−0.028	.8447	0.8433
−0.099	.9317	0.7596	+0.102	.8699	0.0957	−0.012	.8492	0.8592
−0.077	.9386	0.7839	+0.054	.8755	0.1154	+0.014	.8537	0.8750
−0.027	.9511	0.8279	+0.021	.8810	0.1348	+0.055	.8586	0.8923
+0.002	.9584	0.8536	−0.009	.8880	0.1594	+0.078	.8635	0.9095
+0.036	.9636	0.8718	−0.042	.8928	0.1763	+0.137	.8680	0.9253
+0.075	.9709	0.8975	−0.045	.8977	0.1936	+0.217	.8735	0.9447
+0.131	.9761	0.9158	−0.074	.9026	0.2108	+0.294	.8794	0.9655
+0.211	.9830	0.9401	−0.076	.9078	0.2291	+0.342	.8846	0.9838
+0.325	.9945	0.9806	−0.096	.9130	0.2474	+0.347	.8902	0.0035
−0.077	491.9147	0.7392	−0.094	.9196	0.2707	+0.313	.8947	0.0194
−0.109	.9213	0.7624	−0.077	.9251	0.2900	+0.234	.9034	0.0500
−0.084	.9321	0.8004	−0.064	.9328	0.3171	+0.163	.9089	0.0693
−0.057	.9390	0.8247	−0.032	.9383	0.3365	+0.115	.9138	0.0866
−0.018	.9460	0.8493	−0.018	.9435	0.3548	+0.075	.9204	0.1098
+0.016	.9526	0.8726	+0.008	.9487	0.3731	+0.036	.9266	0.1316
+0.251	508.8931	0.4994	+0.037	.9539	0.3914	+0.016	.9315	0.1489
+0.225	.9007	0.5262	+0.079	.9591	0.4097	−0.031	.9374	0.1697
+0.176	.9063	0.5459	+0.152	.9647	0.4294	−0.046	.9423	0.1869
+0.144	.9118	0.5653	+0.175	.9702	0.4488	−0.066	.9478	0.2063
+0.075	.9174	0.5850	+0.237	.9782	0.4769	−0.086	.9603	0.2503
+0.038	.9226	0.6033	+0.252	.9838	0.4966	+0.231	535.8798	0.4864
+0.008	.9288	0.6251	+0.239	.9894	0.5164	+0.227	.8874	0.5132
−0.032	.9358	0.6498	+0.221	.9952	0.5368	+0.216	.8923	0.5304
−0.064	.9410	0.6681	+0.173	518.0012	0.5579	+0.176	.8975	0.5487
−0.066	.9462	0.6864	+0.107	.0067	0.5772	+0.123	.9027	0.5670
−0.088	.9511	0.7036	+0.063	.0123	0.5970	+0.083	.9079	0.5853
−0.111	.9563	0.7219	+0.054	.0175	0.6153	+0.038	.9131	0.6036
−0.116	.9615	0.7402	+0.219	.8265	0.4629	+0.007	.9183	0.6219
−0.121	.9670	0.7596	+0.244	.8341	0.4896	−0.007	.9232	0.6392

TABLE Ia. (Continued)

V—C	JD ⊙ 2435000+	Phase	V—C	JD ⊙ 2435000+	Phase	V—C	JD ⊙ 2435000+	Phase
−0m037	535.9284	0.6575	+0m223	536.8922	0.0500	+0m021	574.7036	0.1376
−0.066	.9339	0.6769	+0.164	.8985	0.0722	−0.026	.7122	0.1679
−0.089	.9391	0.6952	+0.101	.9033	0.0891	−0.039	.7167	0.1837
−0.110	.9468	0.7223	+0.081	.9082	0.1063	−0.063	.7220	0.2024
−0.115	.9523	0.7416	+0.030	.9134	0.1246	−0.098	.7265	0.2182
−0.125	.9572	0.7589	+0.004	.9183	0.1418	−0.083	.7310	0.2341
−0.103	.9624	0.7772	−0.021	.9242	0.1626	−0.078	.7359	0.2513
−0.094	.9676	0.7955	−0.038	.9283	0.1770	−0.082	.7411	0.2696
−0.121	536.8006	0.7275	−0.071	.9332	0.1943	−0.073	.7508	0.3038
−0.123	.8089	0.7568	−0.067	.9381	0.2115	−0.074	.7560	0.3221
−0.119	.8134	0.7726	−0.077	.9433	0.2298	−0.048	.7612	0.3404
−0.093	.8183	0.7898	−0.096	.9509	0.2566	−0.072	594.6466	0.3326
−0.093	.8231	0.8067	−0.099	.9561	0.2749	−0.027	.6546	0.3608
−0.079	.8280	0.8240	−0.108	561.6671	0.2520	+0.013	.6598	0.3791
−0.055	.8328	0.8409	−0.082	.6750	0.2798	+0.033	.6647	0.3963
−0.013	.8384	0.8606	+0.079	574.6372	0.9039	+0.083	.6699	0.4146
+0.007	.8429	0.8764	+0.216	.6487	0.9444	+0.125	.6755	0.4343
+0.035	.8478	0.8937	+0.330	.6564	0.9715	+0.173	.6814	0.4551
+0.075	.8530	0.9120	+0.360	.6622	0.9919	+0.207	.6869	0.4745
+0.153	.8586	0.9317	+0.334	.6682	0.0130	+0.233	.6925	0.4942
+0.228	.8638	0.9500	+0.310	.6730	0.0299	+0.212	.6980	0.5135
+0.306	.8693	0.9693	+0.245	.6793	0.0521	+0.175	.7036	0.5332
+0.342	.8766	0.9950	+0.188	.6841	0.0690	+0.116	.7112	0.5600
+0.326	.8818	0.0134	+0.087	.6928	0.0996	+0.073	.7171	0.5808
+0.290	.8870	0.0317	+0.067	.6980	0.1179			

TABLE Ib. Blue observations of XY Leo.

V—C	JD ⊙ 2435000+	Phase	V—C	JD ⊙ 2435000+	Phase	V—C	JD ⊙ 2435000+	Phase
+0m497	473.9600	0.5427	+0m659	484.0331	0.9979	+0m269	508.9969	0.8648
0.388	.9708	0.5808	0.614	.0407	0.0246	0.279	509.0018	0.8821
0.322	.9777	0.6050	0.515	.0490	0.0539	0.278	513.8251	0.8588
0.290	.9843	0.6283	0.453	.0550	0.0750	0.367	.8379	0.9039
0.242	.9913	0.6529	0.253	489.9025	0.6568	0.426	.8438	0.9246
0.204	474.0020	0.6906	0.201	.9143	0.6983	0.503	.8494	0.9444
0.175	.0093	0.7163	0.177	.9195	0.7166	0.596	.8546	0.9627
0.170	.0177	0.7458	0.169	.9251	0.7363	0.601	.8563	0.9686
0.175	.0260	0.7751	0.177	.9324	0.7620	0.660	.8619	0.9884
0.192	482.9528	0.1953	0.192	.9393	0.7863	0.641	.8675	0.0081
0.169	.9618	0.2270	0.238	.9518	0.8303	0.576	.8751	0.0348
0.166	.9684	0.2503	0.275	.9591	0.8560	0.449	.8862	0.0739
0.171	.9736	0.2686	0.326	.9643	0.8743	0.395	.8918	0.0936
0.166	.9792	0.2883	0.365	.9716	0.9000	0.333	.8977	0.1144
0.201	.9858	0.3115	0.415	.9768	0.9183	0.312	.9029	0.1327
0.200	.9875	0.3175	0.514	.9837	0.9426	0.261	.9077	0.1496
0.252	.9976	0.3530	0.650	.9952	0.9831	0.232	.9129	0.1679
0.269	483.0032	0.3727	0.176	491.9220	0.7648	0.212	.9185	0.1876
0.300	.0084	0.3910	0.186	.9328	0.8029	0.190	.9237	0.2059
0.358	.0153	0.4153	0.221	.9397	0.8271	0.172	.9306	0.2302
0.395	.0195	0.4301	0.253	.9467	0.8518	0.174	.9411	0.2672
0.461	.0257	0.4519	0.292	.9533	0.8750	0.172	.9466	0.2865
0.515	.0309	0.4702	0.528	508.8938	0.5019	0.198	.9518	0.3048
0.541	.0361	0.4885	0.516	.9014	0.5287	0.205	.9570	0.3231
0.535	.0417	0.5083	0.448	.9070	0.5484	0.221	.9629	0.3439
0.513	.0483	0.5315	0.413	.9125	0.5677	0.266	.9688	0.3625
0.176	.9494	0.7033	0.357	.9181	0.5875	0.279	.9730	0.3794
0.165	.9570	0.7300	0.315	.9233	0.6058	0.317	.9786	0.3991
0.167	.9626	0.7497	0.278	.9295	0.6276	0.353	.9834	0.4160
0.166	.9681	0.7691	0.233	.9365	0.6522	0.418	.9886	0.4343
0.174	.9734	0.7877	0.208	.9417	0.6705	0.487	.9959	0.4600
0.201	.9796	0.8095	0.192	.9469	0.6888	0.542	514.0060	0.4956
0.233	.9872	0.8363	0.179	.9518	0.7061	0.412	517.8206	0.9222
0.275	.9938	0.8595	0.155	.9570	0.7244	0.517	.8275	0.9465
0.299	.9990	0.8778	0.151	.9622	0.7427	0.596	.8331	0.9662
0.325	484.0042	0.8961	0.139	.9677	0.7620	0.660	.8390	0.9869
0.410	.0105	0.9183	0.149	.9733	0.7817	0.665	.8466	0.0137
0.491	.0181	0.9451	0.179	.9820	0.8124	0.588	.8536	0.0384
0.584	.0234	0.9637	0.196	.9868	0.8293	0.509	.8591	0.0577
+0.641	.0286	0.9820	+0.240	.9920	0.8476	+0.431	.8650	0.0785

TABLE Ib. (Continued)

V—C	JD ⊙ 2435000+	Phase	V—C	JD ⊙ 2435000+	Phase	V—C	JD ⊙ 2435000+	Phase
+0m368	517.8706	0.0982	+0m230	522.9143	0.8507	+0m329	536.8485	0.8961
0.332	.8762	0.1179	0.261	.9196	0.8694	0.373	.8537	0.9144
0.284	.8821	0.1387	0.310	.9251	0.8887	0.448	.8592	0.9338
0.264	.8886	0.1616	0.359	.9307	0.9085	0.532	.8644	0.9521
0.225	.8935	0.1788	0.456	.9369	0.9303	0.606	.8700	0.9718
0.218	.8984	0.1961	0.161	534.8093	0.7187	0.649	.8773	0.9975
0.184	.9032	0.2129	0.168	.8169	0.7455	0.642	.8825	0.0158
0.184	.9084	0.2312	0.162	.8218	0.7627	0.586	.8877	0.0341
0.172	.9136	0.2496	0.158	.8270	0.7810	0.502	.8929	0.0524
0.172	.9202	0.2728	0.178	.8315	0.7969	0.442	.8992	0.0746
0.202	.9258	0.2925	0.190	.8364	0.8141	0.386	.9040	0.0915
0.214	.9338	0.3207	0.216	.8409	0.8300	0.348	.9089	0.1088
0.239	.9390	0.3390	0.240	.8454	0.8458	0.309	.9141	0.1271
0.259	.9442	0.3573	0.266	.8499	0.8616	0.266	.9190	0.1443
0.298	.9494	0.3756	0.305	.8544	0.8775	0.232	.9249	0.1651
0.327	.9546	0.3939	0.351	.8593	0.8947	0.217	.9290	0.1795
0.364	.9598	0.4122	0.396	.8642	0.9120	0.187	.9339	0.1968
0.414	.9654	0.4319	0.455	.8687	0.9278	0.187	.9388	0.2140
0.459	.9709	0.4512	0.504	.8742	0.9472	0.175	.9440	0.2323
0.528	.9789	0.4794	0.604	.8801	0.9679	0.170	.9516	0.2591
0.554	.9845	0.4991	0.646	.8853	0.9862	0.151	.9568	0.2774
0.543	.9900	0.5185	0.648	.8909	0.0060	0.178	561.6678	0.2545
0.498	.9960	0.5396	0.632	.8954	0.0218	0.185	.6758	0.2826
0.433	518.0018	0.5600	0.525	.9041	0.0524	0.364	574.6379	0.9063
0.362	.0074	0.5797	0.441	.9096	0.0718	0.533	.6494	0.9468
0.320	.0130	0.5994	0.413	.9145	0.0891	0.635	.6570	0.9736
0.288	.0182	0.6177	0.362	.9211	0.1123	0.666	.6629	0.9943
0.517	.8272	0.4653	0.277	.9273	0.1341	0.642	.6688	0.0151
0.559	.8348	0.4921	0.281	.9322	0.1514	0.620	.6737	0.0324
0.561	.8400	0.5104	0.242	.9381	0.1721	0.532	.6800	0.0546
0.522	.8456	0.5301	0.216	.9430	0.1894	0.458	.6848	0.0715
0.475	.8508	0.5484	0.199	.9485	0.2087	0.363	.6935	0.1021
0.397	.8578	0.5730	0.167	.9558	0.2344	0.344	.6987	0.1204
0.360	.8630	0.5913	0.172	.9610	0.2527	0.298	.7043	0.1401
0.313	.8678	0.6082	0.534	535.8804	0.4885	0.254	.7129	0.1704
0.271	.8737	0.6290	0.527	.8881	0.5156	0.238	.7174	0.1862
0.251	.8779	0.6438	0.510	.8930	0.5329	0.216	.7227	0.2049
0.221	.8831	0.6621	0.459	.8982	0.5512	0.174	.7272	0.2207
0.200	.8887	0.6818	0.402	.9034	0.5695	0.187	.7317	0.2365
0.190	.8904	0.6878	0.368	.9086	0.5878	0.187	.7366	0.2538
0.153	.8980	0.7145	0.315	.9138	0.6061	0.190	.7428	0.2756
0.229	.9352	0.8455	0.278	.9190	0.6244	0.215	.7515	0.3062
0.256	.9407	0.8648	0.267	.9238	0.6413	0.215	.7567	0.3245
0.301	.9463	0.8845	0.225	.9291	0.6600	0.220	.7619	0.3428
0.350	.9522	0.9053	0.199	.9346	0.6793	0.260	.7675	0.3625
0.454	.9602	0.9334	0.180	.9398	0.6976	0.315	.7734	0.3833
0.541	.9661	0.9542	0.156	.9475	0.7247	0.223	594.6473	0.3351
0.615	.9716	0.9736	0.155	.9530	0.7441	0.265	.6553	0.3632
0.357	522.8400	0.5892	0.149	.9579	0.7613	0.292	.6605	0.3815
0.270	.8508	0.6272	0.150	.9631	0.7796	0.322	.6654	0.3988
0.233	.8588	0.6554	0.152	.9683	0.7979	0.365	.6706	0.4171
0.203	.8643	0.6747	0.153	536.8012	0.7296	0.417	.6762	0.4368
0.185	.8696	0.6934	0.140	.8096	0.7592	0.463	.6821	0.4576
0.172	.8748	0.7117	0.157	.8141	0.7751	0.504	.6876	0.4769
0.155	.8800	0.7300	0.168	.8190	0.7923	0.533	.6932	0.4966
0.140	.8852	0.7483	0.177	.8238	0.8092	0.508	.6987	0.5160
0.138	.8904	0.7666	0.185	.8287	0.8264	0.477	.7043	0.5357
0.146	.8959	0.7860	0.224	.8335	0.8433	0.416	.7119	0.5625
0.180	.9015	0.8057	0.258	.8377	0.8581	+0.350	.7178	0.5832
+0.224	.9088	0.8314	+0.299	.8436	0.8789			

TABLE Ic. Yellow observations of XY Leo, Flower and Cook Observatory.

V—C	JD ⊙ 2436000+	V—C	JD ⊙ 2436000+	V—C	JD ⊙ 2436000+
+0m030	296.5518	+0m276	296.5668	+0m266	296.5952
+0.059	.5529	+0.294	.5709	+0.145	.6015
+0.096	.5581	+0.392	.5820	+0.117	.6025
+0.105	.5591	+0.372	.5862	+0.102	.6060
+0.200	.5636	+0.329	.5872	+0.099	.6070

TABLE Ic. (Continued)

V—C	JD ⊙ 2436000+	V—C	JD ⊙ 2436000+	V—C	JD ⊙ 2436000+
+0^{m}079	296.6108	+0^{m}152	297.5597	+0^{m}212	297.5861
+0.047	.6119	+0.152	.5608	+0.191	.5872
+0.050	.6154	+0.205	.5639	+0.166	.5903
+0.023	.6164	+0.202	.5650	+0.153	.5913
−0.047	297.5347	+0.233	.5681	+0.106	.5958
+0.024	.5406	+0.226	.5691	+0.098	.5969
+0.042	.5417	+0.257	.5726	+0.071	.5997
+0.046	.5448	+0.254	.5736	+0.060	.6007
+0.030	.5458	+0.255	.5768	+0.037	.6038
+0.052	.5490	+0.252	.5778	+0.037	.6049
+0.073	.5500	+0.250	.5820	+0.029	.6080
+0.085	.5552	+0.227	.5830	+0.014	.6090

3. EPOCH AND PERIOD

The newly observed heliocentric times of minimum light are listed in the first column of Table III. From a least-squares solution of the weighted minima from 1953 to 1956 light elements were determined as

$$\text{Pr. Min.} = 2435195.66306 + 0.2841091\ E.$$
$$\pm 1 \text{ (p.e.)} \quad \pm 9 \text{ (p.e.)}.$$

From these elements the residuals for all determinations of minimum light have been computed. They are plotted in Fig. 2 as a function of time. It can be seen that the light elements given above do not satisfy the other observed minima. From 1956 to early 1958 the period had apparently decreased by about 0^d.000002. It should be noted that the alternate minima seem always to have been separated by half a period. The orbit may thus be assumed circular.

In order to compute the phases of the observations listed in Table I the epoch of light variation was rounded off to four decimals and the period to six.

4. OUTSIDE ECLIPSE VARIATIONS

A night-by-night plot of the observations revealed that, with the possible exception of those on JD 2435489 and 2435594, all points could properly be collected into a mean light curve. Analysis of the variations outside eclipse was done by the method of Russell and Merrill (1952). The coefficients, in intensity units of +0.0001, are given in Table IV. For a single observation the probable residual in magnitudes from the computed variation is listed in the last column. While the terms in $\cos 3\theta$ are small and near the limit of accuracy of th observations, it appears that they are real. Indeed alternative determinations of the variations outsid eclipse always uncovered such terms. Terms higher tha $\cos 3\theta$ and $\sin 2\theta$ have coefficients smaller than 0.0010

TABLE II. Magnitudes and colors of comparison stars and XY Leo.

Star	V	$B-V$
BD+18°2306	+9^{m}60±0^{m}04	+0^{m}67±0^{m}01
BD+18°2308	9.55±0.04	0.30±0.01
XY Leo, 0^{p}00	9.92	1.01
XY Leo, 0.25	9.48	0.96
XY Leo, 0.50	9.82	1.00
XY Leo, 0.75	+9.47	+0.96

5. RECTIFICATIONS AND SOLUTIONS

Reflection of the observations about the minim shows secondary to be symmetric and the asymmetry giving rise to the $\sin\theta$ and $\sin 2\theta$ terms to persist withir primary. The bottom of primary minimum is reason ably symmetrical so that removal of the complicatior terms increases slightly the scatter of the deep ob servations but does not affect the depth of eclips appreciably. Within secondary minimum the $\sin\theta$ anc $\sin 2\theta$ terms have opposite algebraic signs, and becaus their coefficients differ at most only in the third decimal these terms have little effect on the shape and depth of the minimum. Various trials for subtracting o dividing out the $\sin\theta$ and $\sin 2\theta$ terms showed the rec tified observations to be insensitive to the choice o procedure. Since there is no theoretical indication tha these terms are associated with areas of constant brightness on either component or on both of them, it was decided to subtract these terms from the obser vations at every phase.

Similar attempts were made to discover if the $\cos 3\theta$ term is best subtracted or divided out, and again the shapes and depths of the rectified minima depend little

TABLE III. Times of minimum light, XY Leo.

JD ⊙ 2430000+	E	$O-C$
5484.0337	+1015	−0^{d}0001
5513.8652	1120	−0.0001
5517.8430	1134	+0.0002
5517.9848	1134.5	0.0000
5534.8892	1194	−0.0001
5536.8782	1201	+0.0001
5574.6646	1334	0.0000
5594.6941	1404.5	−0.0002
6296.5812	3875	−0.0046
6297.5756	+3878.5	−0.0046

t the choice. It was finally decided to include this rm specifically in the rectification for ellipticity.

The yellow observations of JD 2435594 are not col- cted into a mean curve. The equations of rectification yellow light are

$$^{\text{ref}}(y)=0.0326+0.0170\cos\theta+0.0109\cos2\theta,$$

$$'(y)=\frac{g'(y)}{1.0160-0.1019\cos2\theta-0.0016\cos3\theta},$$

$$Nz(y)=0.4605.$$

For the mean coefficient of limb darkening values of 6, 0.8, and 1.0 were investigated. These trials showed 8 to be slightly preferable to the other values, but om one value to another the change was small. With iis rectification the best solution of the yellow ob- rvations shows primary eclipse to be annular and etermines the elements listed in column 2 of Table V.

The blue observations of JD 2435489 and 2435594 em to differ sufficiently from the others at this wave- ngth so that they should be studied separately. ccordingly, these are not combined into the mean ue curve, and it is concluded that the light curve aries in form.

The equations of rectification in blue light are

$$^{\text{ref}}(b)=0.0326+0.0100\cos\theta+0.0109\cos2\theta,$$

$$'(b)=\frac{g'(b)}{0.7963-0.0856\cos2\theta-0.0010\cos3\theta},$$

$$Nz(b)=0.5125.$$

gain, various darkening coefficients were investigated. or $x=0.8$ the eclipses yield the solution listed in olumn 3 of Table V.

The solutions described above are the best which n be derived at each wavelength, but they are not

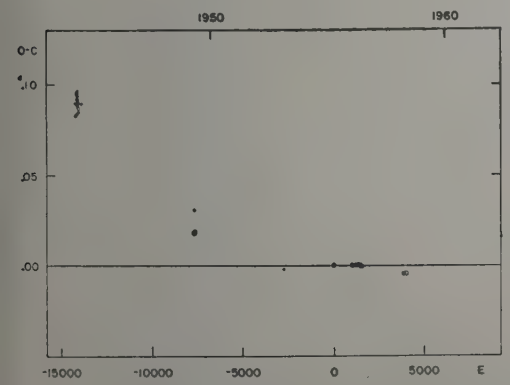

FIG. 2. Residuals from linear elements for XY Leo. The filled cles refer to primary eclipse and the open ones to secondary. he large symbols represent photoelectric observations and the all ones visual observations or estimates.

TABLE IV. Outside-eclipse variations, XY Leo.

Light curve	A_0	A_1	A_2	A_3	B_1	B_2	Residual
Yellow	+9834	−170	−1128	−16	−68	−62	±0m006
Blue	+7638	−100	−965	−10	−60	−50	±0.008

equally satisfactory. In yellow light the depths and the shapes of both minima definitely point to one consistent solution. At the shorter wavelength the shape of secondary minimum is aberrant, and the depth of secondary eclipse is too great to provide strict agreement with the solution for yellow light. The physical cause of this departure from the theoretically expected result may lie in the radiation from the interior hemisphere of the cool star. This is the area which Struve and Zebergs found to show strong *Ca*II emission. Though the spectrographic and photometric observations were made years apart, it may be that this disturbance is stable and distorts the light curve.

It should be emphasized that the tabulated solutions were not the only ones tested. For instance, a change in the mean darkening coefficient does not remove the discrepancies nor does an attempt at allowing for a difference in darkening for the two components. As a final check, theoretical light curves were computed from the depth relation at intervals of 0.1 in k. The possibilities of primary eclipse being either a transit or an occultation were each investigated. The theoretical curves agree best with the observations when primary eclipse is a transit and k is close to 0.4, just as predicted by the original nomograph solution.

6. DISCUSSION

The solutions discussed in the last paragraph have been summarized before (Koch 1959), but they do not agree with the spectroscopy published subsequently. In the observations of Struve and Zebergs two sets of absorption lines are visible, and each set shows the harmonic behavior characteristic of a component of a

TABLE V. Orbital solutions for XY Leo.

	Yellow	Blue	Limiting Yellow
x	0.8	0.8	0.8
k	0.373	0.397	0.618
a_g	0.518	0.519	0.398
b_g	0.476	0.473	0.368
a_s	0.193	0.206	0.246
b_s	0.177	0.188	0.228
$\alpha_0^{\text{pr}}=\alpha_0^{\text{tr}}$	1.028	1.000	1.100
$\alpha_0^{\text{sec}}=\alpha_0^{\text{oc}}$	1.000	1.000	1.000
j	73°3	73°3	90°0
$L_g=L_h$	0.904	0.906	0.748
$L_s=L_c$	0.096	0.094	0.252
$L_g'=L_h'$	0.882	0.886	0.713
$L_s'=L_c'$	0.088	0.073	0.228
$\langle J_h'/J_c'\rangle_{\text{av}}$	1.4	1.9	1.2
z	0.144	0.160	0.144
D	0d063	0d065	0d063

TABLE VI. Limiting dimensions and magnitudes for XY Leo.

	$Star_h$	$Star_c$
Radius	0.63 ⊙	0.39 ⊙
Mass	0.37 ⊙	0.47 ⊙
Density	1.2 ⊙	1.6 ⊙
V	$+10^m87$	$+12^m11$

double star. From the photometric solutions of Sec. 5, however, the ratio of the blue luminosities is on the order of 10:1 so that only one set of lines should be visible.

A possible way out of the dilemma can be indicated. It has already been mentioned that the shapes of the minima in yellow light are accordant, but in the neighborhood of the solution the shape curves run almost parallel to each other rather than intersecting at a decisive angle. There are then a large number of consistent orbital solutions, but the depth line is required for determinacy. The coordinates of the line can be erroneous if there is third light in the system. Lacking spectroscopic proof of this situation one can only make a limiting solution for central eclipses. This has been done and the elements listed in column 4 of Table V. The net effect on the solution has been the derivation of sizes and brightnesses which make the components members of a recognizable W UMa-type system. On the basis of his photometry Kwee (1956) found this device necessary for a solution for W UMa itself. For XY Leo the limit of the third light amounts to 62% of the observed visual brightness of the system, so that a search for the lines of a third star is in order. Should this not be found, careful spectrophotometry would be desirable in order to test the hypothesis of an extensive, luminous shell enveloping the eclipsing pair. So far as photometry itself can go, there is already an indication of third light independent of the orbital solution. Both stars are probably early K type, and the colors discussed in Sec. 2 suggest reddening of about 0^m1 in both $(B-V)$ and $(U-B)$.

The observed difference in visual light between the components is 1^m2 in the limiting solution so that XY Leo would be a double line binary. A legitimate combination of the spectroscopic and photometric solutions, necessarily viewed with much reservation, is then possible. The limiting absolute radii, masses, and densities in solar units and the apparent visual magnitudes are listed in Table VI. Taken at face value these properties describe single M-type stars more closely than K-type stars, but they are on the proper orders of magnitude. Also, for this solution the larger hot star very nearly fills its lobe of the Jacobian surface at least on its outer, cooler hemisphere.

If the correct depth of secondary eclipse were known for the blue observations, the geometry of the limiting solution would presumably be applicable to both light curves.

7. SUMMARY

It is certain that the limiting solution discussed above is wrong, but the degree to which it is incorrect remains unknown. For instance, it is felt that a strong case has been made for the presence of third light, but the percentage of it is conjectural. Similarly, it is not known whether the run of the residuals with time is due to an intrinsically variable period or to light time in an orbit around a third star. These matters and others discussed above indicate that this binary will repay further observation.

ACKNOWLEDGMENTS

This research was done under the same circumstances as the work on AS Eri, and the assistance acknowledged in my paper [1960, *Astron. J.* **65**, 139)] on that star was available for the study of XY Leo. I would also like to thank Dr. P. C. Keenan for his spectrogram and its classification and Dr. O. Struve and Dr. V. Zebergs for the use of their paper in advance of publication.

REFERENCES

Ashbrook, J. 1952, *Astron. J.* **57**, 63.
——. 1953, *ibid.* **58**, 171.
Hoffmeister, C. 1934, *Astron. Nach.* **253**, 199.
Hubble, E. 1934, *Astrophys. J.* **79**, 55.
Johnson, H. L. 1955, *An. d'Ap.* **18**, 292.
Koch, R. H. 1956, *Astron. J.* **61**, 47.
——. 1959, *ibid.* **64**, 52.
Kwee, K. K. 1956, *Bull. Astron. Inst. Neth.* **12**, 330.
Russell, H. N. and Merrill, J. E. 1952, *Contr. Princeton Univ. Obs.* **26**, 54.
Struve, O. and Zebergs, V. 1959, *Astrophys. J.* **130**, 137.
Vyssotsky, A. N. and Balz, Jr., A. G. A. 1958, *Publ. McCormick Obs.* **13**, 59.
Zessewitsch, V. P. 1954, *Izvest. Astron. Obs. Odessa* **4**, 179.

Periods of Fifty-Eight Mira-Type Variables

BALFOUR S. WHITNEY
University of Oklahoma Observatory, Norman, Oklahoma
(Received April 22, 1960)

New periods or epochs have been determined for 42 Mira-type stars. For 16 others, epochs and residuals are provided which may be useful in future studies of their periods.

THIS study was undertaken at the request of Dr. B. V. Kukarkin, President of Commission 27 of International Astronomical Union, who supplied a of 50 stars for which observations were needed. r stars of this list, CN and V547 Aql, BK Cyg, and Sgr, were fainter than the plate limits on all of the plates of their fields in the observatory collection. The plates available for four others, V598 Cyg, VW and ES Del, and RX Vul, were insufficient to provide dates of maxima. A few stars were added to the original list.

New or revised elements are marked with asterisks in columns 2 and 3 of Table I. The pairs of numbers in

TABLE I. Elements and residuals.

tar	E_0 −240000	P	Epochs and residuals
And	28479	177d5*	37,0; 39,−3; 40,−2; 41,−2; 43,1; 45,−5.
Aql	33109*	332.7	0,2; 7,−1; 8,−4; 9,6; 10,0.
Aql	35392*	236:*	−3,1; 0,0; 4,33; 6,5.
5 Aql	27336	292.4*	29,4; 31,−1; 32,−10.
Aur	29200	695	8,−48; 9,−360.
Aur	29625	186.8*	33,1; 37,7; 39,−6.
Cam	27157	285.2	23,−28; 24,−18; 27,5.
Cam	26568	254.2	28,12; 29,10; 31,2; 32,10.
Cam	32425*	411.9*	−1,14; 0,0; 1,−6; 2,0; 3,1; 4,−22; 5,−42:; 8,−5:; 10,0:.
Cam	32490*	362*	−2,−18:; −1,4; 0,−10; 1,10; 2,6; 3,−6; 4,0:; 5,−5; 6,−1; 7,−9:; 9,16:.
CMa	34399*	345:*	0,0; 2,−1:; 4,0:; 6,1:.
Cas	28723	371.7	5,−2; 7,25; 8,−7; 9,−13; 10,20.
Cas	32812*	362.1*	0,−17; 1,6; 2,−1; 3,22; 4,0; 5,−22:; 9,9:; 10,−3:.
Cas	28723*	398.4*	5,5; 7,28; 8,10; 9,21; 10,−37; 11,5; 12,1; 13,−2; 14,−16; 15,1; 16,23:.
Cas	32823*	300.1*	−7,−2; −5,8; −4,7; −2,7; 0,−3; 1,−8; 4,−3; 5,−4; 7,−4; 10,6:.
Cep	34397	277.3	−7,2; −6,25; −4,12; −3,0.
Cep	29440	800:*	3,−130; 4,140:; 5,70:; 6,−90:; 7,−40:.
Cyg	33202*	298.4	−1,−20:; 0,3,; 1,5; 2,−5; 3,3; 5,−9; 6,−2:; 10,−26:.
Cyg	29796	296.3	10,6; 11,5; 12,3:; 13,2; 14,−4; 15,0; 16,−37:; 21,−6:.
Cyg	33072	263	−1,−1; 2,4; 3,3; 6,6.
Cyg	33109*	258.0	−1,−6; 0,7; 2,2; 3,2; 6,−4.
Cyg	24500	284*	29,10; 31,−4:; 32,−6; 33,−28:.
Cyg	28465	352.1	15,+26:; 16,+20:; 19,+23:.
Cyg	26955	458.8*	15,−1; 16,0.
Cyg	29461	338.6*	11,0; 12,6; 13,−7.
Cyg	34194	163.9	−9,11; −8,−3:; −4,22; −2,44.
5 Cyg	33220*	320*	0,−10; 1,0; 2,5; 3,15; 8,−10; 9,0:.
Del	31060*	236.6	−2,3; 3,−10; 4,−1; 6,0; 7,−6; 9,16:; 14,−2:; 18,1:; 20,8; 21,−4:; 23,−2:.
Del	30608*	249.2*	0,0; 1,−7:; 3,4:; 6,7; 7,−22:; 9,−1; 10,−7; 19,5.
Del	31644*	195.2*	−5,7; −4,21; −1,−9; 0,1; 2,−4; 4,−5; 6,8; 8,−1; 19,−3; 21,7; 25,−4:.
SZ Del	26339	236.0*	24,31:; 32,−11; 37,4; 44,−3.
WX Del	25850	526	9,36; 11,−11; 14,−14; 16,34:; 18,22:.
AG Del	26175	239.6*	32,−1; 34,−3; 44,3.
AN Del	26920	194.6*	19,−4; 22,−1; 23,10; 25,−1; 26,−10:; 27,−24; 28,1:; 30,12; 32,−2; 36,−6:; 38,−15:; 41,1:; 45,13:; 47,17; 49,−5.
BB Del	25750	245.4*	20,7; 21,−33:; 23,−14; 24,−20; 26,15; 27,4:; 29,−42; 30,33; 33,12:; 35,−9:; 38,5:; 39,−1:; 41,−1; 42,3:; 44,−32:.
SY Dra	27986	387.7*	7,4; 9,−7; 10,−1; 11,6.
SX Eri	33212	281.6	−10,14; −9,12; −6,6; −5,16; −4,4.
SX Eri	32086*	284.5*	0,4; 2,5; 4,−4; 5,12; 7,2; 8,−2; 12,−6; 13,6:; 17,8:.
UV Eri	26325	432.6*	10,−8; 12,12; 15,−4; 16,3; 17,−27; 21,20:; 22,13:.
BK Her	28298	215.0	38,17:.
DF Her	28620	337.5*	21,12; 22,−45:; 23,18:.
FQ Hya	36720*	355:*	−4,10; −1,10; 0,0.
FT Hya	33358	150:*	10,0:; 13,12:; 20,8.
BC Mon	29670	272.31	8,2; 9,−11; 11,−25; 13,0; 19,−14; 20,14; 23,17:; 24,15:.
BD Mon	27860	366	11,47:.
IK Mon	28495	387	9,13:; 17,−7:; 19,−7:; 20,−7; 21,6:.
AI Oph	35690*	420*	−9,2; −8,−2; −1,−5:; 0,2.
V374 Oph	27957	213.8*	19,−4; 22,−17; 24,−3; 36,8.
V389 Oph	27246	315*	15,−1; 16,0; 27,−3; 29,−5.
TU Peg	33880	322.00	−1,2; 0,0; 1,−2; 2,1; 3,14; 7,1; 9,6.
TV Peg	33851*	247.0	−4,−1; 3,10:; −1,−4; 0,19; 2,−15; 3,3; 9,−4.
AP Peg	32820	300	0,20:; 1,10:; 4,5; 5,0; 6,5; 7,0; 11,−10:.
EG Peg	28003	339.4*	14,−5; 15,4:; 17.9; 21,−12; 25,−21:.
GG Per	28580	277.7*	25,0; 26,1; 27,3.
AH Sgr	35332*	343	0,0; 1,−3; 2,−6; 3,3.
V Sct	12974	252.9*	78,−13; 90,7; 91,5.
SV Sct	13103	310	72,−25:; 74,27:; 75,41:.
WW Ser	33405*	366.6*	0,−3; 1,−2; 2,−1; 8,4; 9,1.
BG Ser	19887	143	98,−41:; 115,28; 118,0.
WX Vul	26189	280.7*	25,−3; 26,2; 30,−1.

column 4 are first, the epoch and second, the residual, *O-C*, both computed with the elements in columns 2 and 3. A colon following a number indicates uncertainty or possibility of abnormal error in the number so marked.

Notes on four stars of Table I follow:

DI Cas. The elements in the first line are of Florja (1949). Those in the second line fit the observations following JD 2432800.

V429 Cyg. This star was fainter than the plate limit (13.5–14.0) on all blue plates. The maxima were determined from estimates of photovisual plates.

AH Sgr. Residuals of the four maxima, computed with the catalogue elements, were close to one-half the period. Perhaps the period in Table I should b halved.

WW Ser. Two maxima deduced from observation by Mündler (1929) gave the epochs and residuals −23,2; −22,0. Eight from observations by Olivier *et a* (1940) gave: −20,17:; −18,54:; −17,57:; −16,51 −15,36; −14,22; −14,22; −12,34:; −11,18.

This work was supported by a grant from th National Science Foundation. Publication costs wer met by the Faculty Research Fund Committee of thi University.

REFERENCES

Florja, N. F., 1949, *Sternberg Pub.* **16**, 187.
Mündler, M., 1929, *Astron. Nach.* **235**, 81.
Olivier, C. P. *et al.*, 1940, *Publ. Univ. of Pennsylvania, Astr. Seri* V, Part III, 45.

THE ASTRONOMICAL JOURNAL VOLUME 65, NUMBER 6 AUGUST, 196

Parallax and Mass-Ratio of the Visual Binary Ho 581 from Photographs Taken With the Sproul 24-Inch Refractor

LAURENCE W. FREDRICK*
Sproul Observatory, Swarthmore College, Swarthmore, Pennsylvania
(Received April 4, 1960)

Measurement and reduction of plates taken with the Sproul refractor over the intervals 1919–1923 and 1934–1958 yield $+0''.016 \pm 0''.004$ for the relative parallax and $+0''.079 \pm 0''.004$ for the semi-axial major of the photocentric orbit. An absolute parallax of $=0''.0181 \pm 0''.004$ was adopted.

The small value of the parallax does not permit a good determination of the combined mass of A and B. The mass function is found to have the unusual value of 0.32 to 0.68, the fainter component being the more massive.

THE visual binary Ho 581 = BD+41°3535 = ADS 13125 = HD 188753; $19^h51^m.6$, +41°36′ (1900), has a period of $25^y.69$ and has been observed since 1895. The apparent visual magnitude is 7.36 and the spectral type is dK0.

A parallax determination by Miller (1926) from photographs taken at Sproul during 1919–1923 yielded $+0''.001 \pm 0''.011$ for the relative parallax. Observations began again in 1934 and continued through 1958 in order to cover the orbit as well as obtain a parallax.

TABLE I. Normal places of residuals.

Epoch	Σp	Σn	v_x unit 0.0001	v_y mm
1921.63	30	30	+3	−3
38.36	11	8	−1	−2
44.21	36	14	−9	+2
49.23	35	14	+1	+4
53.40	30	14	−2	+1
57.19	40	17	+6	−4

* Now at Lowell Observatory.

The procedure of van de Kamp and Lippincott (194 was followed. A total of 803 exposures were measured o 262 plates taken on 97 nights with a total weight of 18. The recent exposure times were about 12 min. Fou reference stars of average photovisual magnitude 10. were used. Ho 581 has been reduced 2.8 mag. by mean of a rotating sector. All plates have been measured b the author on the Gaertner measuring machine.

The images on the Sproul plates are well blende since the separation of the two components nev exceeds $0''.45$ or $0^{mm}.024$; it is assumed the weighte center of light has been measured. The solution wa made from the nightly means using the equations condition,

$$\xi = c_x + \mu_x t + \pi P_\alpha + \alpha Q_\alpha,$$
$$\eta = c_y + \mu_y t + \pi P_\delta + \alpha Q_\delta,$$

where the symbols have their usual meaning, t counted from 1950.000.

The orbital factors (Q_α, Q_δ) were determined fro the elements given by Van Biesbroeck (1927):

$$P = 25^y.69 \quad e = 0.52 \quad T = 1911.37$$
$$\omega = 245°.0 \quad \Omega = 34°.6 \quad i = 39°.2.$$

Separate solutions in right ascension and declination ›ld

	p.e.	wt
$\mu_x = -0^{mm}.001375 = -0''.02595 \pm 0''.00022$		22 663
$\mu_y = +0.015398 = +0.29056 + 0.00024$		14 936
$\pi_x = +0.000780 = +0.0147 \pm 0.0043$		60.40
$\pi_y = +0.001092 = +0.0206 \pm 0.0075$		15.11
$\alpha_x = +0.004845 = +0.0914 \pm 0.0065$		26.22
$\alpha_y = +0.003596 = +0.0678 \pm 0.0054$		29.24

›. $1_x = \pm 0.00175 = \pm 0.0331$
›. $1_y = \pm 0.00154 = \pm 0.0290$.

ıe agreement between the values determined from x ıd y separately is good for π and fair for α. The com- ıed solution for both coordinates yields

	p.e.	wt
$\mu_x = -0^{mm}.001367 = -0''.02580 \pm 0''.00020$		24 254
$\mu_y = +0.015381 = +0.29024 \pm 0.00023$		18 720
$\pi = +0.000830 = +0.0157 \pm 0.0036$		75.55
$\alpha = +0.004182 = +0.0789 \pm 0.0042$		55.48

›. $1 = \pm 0.00164 = \pm 0.0309$.

The residuals from this solution reveal no significant nd or deviations (Table I).

The present value for the relative parallax $+0''.0157$ $\pm 0''.0036$ supersedes the earlier Sproul determination ›sed on part of the present material. For the reference stars, at galactic latitude $+9°$, an annual parallax of $0''.0024$ is found according to Vyssotsky (1948) and $0''.0029$ according to Binnendijk (1943). Adopting the mean $0''.0026$, we find $+0''.0183 \pm 0''.0036$ (p.e.) for the absolute parallax of Ho 581.

The masses are evaluated in the usual manner (van de Kamp 1945). The difference in magnitude of the two components is 0.5 according to Van Biesbroeck (1927), from which $\beta = 0.387$. Using $0''.27$ for the semi-axis major, as communicated by Van Biesbroeck, we have $B - \beta = 0.292$, whence $B = 0.679$. This yields the rather unusual mass ratio: $M_B/M_A = 2.1$. The sum of the masses is found to be $M_A + M_B = 5.1\odot$, hence the individual masses are $M_A = 1.6\odot$, $M_B = 3.5\odot$. These values are uncertain. The absolute visual magnitudes of the two components are found to be 4.2 and 4.7, thus placing them both slightly above the main sequence at K0 in the H-R diagram.

This investigation was partially supported by a grant from the National Science Foundation.

REFERENCES

Binnendijk, L., 1943, *Bull. Astron. Inst. Neth.* **10**, 9.
Miller, J. A., 1926, *Sproul Obs. Publ.* No. 8, 52.
Van Biesbroeck, G., 1927, *Yerkes Publ.* No. 5 (I), 246.
van de Kamp, P., 1945, *Astron. J.* **51**, 161.
van de Kamp, P. and Lippincott, S. L., 1949, *Astron. J.* **55**, 16.
Vyssotsky, A. N. and Williams, E. T. R., 1948, *Publ. McCormick Obs.* **10**, 33.

Parallax and Orbital Motion of Hu 575 = ADS 9352 From Photographs Taken With the 24-Inch Sproul Refractor

Sarah Lee Lippincott
Sproul Observatory, Sarthmore College, Swarthmore, Pennsylvania

(Received April 4, 1960)

Measurement and reduction of plates taken with the Sproul refractor over the interval 1933–1959 yield $+0''.046 \pm 0''.007$ (p.e.) for the mean relative parallax of ADS 9352 AB and its distant proper motion companion C and $+0''.014 \pm 0''.016$ for the semi-axis major of the photocentric orbit of AB. The small value of the parallax combined with the uncertainty in the orbital elements does not permit a good determination of the combined mass of A and B. The mass ratio is found to be 0.55 to 0.45.

HE visual binary ADS 9352 = Hu 575; $14^h38^m.0$ $+19°55'$ (1900) has a period 51.29 (Dommanget 51), and semi-axis major $0''.63$ (Muller 1951). The nbined visual magnitude is 9.08 with $\Delta m = 0.28$ ggen 1956). Van de Kamp (1936, 1939) discovered proper motion companion C, BD $+20°3009$, at a tance of 135″ in a position angle 309°. In the current estigation, both AB and C were measured. The otovisual magnitude of C is 10.06 (Eggen 1956). The ctra of AB and C are M0 (Vyssotsky 1946).

The procedure described in previous Sproul publi- ions has been followed (van de Kamp and Lippincott 9). ADS 9352 C appears fainter than desirable on ny plates so that often lower weights were given to plate solutions and occasionally C was not measured. A total of 508 exposures for AB and 499 for C were measured on 171 plates taken on 60 nights with total weights of 123 and 102, respectively. The regular exposure was $2\frac{1}{2}$ min. from 1946 on. The brightness of ADS 9352 was reduced 2.0 mag. by means of a rotating sector. The plates were measured on the St. Clair-Kasten machine by Mrs. Mary Jackson.

The orbital factors were computed from Dommanget's (1951) elements except for a which is taken from Muller's determination (1951), since subsequent observations show Dommanget's value to be too small:

$P =$	$51^y.29$	$i =$	$122°.18$
$e =$	0.066	$\omega =$	38.40
$T =$	1931.61	$\Omega =$	$+2.53$.

Separate solutions in right ascension and declination yield the following results:

AB		p.e.	wt
μ_x	$=-0.0138173^{mm}=-0''.26073\pm0''.00295$		362
μ_y	$=-0.0093471=-0.17638\pm0.00076$		2579
π_x	$=+0.001772=+0.0334\pm0.0093$		35.36
π_y	$=+0.002013=+0.0380\pm0.0134$		8.29
α_x	$=-0.007958=-0.1502\pm0.0636$		0.78
α_y	$=+0.001467=+0.0277\pm0.0134$		8.60
p.e. 1_x	$=\pm0.00297=\pm0.0560$		
p.e. 1_y	$=\pm0.00206=\pm0.0389$		

C			
μ_x	$=-0.0136923^{mm}=-0''.25837\pm0''.00105$		3612
μ_y	$=-0.0093680=-0.17677\pm0.00078$		3567
π_x	$=+0.002649=+0.0500\pm0.0117$		29.68
π_y	$=+0.004089=+0.0772\pm0.0173$		7.26
p.e. 1_x	$=\pm0.00334=\pm0.0630$		
p.e. 1_y	$=\pm0.00248=\pm0.0468.$		

A combined solution for π and α in both coordinates was made for AB and a similar solution for C. The agreement of the μ and π values leaves no doubt about the physical connection between AB and C.

A joint solution for AB and C was, therefore, made for parallax, combining right ascension and declination, with the following results:

	AB	C
μ_x	$=-0''.25341$	$-0''.25840$
μ_y	$=-0.17592$	-0.17659
α	$=+0.014\pm0''.016$	
$\pi_{AB,C}$	$=+0.00241^{mm}=+0''.046$	
p.e. $1_{AB,C}$	$=\pm0.0026^{mm}=\pm0''.049.$	

The parallax determinations of AB and C are not independent (van de Kamp and Damkoehler 1953). This is borne out by the similar trends in the normal points given in Table I based on residuals from the joint solution. For further use, we adopt $+0''.046\pm0''.007$ for the relative parallax and probable error of the AB, C system.

The reduction to absolute parallax is made in the usual manner (Lippincott 1958), considering the average magnitude and spectral type of the three star

TABLE I. Normal points of residuals.

	AB					C			
Epoch	Σn	Σp	v_x unit	0.0001	v_x mm	Σp	v_x unit	0.0001	m
1936.08	5	6	+16		+ 2	5	+ 4		+
40.14	7	11	+ 3		−10	10	+ 7		−
43.36	5	10	−14		− 1	10	−13		+
46.11	5	10	+ 2		+ 3	8	+ 6		−
47.56	9	22	−12		+ 8	19	− 4		−
49.79	10	26	+ 8		− 4	21	+ 3		+
52.35	10	18	0		+ 2	13	− 3		+
57.23	4	9	− 3		+ 8	8	−12		+
59.32	5	11	+ 6		− 9	8	+19		−

reference system, 11.6, G7, at galactic latitude +62 The present material thus yields $\pi_{abs}=+0''.050\pm0''.0$

The only other trigonometric parallax determinati for ADS 9352 was carried out at the McCormick O servatory: $\pi_{abs}=+0''.023\pm0''.013$ (Jenkins 1952). T weighted mean absolute parallax adopted for furth use is $+0''.044\pm0''.006$. With this value, the adopt $a=0''.63$ gives 14 ± 2 a.u. yielding $M_A+M_B=1.$ $\pm0.46\odot$, the p.e. in both cases arising solely from t p.e. of the parallax. Adopting Eggen's value $\Delta m=0.2$ $\beta=0.43$, we derive the mass ratio $B=\alpha/a+\beta=0.$ ±0.02 (p.e.) taking into account only the p.e. of α.

Thus, we find $M_A=0.61\odot$ and $M_B=0.50\odot$, valu which must be taken with reservation in view of t large percentage error in the sum of the masses. T absolute visual magnitudes for the A, B, and C cor ponents are 7.9, 8.2, and 8.3, respectively.

This investigation was partially supported by grant from the National Science Foundation.

REFERENCES

Dommanget, J. 1951, *Ann. Obs. R. Bel.* **5**, 181.
Eggen, O. J. 1956, *Astron. J.* **61**, 372.
Jenkins, L. F. 1952, *General Catalogue of Trigonometric Stel Parallaxes.*
Lippincott, S. L. 1958, *Astron. J.* **63**, 230.
Muller, P. 1951, *Bull. Astron.* **16**, 208.
van de Kamp, P. 1936, *Publs. Astron. Soc. Pacific* **48**, 313.
van de Kamp. P. 1939, *Astron. J.* **48**, 80.
van de Kamp, P. and Damkoehler, J. E. 1953, *Astron. J.* **58**, 2
van de Kamp, P. and Lippincott, S. L. 1949, *Astron. J.* **55**, 16.
Vyssotsky, A. N. 1946, *Astrophys. J.* **104**, 234.

The Elements and Ephemeris of Comet Wirtanen 1948 *b*

PAUL HERGET
Cincinnati Observatory, Cincinnati, Ohio
(Received May 20, 1960)

A numerical integration and orbit correction were made for the orbit of Periodic Comet Wirtanen 1948 *b*. The orbit correction is based on 23 observations, nine in 1948, 14 in 1954. The ephemeris for the 1961 apparition is furnished.

OMET Wirtanen, 1948 *b*, was discovered at the Lick Observatory on January 17, 1948, observed ne times during 54 days in 1948, and 14 times during days in 1954. The following elements (Table I) and hemeris (Table II) were derived by means of the

TABLE I. Elements.

och 1947 Dec. 1.0 ET=JDE 2432520.5				
359°71618		(1950.0)	*P*	*Q*
0.14685682	ω	343°51972	+0.33386927	−0.91398242
3.558009	Ω	86.51027	+0.88877605	+0.22374415
0.5404842	*i*	13.35648	+0.31401982	+0.33848883
och 1954 Aug. 26.0 ET=JDE 2434980.5				
1°41280		(1950.0)	*P*	*Q*
0.14739592	ω	343°52165	+0.33421512	−0.91376935
3.549328	Ω	86.48588	+0.88869395	+0.22393309
0.5420992	*i*	13.37709	+0.31388422	+0.33893883
och 1961 May 1.0 ET=JDE 2437420.5				
0°81742		(1950.0)	*P*	*Q*
0.14778202	ω	343°50271	+0.33480540	−0.91350099
3.543143	Ω	86.46745	+0.88854581	+0.22441312
0.5433300	*i*	13.38955	+0.31367451	+0.33934452

TABLE II. Ephemeris.

60—61 0^h UT	R. A. (1950)	Decl.	Δ	*r*	mag.	mag.
ne 15	23^h 02^m3	−19° 47′	2.630	3.046	20.2	21.4
25	23 08.2	−20 15	2.450	2.990		
ly 5	23 12.5	−20 57	2.279	2.934		
15	23 14.9	−21 56	2.120	2.876		
25	23 15.1	−23 11	1.977	2.819		
ıg. 4	23 12.9	−24 38	1.852	2.761	19.4	20.7
14	23 08.2	−26 13	1.750	2.702		
24	23 01.1	−27 48	1.672	2.644		
;p. 3	22 52.4	−29 13	1.620	2.585		
13	22 42.9	−30 19	1.593	2.526		
23	22 33.8	−30 58	1.590	2.467	18.6	19.4
ct. 3	22 26.5	−31 06	1.607	2.407		
13	22 21.7	−30 44	1.640	2.349		
23	22 20.1	−29 56	1.686	2.290		
ov. 2	22 21.8	−28 46	1.739	2.232		
12	22 26.7	−27 16	1.797	2.175	18.6	19.1
22	22 34.5	−25 29	1.856	2.118		
ec. 2	22 44.9	−23 29	1.915	2.063		
12	22 57.5	−21 14	1.971	2.009		
22	23 12.0	−18 48	2.023	1.957		
an. 1	23 28.1	−16 10	2.072	1.908	18.6	18.9
11	23 45.7	−13 22	2.116	1.860		
21	00 04.5	−10 24	2.156	1.816		
31	00 24.5	−07 19	2.193	1.775		
eb. 10	00 45.6	−04 07	2.226	1.738		
20	01 07.8	−00 50	2.257	1.705	18.6	18.6
far. 2	01 30.9	+02 28	2.287	1.677		
12	01 55.1	+05 45	2.317	1.654		
22	02 20.4	+08 59	2.348	1.636		

TABLE II.—*Continued.*

1960—61 0^h UT	R. A. (1950)	Decl.	Δ	*r*	mag.	mag.
Apr. 1	02 46.7	+12 04	2.379	1.624		
11	03 14.0	+14 59	2.413	1.619	18.6	98.5
21	03 42.3	+17 39	2.450	1.619		
May 1	04 11.5	+20 00	2.489	1.626		
11	04 41.5	+22 01	2.531	1.638		
21	05 12.0	+23 39	2.576	1.656		
31	05 42.7	+24 52	2.624	1.680	18.9	18.9
1961—62 0^h UT						
Oct. 28	11 47.5	+12 11	3.048	2.416	20.0	20.8
Nov. 7	12 03.2	+11 03	3.014	2.475		
17	12 17.9	+10 04	2.969	2.534		
27	12 31.3	+09 15	2.915	2.593		
Dec. 7	12 43.6	+08 38	2.851	2.652		
17	12 54.3	+08 13	2.779	2.711	20.0	21.0
27	13 03.6	+08 02	2.701	2.769		
Jan. 6	13 11.0	+08 05	2.620	2.827		
16	13 16.5	+08 24	2.539	2.885		
26	13 19.8	+08 57	2.461	2.942		
Feb. 5	13 20.7	+09 44	2.390	2.998	19.9	21.2
15	13 19.2	+10 42	2.332	3.054		
25	13 15.3	+11 47	2.291	3.110		
Mar. 7	13 09.4	+12 55	2.272	3.165		
17	13 01.8	+13 57	2.278	3.219		
27	12 53.3	+14 49	2.312	3.272	20.0	21.5
Apr. 6	12 44.8	+15 26	2.375	3.325		
16	12 36.8	+15 44	2.466	3.378		
26	12 30.1	+15 44	2.582	3.429		
May 6	12 25.1	+15 27	2.720	3.480		
16	12 22.0	+14 55	2.876	3.530	20.7	22.3

TABLE III.

JDE—2430000	cosδ Δα	Δδ	cosδ Δα	Δδ	Place
2567	+0″1	−0″3	−2″0	−0″5	Lick
2568	(−29.0	−40.7)	(−31.0	−40.9)	Lick
2569	+0.2	+0.3	−1.8	0.0	Lick
2570	+5.8	−1.0	+3.9	−1.2	Yerk
2579	+1.4	+0.2	0.0	0.0	Yerk
2579	+3.8	+1.5	+2.5	+1.3	Yerk
2580	−1.4	−0.6	−2.7	−0.8	Lick
2621	+1.4	+1.0	+1.5	+0.5	Lick
2621	−0.3	−0.7	−0.2	−1.2	Lick
4994	+24.8	+1.0	+1.0	−1.5	Lick
5011	+20.0	+1.2	−2.7	+0.5	Lick
5012	+23.4	+1.3	+0.7	+0.6	Lick
5017	+23.3	+0.3	+1.0	+0.2	Lick
5018	+24.1	+0.8	+1.8	+0.7	Lick
5018	+18.7	+2.0	−3.6	+1.9	McD
5019	+25.2	+1.0	+3.0	+1.0	McD
5019	+20.2	−0.2	−2.0	−0.2	McD
5039	+24.7	−1.7	+3.7	0.0	McD
5039	+21.4	−1.2	+0.4	+0.5	McD
5041	+19.5	−2.4	−1.4	−0.5	McD
5041	+18.6	−0.9	−2.3	+1.0	McD
5043	+20.7	−1.8	0.0	+0.2	Lick
5044	+21.8	−2.7	+1.0	−0.7	Lick

standard IBM 650 electronic computer programs which are in regular use at the University of Cincinnati for the determination of minor planet orbits. All the observations were collected by B. G. Marsden, Yale University, and the author gratefully acknowledges this assistance. The preliminary elements, by G. Merton, were adopted from IAU Circular 1474 as follows:

Epoch—1947 Dec. 1.0 ET = JDE 2432520.5

M_0	359°71645		(1950.0)	P	Q
n	0.14685577	ω	343°51838	+0.33389623	−0.91397397
a	3.558026	Ω	86.50995	+0.88876847	+0.22377176
e	0.5404925	i	13.35616	+0.31401260	+0.33849338.

The perturbations were computed by the method described in *Astronomical Journal* **59**, 267 (1954). The resulting residuals before and after the differential correction are shown in Table III, and the correcti and their probable errors are shown in Table Osculating elements are given at three epochs three successive perihelia, and an extended ephem is given during the next apparition. The observ conditions are not too favorable, especially after c junction with the sun. The two values of the magnit depend upon the diminution of brightness according $1/r^2$ or $1/r^4$ of the heliocentric distance.

TABLE IV.

$\delta\psi_x$	+1″18± 3″58	δM_0	−0″97±3″39
$\delta\psi_y$	−1.32± 6.53	δe	−1.71±1.76
$\delta\psi_z$	+5.79±12.96	$\delta a/a$	−0.9854±0.045

THE ASTRONOMICAL JOURNAL VOLUME 65, NUMBER 6 AUGUST, 1

On the Computation of Nearly Parabolic Two-Body Orbits

CHARLES E. HERRICK
Flight Performance and Guidance Analysis Group, Convair (Astronautics) Division of General Dynamics Corporation, San Diego 12, California

(Received May 31, 1960)

A solution is given for the accurate computation of time in nearly parabolic two-body orbits which employs the true anomaly as the angular variable. It yields accuracy unattainable by any method found in the literature.

I. INTRODUCTION

HISTORICALLY, difficulties have been encountered in the computation of nearly parabolic two-body orbits. These difficulties have arisen from the use of parameters and variables that rapidly become indeterminant as the parabolic orbit is approached, or from the basic form of the solutions employed. The solution that is given departs from the traditional approach exemplified by the method of Gauss (Herget, 1948), and provides for the accurate computation of time in such orbits directly as a function of true anomaly. This solution was developed to provide for the accurate computation of the reference conic sections employed in an Encke's method calculation of the trajectories of lunar and interplanetary probes. It is applicable to the problems of comet orbits.

II. GENERAL DISCUSSION

The reasons for employing the true anomaly rather than the eccentric anomaly in describing the motion of a body in a nearly parabolic orbit (the same reasoning applies to the hyperbolic equivalent of the eccentric anomaly in nearly parabolic hyperbolic orbits) are manifest in several ways:

(a) From the geometry of the problem (Fig. 1), it is apparent that the eccentric anomaly E is not a favora variable with which to describe the motion until body is at a considerable distance from the attract body. This results because it is an angular measure coordinate system (center of ellipse), that is far remo from the region in which the motion is taking place the orbit close to the attracting body is computed f E, a given percentage error in E results in much la errors in the computed quantities. This situat becomes worse as the orbit approaches the parab orbit because the center of the ellipse, in the li moves to infinity, so that E is unaffected by the mo ment of the orbiting body.

(b) When considered from a numerical standpoint is found that losses in numerical significance result f three basic computations when the eccentric anom is taken as the primary angular variable. These are computation of the semi-major axis a; the computat of E from Kepler's equation when time is given, or versa; the computation of the radial distance

$$r = a(1 - e\cos E).$$

Such losses in significance are in essence simpl numerical manifestation of the indeterminancy of geometry, and cannot be avoided by an ingeni

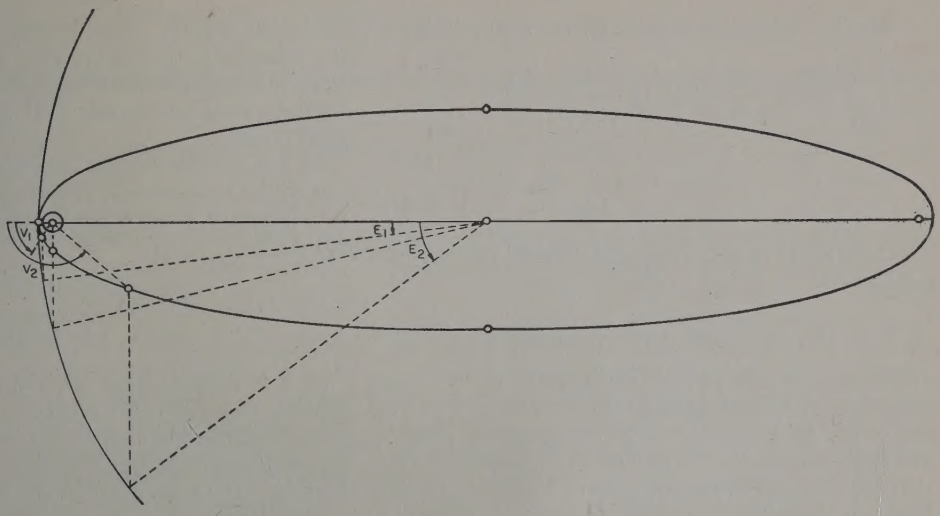

G. 1. Geometry of the problem.

gling of the basic equations while retaining the entric anomaly as the primary angular variable.

(c) When the position and velocity are computed in ns of the true anomaly it is found that the maximum ificance can be maintained in the computations. parameters that enter into such computations, the ilatus rectum p and the eccentricity e can be com-ed with no difficulty.

pon careful consideration it is clear that what is led is an appropriate solution to the areal-time erential equation in terms of the true anomaly. No solution could be found in the literature that quately meets the requirements of the problem. sequently a new solution was developed that yields maximum accuracy and is efficient in machine putation. The solution results from an expansion ne elliptical, (or hyperbolic) orbit about a parabolic t. The transformation of variables used for this nsion is well known to astronomers, but the form ne final solution is new.

III. DERIVATION OF THE SOLUTION

he differential equation to be solved to obtain a tion for the time as a function of true anomaly is llows:

$$r^2dv/dt=(GM)^{\frac{1}{2}}p^{\frac{1}{2}}, \tag{1}$$

re v is the true anomaly, GM the product of the ersal gravitational constant and the mass of the acting body, and r is given by

$$r=p/(1+e\cos v).$$

r making the substitution

$$x=\tan(v/2) \quad \text{and} \quad \lambda=(1-e)/(1+e),$$

(1) becomes

$$\frac{(GM)^{\frac{1}{2}}(1+e)^2}{2p^{\frac{3}{2}}}dt=\frac{1+x^2}{(1+\lambda x^2)}dx. \tag{2}$$

Integrating by parts, one obtains

$$\int\frac{1+x^2}{(1+\lambda x^2)^2}dx=\frac{-e}{1-e}\frac{x}{1+\lambda x^2}+\frac{1}{1-e}\frac{1}{\lambda^{\frac{1}{2}}}\tan^{-1}\lambda^{\frac{1}{2}}x \quad \text{Elliptical}$$

or,

$$+\frac{1}{1-e}\frac{1}{(-\lambda)^{\frac{1}{2}}}\tanh^{-1}(-\lambda)^{\frac{1}{2}}x \quad \text{Hyperbolic.}$$

When expanded in series it can be shown that

$$\lambda^{-\frac{1}{2}}\tan^{-1}\lambda^{\frac{1}{2}}x=(-\lambda)^{-\frac{1}{2}}\tanh^{-1}(-\lambda)^{\frac{1}{2}}x$$
$$=x\{1-\tfrac{1}{3}\lambda x^2+\tfrac{1}{5}[(\lambda x^2)^2]-\dots\}.$$

From Kepler's equation, letting $\sin E=\lambda^{\frac{1}{2}}x/(1+\lambda x^2)$, $E=2\tan^{-1}\lambda^{\frac{1}{2}}x$,

$$\frac{(GM)^{\frac{1}{2}}(1+e)^2}{2p^{\frac{3}{2}}}t=\frac{-e}{1-e}\frac{x}{1+\lambda x^2}+\frac{x}{1-e}\left(1-\frac{\lambda x^2}{3}+\frac{(\lambda x^2)^2}{5}-\dots\right). \tag{3}$$

The problem remaining is the removal of the indeterminancy on the parabolic boundary solution. This can be done by multiplying the numerator and denominator of the first term in the series by $1+\lambda x^2$, and adding the resultant expression to the first term in the integral, that is,

$$\frac{-e}{1-e}\frac{x}{1+\lambda x^2}+\frac{x}{1-e}=\frac{x}{1+\lambda x^2}+\frac{1}{1+e}\frac{x^3}{1+\lambda x^2}.$$

The indeterminancy in the remaining terms in the series can be eliminated by dividing term by term by $1-e$.

Collecting terms, one obtains for the final solution

$$\frac{(GM)^{\frac{1}{2}}(1+e)^2}{2p^{\frac{3}{2}}}t=\frac{x}{1+\lambda x^2}+\frac{x^3}{1+e}\left(\frac{1}{1+\lambda x^2}-\frac{1}{3}\right)+\frac{x^3}{1+e}\sum_{n=1}^{\infty}(-1)^{n+1}\frac{(\lambda x^2)^n}{2n+3}.$$

This solution is valid for elliptical parabolic and hyperbolic orbits.

IV. DISCUSSION OF THE SOLUTION

The gain in computation efficiency of this solution over those of the traditional methods results from the use of the true anomaly as the independent variable and from the rational fraction form. It should be noted that $\lambda x^2=\tan^2(E/2)$ appears only as a small correcting factor in the solution. The major terms are directly a function of true anomaly. Since there is no way of converting these terms to equivalent expressions in eccentric anomaly without loss of numerical significance, it is clear that for accurate computation the true anomaly must be retained as the primary variable.

The series part of the solution is rapidly convergent in the regions of interest. It is uniformly and absolutely convergent for $|\lambda x^2|<1$. The errors in the solution due to losses in significance in forming λ [where $\lambda=(1-e)/(1+e)=(1-e^2)/(1+e)^2$] can be shown to be negligible provided $x^2\leq 10(1+e)^2$. For orbits with $e\cong 1$, this yields $v\cong 175°$. Thus, in practice, the limitation the solution is the convergence of the series and losses in significance in forming λ, since the value o generally does not exceed 175° in the applications most interest.

At large values of true anomaly significance can lost in the computation of r because $e\cos v$ is appro mately minus 1. Such losses can be avoided by co puting

$$r=\frac{p}{1+e}\frac{1+x^2}{1+\lambda x^2}.$$

If it is desired to let the time be the independe variable in a particular problem, then an iteration $x=\tan(v/2)$ is required. It has been found conveni in practice to employ Newton's method for such iteration. The first derivative, used in Newton's meth to increase the rapidity of convergence, can be obtai from Eq. (2).

V. ACKNOWLEDGMENT

I should like to express my indebtedness to Dr. P Herget, Director of the Cincinnati Observatory, for discussions that we have had on this problem.

REFERENCES

Herget, Paul, 1948, *The Computation of Orbits* (Published priva by the author), p. 34.

NOTICES

Notice Concerning the Lick Observatory Double-Star Catalogue Projects

HAMILTON M. JEFFERS
Lick Observatory, Mount Hamilton, University of California

URING the past few years two double-star catalogue projects have been under way at the Lick ervatory, both largely supported by National nce Foundation grants.

he first is a catalogue of double star measures. All sures made since the closing date of R. G. Aitken's *General Catalogue of Double Stars . . .*, 1927.0, h of −20° declination, have been recorded on IBM ls, up to the commencement of 1958. The number neasures so entered is about 96 000. The rather con-rsial question of limits, of distance or brightness, inclusion or rejection from the catalogue has been ided by not imposing limits. Even wide "proper ion" pairs have been included. We hope that the nber of objects inadvertently omitted from our com-tion will prove to be small.

he second Lick Observatory project is an Index alogue of double stars north of −20° declination, n about 35 000 entries. All objects contained in the rnham catalogue, and in the Aitken catalogue, are uded, together with the pairs rejected from the ken catalogue, and those more recently discovered. rt part of the Index Catalogue south of −19°, cover-the southern third of the sky, with about 18 000 ries, was compiled by Dr. W. H. van den Bos during year before his retirement, in 1956, as Director and ronomer at the Union Observatory, Johannesburg. e northern and southern Index catalogues list the ble stars, with their positions for 1900 and 2000, the es of first and last measures with the corresponding ition angles and distances, together with data as to discoverer, the magnitudes, the spectral type, the per motion, etc., with occasional additional informa-n in the form of notes. The project is described in ail in an article by W. H. van den Bos and myself, nted in the *Publications of the Astronomical Society he Pacific* **69**, 322 (1957). The general plan for the lex Catalogue has been approved by the Double Star mmission of the International Astronomical Union. As a part of the over-all project, we have entered on M cards the complete list of southern double-star asures. There are about 95 000 observations of 18 700 rs. This was done with the cooperation of Dr. van n Bos, from a microfilm copy of the cards maintained the Union Observatory.

The catalogue of measures of pairs north of −20°, de since 1927.0, commenced with a new manuscript d catalogue begun by Dr. R. G. Aitken after the blication of his *New General Catalogue of Double rs . . . .* This manuscript catalogue was kept up after Dr. Aitken's retirement in 1936, at first by Dr. Aitken himself. Later, owing to lack of personnel and to the dislocations incident to the second World War, it was not possible to maintain it so well, so that by 1946 it was in a quite unsatisfactory state. A suggestion by Mrs. Dorothea Havens Chappell, who had worked for some time upon the manuscript, that the catalogue of measures be transferred to IBM punched cards, was investigated and favorably acted upon. Since the retirement of Mrs. Chappell we have been fortunate in having the very efficient assistance of Mrs. Frances Greeby, who is competent both in compiling the data and in operating the punching machine. By 1957 all the measures were recorded on IBM punched cards, and all new measures that reach us as publications or in manuscript form have been, or will be, so recorded. The entries are complete, so far as we know, up to 1958.0. At this time the recording of observations was suspended in order to concentrate efforts on the second catalogue project, that of the Index Catalogue.

The background of the Index Catalogue is described in the before-mentioned article in the August, 1957, issue of the *Publications of the Astronomical Society of the Pacific*. This type of catalogue appeared to be the most practical from the economic and feasibility points of view. In some respects it will not replace the earlier catalogues, in particular S. W. Burnham's *General Catalogue* and R. G. Aitken's *New General Catalogue*. It will not, of course, attempt to list observations. The manuscript of the northern section (north of −20° declination) of the Index Catalogue, being prepared at the Lick Observatory, is nearly finished. The magnitudes, spectral types, and proper motions have been entered from the standard sources. After the completion of the manuscript it will be necessary to bring the observation catalogue up to date, and then, on the basis of the most recent measures, to revise the Index Catalogue. The same will have to be done for the objects in the sky south of −19°, the Union Observatory catalogue of observations, and the southern Index catalogue, compiled by van den Bos before 1957.

It is not believed that it will be expedient to publish the catalogue of observations. The material, however, will be available to those who desire it. We propose that requests for lists of measures of any double stars will be filled by printing the data from the cards on sheets of paper, with the aid of the automatic IBM typewriter. This can be done at a moderate cost to be paid by the person requesting the service. The Index Catalogues, on the other hand, may merit a wider distribution. It is

the hope of Professor van den Bos and myself that the northern and southern sections can be distributed together, as a unit, to those interested. It is planned to publish the material as a single volume, with appropriate indices and explanations, that will contain the essential data on double stars over the entire sky, from pole to pole. Inasmuch as the two sections of the Index Catalogue will be recorded on special IBM cards, the complete material could also be made available in the form of a duplicate of the card file of the approximately 50 000 cards, a form that would have the advantage of flexibility if not that of compactness.

Although the immediate objectives are to complete the observation and the Index catalogues, and to publish the latter, it is planned at the Lick Observatory to maintain into the future both these catalogues as a continuing project. Supplements to the Index Catalogue, or revisions of it, will be prepared when su additions are needed.

The date of January 1, 1961, has been set as th beyond which no double-star observations of old or n pairs shall be considered in the published Index Ca logue now planned. July 1, 1961, is the date now set the completion of the entire project.

The purposes of this note are, first, to make kno to those astronomers who are interested, the state advancement of the Lick Observatory double-star ca logues, together with the general details of their natu and contents. Second, we would like to request th those observers having lists of measures as yet unpu lished, will either publish them in the near future, transmit to us a manuscript copy of the material, order that the catalogues may take into account t most recent double-star measures.